Colorado

Agricultural and Mechanical College

Department of Civil Engineering

INFLUENCE OF SHAPE ON THE FALL VELOCITY OF SEDIMENTARY PARTICLES

By

E.F. Schulz, R.H. Wilde, and M.L. Albertson

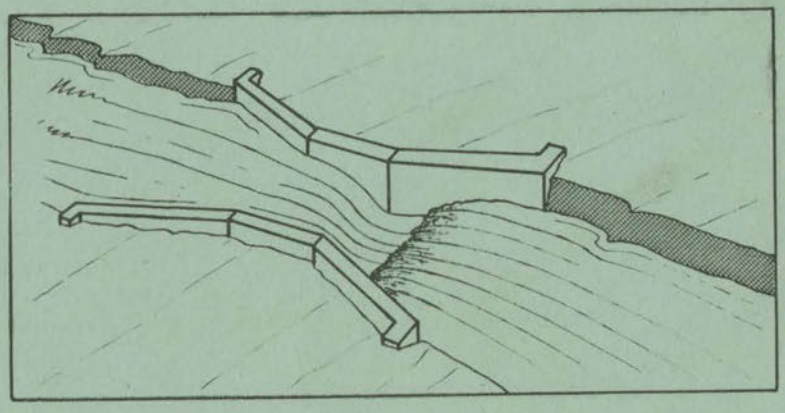

Fort Collins, Colorado

Report No. 53-10 May 1953

INFLUENCE OF SHAPE ON THE FALL VELOCITY

of

SEDIMENTARY PARTICLES

by
E. F. Schulz, R. H. Wilde, and M. L. Albertson
Civil Engineering Section
Colorado Agricultural Experiment Station
Fort Collins, Colorado

prepared for
District Engineer
Omaha District
Corps of Engineers, Department of the Army
under Contract No. DA-25-075-eng 2266

through the
Colorado A & M Research Foundation

TABLE OF CONTENTS

LIST OF TABLES

LIST OF FIGURES

NOTATIONS AND DEFINITIONS

Symbol	Units	FLT Dimensions	Definition
A	$(cm)^2$	L^2	Maximum projected area of a particle.
A_n	$(cm)^2$	L^2	Projected area of a sphere of the same volume as the particle, $A_n = \frac{d_n^2}{4}$.
a	mm	L	Major axis of a particle.
b	mm	L	Intermediate axis of a particle.
c	mm	L	Minor axis of a particle
C_D	-	-	Drag coefficient, $C_D = \frac{F/A}{\rho \frac{w^2}{2}} = \frac{F/d_n^2}{\rho \frac{w}{2}}$.
C_s	-	-	Size coefficient $C_s = \frac{F}{\rho_f v^2}$
C_w	-	-	Velocity coefficient, $C_w = \frac{\Delta \gamma v}{\rho_f w^3}$
d	mm	L	Diameter of circle equal in area to the vertical projection of a particle when falling in its most stable position.
De	mm	L	Diameter of smallest circle completely circumscribing largest projected area of a particle.
de	mm	L	Diameter of a circle equal in area to projected area of a particle.
dj	mm	L	Inside diameter of the fall-column.
d_n	mm	L	Nominal diameter (diameter of a sphere having the same volume as a particle).

Symbol	Units	FLT Dimensions	Definition
d_s	mm	L	Sedimentation diameter (diameter of a sphere of the same fall velocity and same specific gravity as the particle in the same fluid under the same conditions).
d_{sv}	mm	L	Sieve diameter (sieve opening of the sieve preceding the sieve on which the particle was retained).
F	gm	F	Net gravitational force on the particle falling in the fluid, $F = \frac{\pi}{6} d_n^2 (\rho_p - \rho_f) g$.
g	cm/sec^2	L/T^2	Acceleration of gravity (980.7 cm/sec^2).
k	-	-	Volume constant proposed by Heywood (k = volume of particle/ $d^3 = \frac{\pi}{6} (\frac{d_n}{d})^3$).
K	-	-	Shape coefficient proposed by Malaika ($K = v/v_s$).
K_d	-	-	Ratio of nominal diameter to sedimentation diameter d_n/d_s.
K_w	-	-	Ratio of sieve diameter to sedimentation diameter d_{sv}/d_s.
m	-	-	Boundary correction for experimental drag coefficient.
Re	-	-	Reynolds number (usual form - wd/η although some special variations occur in this report).
Se	cm^2	L^2	Surface area of a sphere having the same volume as a particular particle.
S	cm^2	L^2	Surface area of a particle.
sf	-	-	Corey shape factor = $c/\sqrt{ab}$.
V	cm^3	L^3	Volume of particle.

Symbol	Units	FLT Dimensions	Definition
v	cm/sec	L/T	Fall velocity in data of Serr, Corey, Malaika and Wilde.
v_s	cm/sec	L/T	Fall velocity of a sphere having same volume as a particle as used in Malaika's data.
w	cm/sec	L/T	Fall velocity as used in this report.
ϵ	-	-	Particle roughness parameter.
μ	gm sec/cm^2	FT/L^2	Dynamic viscosity.
ν	cm^2/sec	L^2/T	Kinematic viscosity = μ / ρ.
ρ_f	gm sec^2/cm^4	FT^2/L^4	Mass density of fluid.
ρ_p	gm sec/cm^4	FT^2/L^4	Mass density of particle.
ϕ	-	-	Shape factor proposed by Wadell (= de/De).
ψ	-	-	Shape factor proposed by Wadell (= Se/S).
Ω	-	-	Shape factor proposed by Krumbein ($= \sqrt[3]{(b/a)^2(c/b)}$.

FOREWORD

This report summarizes a number of years of research in sediment engineering conducted in the hydraulics laboratory at Colorado Agricultural and Mechanical College. Under the direction of Dean N. A. Christensen, Eugene Serr III proposed in a Master's thesis as a shape factor, a simple ratio of sedimentation diameter to sieve diameter. Later under the direction of Professor M. L. Albertson, Head of Fluid Mechanics Research, A. T. Corey, R. H. Wilde and E. F. Schulz conducted investigations using a shape factor porposed by Corey and natural sedimentary materials from different sources ranging in size from 1/4 mm sand to 1 in. gravel. During this same period under the direction of Professor J. S. McNown at State University of Iowa, Jamil Malaika conducted experiments in oil using steel particles with regular geometric shapes.

In 1952 a grant was made available to Colorado Agricultural and Mechanical College through its Research Foundation, by the Corps of Engineers, Department of the Army, for the purpose of assembling this report and obtaining the data for the gravel particles dropped in oil. Mr. Don C. Bondurant, represented the sponsor and much credit is due him for his efforts and suggestions.

The authors are indebted to Mr. E. W. Lane of the U. S. Bureau of Reclamation for his encouragement and for supplying the initial incentive for this series of studies of shape. They are also indebted to Dr. D. F. Peterson, Head of the Department of Civil Engineering, for his encouragement and for reviewing this report.

In the interest of maximum utility, all of the available measurements and other data have been included in the Appendix. The authors hope that in this way the data will be available to others for future improvement in the techniques of sediment engineering.

ABSTRACT

Techniques used in modern sediment engineering require knowledge of the fall velocity of sediment particles in water. Under certain conditions the fall velocity of a sphere can be computed using Stokes Law. Stokes Law, however, considers only the viscous forces on the particle. The resistance of particles falling in water is attributed to (1) viscous deformation of the fluid, and (2) inertial losses in the fluid caused by acceleration (both tangential and normal acceleration) of the fluid around the particle. The Reynolds number (a ratio of the inertial forces to the viscous forces) is a dimensionless parameter which expresses the relative importance of the inertial forces to the viscous forces in the motion of the fluid around the particle. Stokes Law is valid when the viscous forces are the predominate cause of the resistance of the particle. As Reynolds numbers become greater than 1.0 the inertial forces assume greater importance and any equation which considers only the viscous forces (such as Stokes Law) becomes less and less valid. A quartz sphere approximately 0.1 mm diameter falling in water at 20°C (67°F) would have a Reynolds number of 1.0.

To study the fall velocity of natural particles, dimensionless parameters were employed to give general solutions to the equations involved. The principal parameters employed were the Reynolds number (ratio of inertial forces to viscous forces), the drag coefficient (intensity of drag force) and the shape factor. Particles were selected at random from a number of samples of sediment having different geographical and geologic origins. The shape factor of these particles was measured. The particles were then dropped in water and the fall velocity measured. By measuring the weight, the volume, the fall velocity and the shape of the particle, the dimensionless parameters previously listed could be computed and a graph of drag coefficient versus Reynolds number with the shape factor as a third variable could be prepared. The particles studied in this manner ranged in size from 0.25 mm to 25 mm. To verify the results from the tests on the small particles, the gravel-sized particles were also dropped in oil. Because of the viscosity difference between the water and the oil, the larger gravel-sized particles had Reynolds numbers between 1.0 and 500 when dropped in oil. It was found that the affects of surface roughness could not be ignored; therefore, data obtained from the extremely rough particles were separated from the more rounded material by plotting on separate graphs.

The data obtained by Krumbein and Malaika in tests on artificial particles were also plotted on these two graphs.

Other information regarding the extent of variation of the shape factor, relation of average shape factor to sieve size, relation of sieve size to nominal diameter and intermediate axes, relation of sieve diameter to sedimentation diameter and shape factor have also been investigated. All the available data have been assembled in the Appendix.

Chapter I

INTRODUCTION

The success of many irrigation and flood control projects has been seriously hampered because of man's inability to cope with the problems brought about by the presence of large quantities of sediments or other problems associated with sedimentation. Some of these might have been avoided in the design stage had present day information and knowledge been available to the designers. Other difficulties because of sediment encountered in the current operation of irrigation and river control projects might at least be alleviated, if not eliminated, by a better understanding of factors involved in the process of sedimentation.

Sediment problem in engineering

Modern sediment engineers have been greatly handicapped by the lack of physical measurements required to describe fully the forces governing the movement of sediments. Recently, theoretical methods have been developed for describing the movement of sediment and predicting the amount of sediment being transported in streams. To employ these theoretical methods, certain average hydraulic properties of the sediment and also the extent of variation of these properties from the average must be known.

Fall velocity -- a fundamental property of sediment

Salient among these sediment properties is the terminal fall velocity or settling velocity. Investigators have known for considerable time that the fall velocity is an important consideration in reservoir sedimentation; however, recent research has shown that the stream velocity required to move particles along a stream bed is also directly related to the fall velocity.

Factors affecting fall velocity

Many factors influence the terminal velocity or fall velocity of a single isolated particle, the most important factors generally considered are size, shape, density of the particle, proximity of boundaries, particle concentration, and viscosity of the fluid. Although it is difficult to isolate these factors and study them individually, certain

generalized statements can be made concerning them.

Particle size:- The size usually is considered the most important variable and is sought as a criterion to determine which forces will have predominant action on the particle moving in the fluid. Size would be an easy variable to measure if all sedimentary particles were of regular geometric shape such as a sphere. The exact size of the larger particles like gravel can be determined easily because the particles are large enough to handle, examine, and measure.

Sieving is most often employed to determine the size of a particle wherein the sediment size is usually described by arbitrary sieve-size ranges. The sediment size scale is shown in Table 1.

Particle shape:- The shape of the particle, although secondary in importance to size, cannot be ignored because many of the differences and discrepancies of the fall velocity for a particular size can be explained by measuring or describing the shape.

Particle density:- The particle density is relatively unimportant because the density of common sedimentary particles varies between narrow limits. Actually, the important factor associated with particle density is the particle density relative to the density of the fluid medium. If the fluid medium is water, the relation can be simply expressed as the specific gravity of the particle. Since quartz and the silicas occur so frequently in natural sediments, the average specific gravity of sediments is commonly assumed to be 2.65. The average specific gravity of common sedimentary minerals is shown in Table 2.

Table 2

Specific Gravity of Common Sedimentary Minerals[a]

Mineral	Specific Gravity
Beryl	2.75 - 2.8
Biotite	2.8 - 3.2
Calcite	2.72
Coal	2.3
Dolomite	2.85
Galena	7.4 - 7.6
Garnet	3.5 - 4.3
Muscovite (mica)	2.76 - 3.1
Microcline (Feldspar)	2.54 - 2.57
Orthoclase (Feldspar)	2.57
Quartz (calcedony)	2.65

[a] From Dana's Handbook of Minerology

Table 1

Sediment Grade Scale[/a]

(Subcommittee on Sediment Terminology, A.G.U.)

Size in Millimeters		Microns	Inches	Approx. Sieve Mesh Openings per Inch		Class
				Tyler	U. S. Standard	
4000-2000			160-80			Very large boulders
2000-1000			80-40			Large boulders
1000-500			40-20			Medium boulders
500-250			20-10			Small boulders
250-130			10-5			Large cobbles
130-64			5-2.5			Small cobbles
64-32			2.5-1.3			Very coarse gravel
32-16			1.3-0.6			Coarse gravel
16-8			0.6-0.3	$2\frac{1}{2}$		Medium gravel
8-4			0.3-0.16	5	5	Fine gravel
4-2			0.16-0.08	9	10	Very fine gravel
2-1	2.00-1.00	2000-1000		16	18	Very coarse sand
1-1/2	1.00-0.50	1000-500		32	35	Coarse sand
1/2-1/4	0.50-0.25	500-250		60	60	Medium sand
1/4-1/8	0.25-0.125	250-125		115	120	Fine sand
1/8-1/16	0.125-0.062	125-62		250	230	Very fine sand
1/16-1/32	0.062-0.031	62-31				Coarse silt
1/32-1/64	0.031-0.016	31-16				Medium silt
1/64-1/128	0.016-0.008	16-8				Fine silt
1/128-1/256	0.008-0.004	8-4				Very fine silt
1/256-1/512	0.004-0.0020	4-2				Coarse clay
1/512-1/1024	0.0020-0.0010	2-1				Medium clay
1/1024-1/2048	0.0010-0.0005	1-0.5				Fine clay
1/2048-1/4096	0.0005-0.00024	0.5-0.24				Very fine clay

[/a] Rouse et al., Engineering Hydraulics, John Wiley, 1950, p. 776.

Fluid viscosity:- The fluid viscosity plays an important role in the fall velocity of a particle. When the particle is moving slowly, any differences in the viscosity of the fluid cause changes in the fluid drag on the particle. Viscosity varies considerably with changes in temperature but only slightly with changes in pressure. In fact, the variation with pressure is so small that it can be ignored so that viscosity is considered a function of temperature only. The fluid properties of density, dynamic viscosity, and kinematic viscosity of water are plotted as a function of temperature in Fig. 1.

Present techniques used in sediment analysis

Presently accepted techniques used in sediment analysis will be briefly described. Complete detailed descriptions of these tests can be obtained from the Proceedings of the American Society for Testing Materials or the reports of the Cooperative Federal Interagency Project (1) (2).

Geometric size and submerged weight are the primary properties of a sediment particle which influence its behavior in resisting the forces to which it is subjected by the fluid both while in suspension and while on or near the bed. Because the weight of a particle is sometimes considered to be synonymous with size (since specific gravity is so near a constant for most natural water-borne sediments), the size thereby becomes the most important property of sediment and of greatest significance in sediment engineering. The properties of particle shape, fluid density and fluid viscosity all are associated with the drag or resistance of the particle and are therefore associated with the force which can be mobilized to act on the particle.

Sieve and sedimentation analysis:- Size is determined by several different methods depending on the relative size of the particles. If the particles are very large (coarse gravel and larger), the particles are usually measured using calipers or a scale. Since these particles are seldom encountered in sedimentation studies except for scour or bed-load studies in steep mountain streams, the technique of size determination can be one of considering each particle individually.

For the size range from fine sand (1/16 mm) to medium gravel (16 mm) the usual method of size determination is by sieving and the measured size is termed the sieve diameter (23:775). Sieving sorts the particles according to a range of sizes and it is assumed that the particles are sorted according to their intermediate axes (b dimension). This is true only if the particles are thoroughly agitated for a

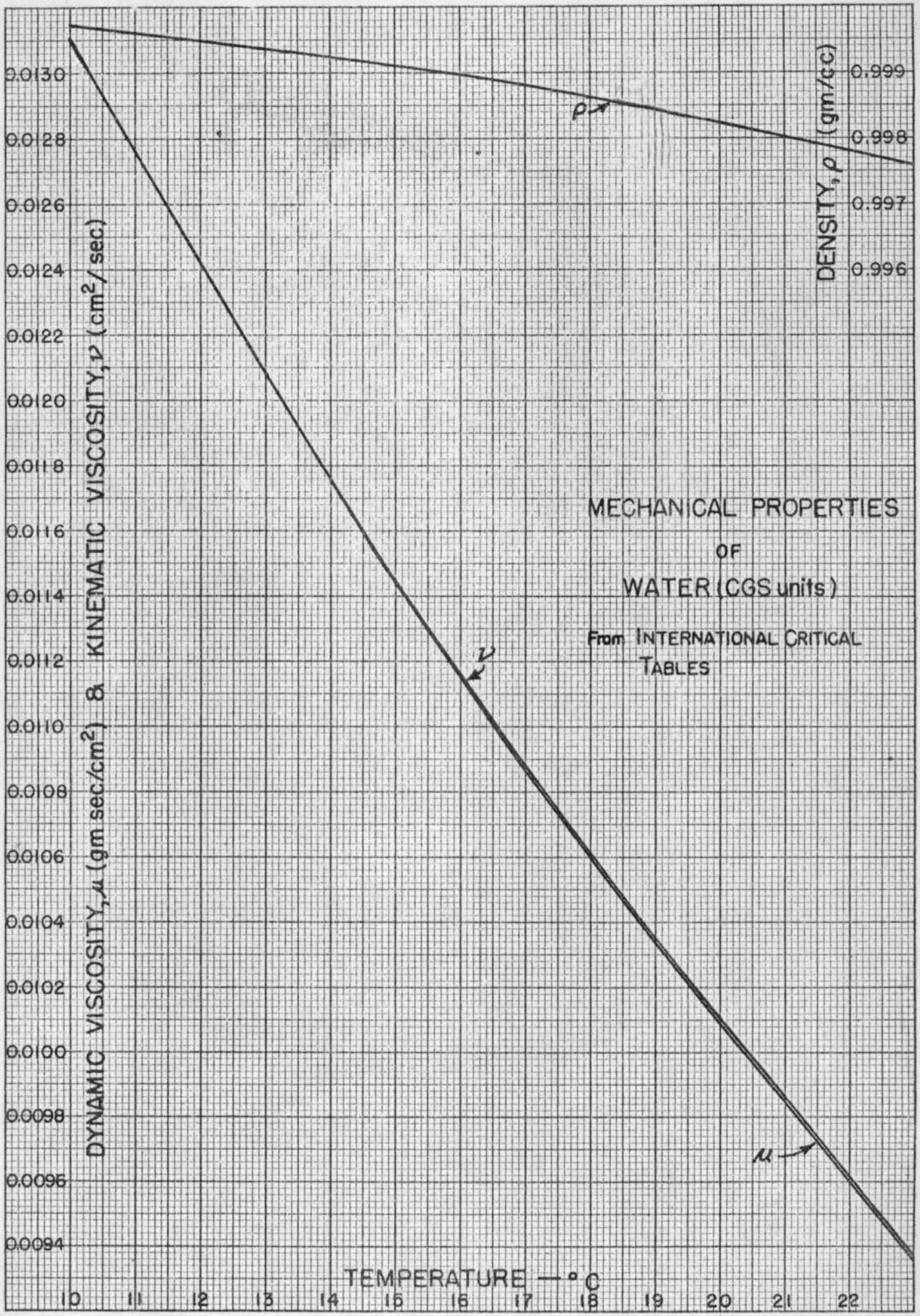

Fig. 1

sufficient period of time. The range of sizes present in any sieve fraction depends on the difference in sizes of the sieve openings of the "retained" sieve and the "passing" sieve.

Sieving is quite often considered an unreliable method of size determination for particles smaller than the No. 200 sieve (approx. 1/14 mm) (23:775). The size distribution of particles smaller than silt size (1/16 mm) is determined by using any one of a number of methods classified as sedimentation methods (1).

The sedimentation methods sort the particles according to the hydraulic properties rather than by actual physical measurements and the size is then termed the sedimentation diameter. The properties of shape and specific gravity are indeterminably confused with the size analysis when the sedimentation methods are used.

Specific gravity:- Because the relative weight of the sediment in the fluid is the desired variable, specific gravity is usually determined instead of density. Considerable variation in specific gravity exists in particles of large size (larger than gravel - 4 mm) because the mineral composition depends upon the parent rock. In nature most sands are composed of quartz (SG = 2.65). Therefore, the specific gravity of sand is approximately 2.65. The fine materials (silt and clay -- sizes less than 1/16 mm) are more often fragments of feldspars and micas (SG = 2.5 to 2.7) and therefore these fine materials tend to have a lower specific gravity (23:777).

The foregoing discussion has shown how the specific gravity varies as the size decreases from large boulders to fine clay. In certain problems these variations in specific gravity could easily account for large discrepancies in fall velocity.

Lack of a shape standard:- Of all the variables influencing the fall velocity, only shape lacks an easy and widely accepted definition. This lack of generally accepted and easily measured standard has hampered many refinements of technique in modern sedimentation engineering. Because there has been considerable confusion in describing shape, a review of the existing literature is appropriate and helpful in formulating a satisfactory and useful method of describing shape.

Chapter II

REVIEW OF LITERATURE

With the more complete utilization of stream flow to fill the expanding needs of irrigation and the increasing demands for municipal and domestic water supplies, the problems resulting from the presence of sediments in the streams and sedimentation in the stream beds and reservoirs have become evident and in many cases aggravated. In utilizing this stream flow, means have been devised for separating the wanted water from the unwanted sediment. In many cases much of the sediment has been discharged back into the stream, thus increasing the concentration of the sediment load downstream. The problems of predicting and controlling the action of these sediment-laden streams have been increased and in many cases today are completely unsolved. To employ the turbulence theory on these problems, more must be known about the fall velocity.

The most apparent use of the fall velocity concept is in predicting the time required for a particle to settle through a known distance in a body of quiet water. By this means the length of time may be determined that water must be retained quietly in a settling basin in order to separate the sediment from the water. The fall velocity is useful also in predicting the location of the sediment deposits in existing or potential reservoirs.

Another need for knowing the fall velocity was demonstrated by Krumbein (8) and Rubey (26) who found that the critical velocity of the stream when the particles on the bed of the stream moved into suspension was related to the fall velocity of the particles in quiet water. Thus to prevent movement of the bed material into suspension, the stream velocity must not exceed the critical velocity of the particles comprising the bed material. If in a stream the particles need to be kept in suspension, the fall velocity to a large extent determines the intensity of turbulence required to prevent sedimentation.

Finally, perhaps the most important need for knowledge of the fall velocity is the use of the fall velocity in the formulae for computing the quantity of material being moved in a stream as suspended sediment and also as bed load.

Early research

Sir George Stokes (19) was first to show concern about the fall velocity of particles. In 1846 he derived an equation for viscous conditions, later called Stokes law, which defined the fall velocity of spheres falling under the action of gravity in a fluid medium of known viscosity. Stokes law is expressed as follows

$$w = \frac{\gamma d^2}{\mu 18} (SG_p - SG_f)$$

where

- w - fall velocity,
- d - diameter of the sphere,
- SG_p - specific gravity of the particle,
- SG_f - specific gravity of the fluid,
- γ - specific weight of water,
- μ - dynamic viscosity.

Later metallurgical engineers, concerned with ore dressing problems, recognized that there was a significant difference in the fall velocity of different rock particles. In 1908 Richards (24), a mining engineer, studied the fall velocities of crushed quartz and galena particles. Richards studied sieve fractions ranging in size from 0.32 to 11.93 millimeters. He observed that the drag coefficient was no longer a function of Reynolds number for particles larger than 1.55 mm diameter. Furthermore, this anomaly occurred differently for the quartz and galena. He sought to explain the difference on the basis of the difference in the specific gravity of the two materials. Closer investigation might have disclosed to Richards that this difference could not be attributed to a difference in specific gravity, but to the shape which was different for the quartz and galena. The explanation was pointed out years later.

Recent research

In 1933 Rubey (26) using Richard's data and additional data of his own recognized that the fall velocities follow two different laws. He found that for particles smaller than about 0.14 mm sieve diameter Stokes law seemed to be valid and he called this range the viscous range because the particle motion could be completely described by the action of the viscous and gravity forces. Rubey developed an equation for the particles larger than 0.14 mm. He stated that this second law applied to the "impact" range because the resistance to motion in this range was caused by the "impact" of the fluid. His equation consisted essentially of Stokes law combined with a correction for "impact." The use of the word

"impact" does not conform to the present-day concept of the term. Rubey also found that it was necessary to use an additional correction coefficient to make the galena data conform to his curve, which had been derived from the data for the quartz grains. He suggested that the difference in this coefficient for the quartz and galena was because of the difference in the characteristic shape of the crushed quartz and galena particles.

In 1934 A. P. Zegrzda (42), a Russian engineer, plotted some original experimental data together with other available data on a type of C_D:Re graph.[a] When plotted in this manner, three logical ranges appeared. Zegrzda called the first range (Reynolds number less than 1.0 where Stokes law is valid) the "streamline stage", the second range the "intermediate stage" (Reynolds number 1.0 to 1000), and the third range the "turbulent stage" (Reynolds number greater than 1000). In the latter range the drag coefficient remained constant and was therefore independent of Reynolds number. He found that the drag coefficient varied greatly for any particular value of Reynolds number depending upon the shape of the particle. He plotted his data using the sieve diameter as the characteristic length in both the drag coefficient and the Reynolds number.

Zegrzda used both smooth spherical balls and "natural sediment" particles of sand. To obtain fluids of different density and viscosity he used water and different petroleum products. In this way he could vary the viscosity by dropping the same particle in the different fluid mediums. He found that data using the smooth balls plotted a smooth curve on the C_D:Re graph regardless of the fluid medium used. On the other hand he found that the curves for the sand grains dropped in water would not fit the curves for the same sand grains dropped in the oil. He explained that this discrepancy was caused by the influence of the relatively rough, irregular surface of the sand grains on the flow pattern around the particle. Therefore, he recommended that for sedimentation studies, water only be used as the fluid medium.

Actually the affects of the fluid are completely accounted for when using the Reynolds number parameter. The influence of the fluid on the particle is one of viscosity. When the Reynolds number is high ($Re > 10{,}000$) the viscous forces, while still present, are of minor importance relative to inertial forces. This relationship is true for any particular Reynolds number, regardless of the fluid used. The validity of the assumption that Reynolds number completely

---

[a] A short English summary of Zegrzda's paper is presented in the appendix.

accounts for the effects of the viscosity of the fluid was later verified by Malaika.

In 1935 Wadell (35)(36) attempted to evaluate the shape parameter by means of the sphericity of the particle. He defined sphericity as the ratio of the surface area of a sphere having the same volume as the particle to the actual surface area of the particle. He also suggested the presently accepted definition of sedimentation diameter (i.e., the diameter of a sphere having the same terminal velocity and specific gravity as the natural particle falling in the same fluid.)

Wadell's conclusions were based on sound theoretical considerations. He also recognized the impractical nature of his concept of sphericity because the true surface area of individual small particles is virtually impossible to obtain. Therefore, he redefined the sphericity as the ratio of the diameter of a circle equal in area to the projected area (obtained when the particle rests on one of its larger faces) to the diameter of the smallest circle circumscribing the projected area. The projected area was measured by tracing around a magnified projection of the particle with a planimeter. The area of the circumscribing circle was obtained by placing a specially-constructed circular grid over the projected image and observing the diameter of the smallest circle which surrounded the image. The weakness of Wadell's simplified sphericity coefficient lies in its lack of any consideration of the "thickness" of the particle with respect to the measured projected area.

In 1938 H. Heywood (6), a British investigator, studying the "fineness" of rock crusher materials suggested a "volume constant" as a shape parameter. The volume constant, k, was defined as:

$$k = \frac{\text{volume of particle}}{d^3}$$

where d = diameter of a circle of area equal to the projected area of the particle when placed in its most stable position.

Heywood prepared a nomograph (1:44) which could be used to determine the fall velocity of the particle provided the volume constant k could be determined. The volume constant could be estimated using a table of "k" values published for a number of particles used as examples. The weakness of Heywood's concept lies in the estimation of the volume constant.

In 1942 W. C. Krumbein (8) in studying the "flume behavior"

of particles formed of molded portland cement mortar, verified the relationship between fall velocity and critical velocity of a stream of water required to move a particle on the bed. Because he made artificial particles, he could control the shape, density, volume, and nominal diameter. The latter three variables were held constant for all the particles. Krumbein suggested the following expression for the shape parameter:

$$\Omega = \sqrt[3]{(b/a)^2 (c/b)}$$

where a - the longest axis of the particle,
b - the intermediate axis of the particle,
c - the shortest axis of the particle.

His investigations showed this shape parameter was related to the sphericity as defined by Wadell. He plotted the b/a ratio versus the c/b ratio and drew lines of equal sphericity on the plot; thus the true sphericity could be determined using definite and measurable dimensions a, b and c.

J. W. Stanley (33) was puzzled by difference in the size analysis curves obtained from the same sediment sample when a sieve analysis and a sedimentation analysis were compared. He found that sieve analyses and sedimentation analyses yielded the same results when a sample of spheres of uniform specific gravity was used. He explained the difference in the two size analysis curves by pointing out that some of the particles of similar sieve size must have different fall velocities and that the difference in fall velocities must be caused either by a difference in the shape of the particles or by a difference in the specific gravity of the particles.

In 1948 E. F. Serr (31) compared the difference between the sieve diameters and the sedimentation diameters of ten samples of sand obtained from widely different sources. He studied eight sieve fractions between the No. 10 and No. 100 Tyler standard sieves. He suggested using the ratio of the sedimentation diameter to the sieve diameter as the shape of the particle. Serr found little difference in the sieve diameter and the sedimentation diameter for the particles corresponding to the No. 100 sieve size indicating that shape had little influence on the fall velocity of small particles (approx. 1/16 mm) because they were in the viscous range of Reynolds number. He also found that the drag coefficients for the most angular samples became independent of Reynolds number at a nominal diameter of about 1.4 mm. For the more spherical particles this does not occur until the nominal diameter becomes as large as 7 mm to 10 mm which was out of the range of Serr's work.

In 1949 A. T. Corey (3) working with discrete individual sand particles suggested a simplified shape parameter which

he called the shape factor sf:

$$sf = \frac{c}{\sqrt{ab}}$$

where a - the longest (or major) axis of the particle,
b - the intermediate axis of the particle,
c - the shortest (or minor) axis of the particle.
All axes were mutually perpendicular.

Corey selected 10 representative sand particles from each of 5 sieve fractions between the No. 4 and the No. 14 mesh Tyler standard sieve. He examined in this manner sand samples from four different sources. He found that the fall velocity for two particles of the same weight and falling in the same fluid medium could vary as much as 100 percent depending upon the shape of the particle. Thus demonstrating that for a fundamental study, the individual particles must be studied. Corey selected the expression $c/\sqrt{ab}$ for his shape factor because he and others found that the particles usually oriented themselves in the fluid so that they presented the greatest resistance to the passing fluid. Thus the maximum projected area as discussed by Wadell, Heywood, and Krumbein is oriented normal to the path of motion. The projected area can be approximated by the ab term and the c term corresponds to the thickness which was not accounted for in Wadell's simplified sphericity coefficient. Hence the form $c/\sqrt{ab}$ is a logical dimensionless shape parameter expressing the relative flatness of the particle.

Corey expressed the drag coefficient and Reynolds number in two different forms:

$$C_D = \frac{F/ab}{\rho w^2/2}$$

$$Re = \frac{wb}{\nu}$$

and

$$C_{D_n} = \frac{F/d_n^2}{\rho w^2/2}$$

$$Re_n = \frac{wd_n}{\nu}$$

where

C_D - drag coefficient,

C_{D_n} - drag coefficient (using nominal diameter),

Re - Reynolds number,
Re_n - Reynolds number (using nominal diameter),

F - force causing motion (buoyant weight of particle),

ρ - mass density of fluid,
w - fall velocity of particle,
a - major axis of particle,
b - intermediate axis of particle,
c - minor axis of particle,
d_n - nominal diameter of particle,

ν - kinematic viscosity of the fluid, μ/ρ,
μ - dynamic viscosity of the fluid.

When he plotted C_D versus Re, using the first two expressions for Re and C_D, he found difficulty in drawing the lines of constant shape factor. On the other hand he found it reasonably simple to draw lines of constant shape factor through his experimental data when Re and C_D were expressed in terms of nominal diameter. He concluded then that the nominal diameter should be used for the characteristic length and area in the Reynolds number and drag coefficient parameters.

In 1949 Jamil Malaika (11) reported the resistance characteristics of twelve machined steel shapes. He dropped these particles in six different types of oil and also varied the temperature. This technique permitted him to vary the Reynolds number between Re = 0.001 and Re = 1000.

Malaika also spent considerable time investigating the proper position to release the particles in order that stable motion might occur when the particle was released. He used a unique electromagnet to hold the steel particle prior to release. Krumbein (8), Rubey (26), and others (23) had previously stated that the particles would tend to orient themselves until the maximum cross section was normal to the direction of motion. Malaika observed this stability over a wide range of Reybolds number. His findings are summarized as follows:

1. Zone of deformation drag (Re $<$ 0.1).
   Particles were stable in any position provided the center of gravity of the particle and center of resistance were on a line parallel to the path of motion.

2. Zone of surface drag (0.1 $<$ Re $<$ 500).
   The particles oriented themselves so that the largest cross section was normal to the path of motion. The particles were quite stable in this position.

3. Zone of eddy formation (Re $>$ 500).
   Formation of eddies in the wake affected the stability of the orientation of the particle.

In 1950 McNown and Malaika (14) developed a shape parameter in the form

$$c/\sqrt{ab}.$$

It is interesting that Corey and Malaika and McNown working independently both used the same basic parameter for the simplified shape factor. McNown and Malaika related the sieve diameter and the sedimentation diameter by a factor K,

$$K = \frac{w_s}{w},$$

where ws is the fall velocity of a sphere with diameter equal to the nominal diameter of the particle (sedimentation diameter),

w is the fall velocity of the particle.

A graph of K versus $c/\sqrt{ab}$ in parameters of b/c was presented based on Malaika's previous data taken from his experiments with the twelve machined steel particles dropped in various types of oil.

Corey's simplified shape factor (which was also developed by McNown and Malaika) is simple and therefore practical to use, is in dimensionless form and therefore a perfectly general form of the shape factor, and is a simple and direct method relating the difference between the sieve analysis and the sedimentation analysis of the same sediment sample.

Summary

Although the drag characteristics of spheres and disks and other regular geometric shapes have been thoroughly studies, the behavior and characteristics of natural particles have been investigated only recently. A description of the shape of natural particles is Wadell's coeffi- of sphericity ($\psi = \frac{s}{S}$). The determination of this coefficient is difficult and, while its importance should be recognized, it is too impractical to be of general use. Other proposed methods for describing the shape of a natural particle involves either the measurement of:

1. The maximum projected area, or
2. The length of the three mutually perpendicular axes.

Because of the relative ease in measuring the three axes, the latter method is preferred. Corey advocated the use of his simplified shape factor ($sf = c/\sqrt{ab}$) and this shape

factor was also used by McNown and Malaika (14), Wilde (41), and Schulz (29). Corey, Wilde, and Schulz have assembled considerable data on natural sedimentary particles and they have shown that, within certain stated limitations of average particle roughness and average specific gravity, the Corey shape factor is practical and involves a minimum amount of labor to measure and compute.

Chapter III

THEORETICAL ANALYSIS

Fundamental principles

The fundamental principles of fluid mechanics involved in the study of fall velocity are the basic laws of motion. The forces producing the motion and the drag or resistance will be analyzed.

Basic assumptions:- In expressing the most fundamental drag equation to be considered in studying the fall velocity of a particle it must be assumed that:

1. The fluid is of uniform density.
2. The fluid is of uniform viscosity.
3. The motion of the particle in a direction normal to the mean falling path (usually vertical) is negligible and involves no lateral acceleration of the particle (falling straight.)
4. The particle is not accelerating in mean falling path.

If these assumptions are met, the submerged weight F of the particle (called the activating force) is exactly equal to the drag forces on the particle (which is moving steadily through the fluid of uniform density and viscosity). The cause of the drag can be explained using the principles of both laminar and turbulent flow.

Laminar flow:- Laminar flow is a result of the fluid property called viscosity, which Rouse (23:75) defines as "that property of a liquid or gas which gives rise to an internal stress opposing deformation of the fluid during flow." Viscosity also may be defined as the ratio of the gradient of momentum flux to the rate of diffusion of momentum per unit area in the direction of the gradient. Any relative motion between a particle and the fluid causes internal viscous stress in the fluid medium and produces a deformation of fluid adjacent to the particle. Drag on the particle is a result of transfer of momentum by molecular diffusion from the moving particle to the fluid.

Turbulent flow:- The distinction between laminar and turbulent flow can be made by considering the difference between the molecular (or laminar) diffusion of momentum as compared with the molar (or turbulent) diffusion of momentum. The diffusion by molecular action is sufficiently slow that its effect may be felt over a widespread region (by deformation) without becoming unstable. Turbulent (or molar) diffusion however, is a result of the gradient of momentum flux being so great that the flow becomes unstable and turbulent mixing results. With turbulent diffusion, finite masses of fluid are moving in a somewhat random fashion through the fluid and the mixing process is much more rapid and intense. These phenomena are involved to varying extents in the different types of drag experienced by sediment particles. One of the most important variables associated with drag is the Reynolds number (a ratio of the inertia forces to the viscous forces involved in the flow) which may be used as a criteria for determining the type of drag which exists on a sediment particle.

Cause of drag:- The drag forces on a particle are a result of either one or both of:

1. The shear along the boundary of the particle in the direction of motion. This is called Surface Drag.

2. The pressure difference between the upstream and downstream side of the particle. This is called Pressure Drag.

Because most sediment particles are relatively short even in their greatest dimension, the drag resulting from shear along the boundary in the direction of motion (surface drag) is of secondary importance except for low Reynolds numbers.

Discussion of the C_D:Re diagram

The drag on the particle can be classified as one or a combination of two different types of drag (21:209)

1. Deformation drag.
2. Form drag.

Deformation drag is principally the result of viscous forces and is characterized by a flow pattern where the deformation of the fluid laminae is widespread. Form drag results from inertial forces and is characterized by a flow pattern in which there is a separation. The relative importance of these two types of drag depends on the Reynolds number.

Low Reynolds numbers:- At low Reynolds numbers ($Re < 0.1$) the effects of the inertial forces caused by the motion of the

particle may be ignored and the drag on the body is exclusively one of deformation, caused by viscous stress. Deformation drag may be classified further as a combination of surface drag due to boundary shear and pressure drag due to the form of the projected area. The motion in this range is characterized by a "widespread distortion of the basic flow pattern" (19:232) and is defined mathematically by Stokes Law (19:158) for spheres.

$$F = 3\pi d_{\mu} w$$

and (9:605) (4:74) for disks:

$$F = 8 d_{\mu} w$$

where

F - net gravitational force,
d - diameter of the particle,
μ - dynamic viscosity of the fluid,
w - terminal or fall velocity of the particle.

As shown in Fig. 2, Stokes Law for spheres may be plotted on the C_D:Re graph as a straight line:

$$C_D = 24/Re$$

and the equation for disks may be rearranged as

$$C_D = 20.37/Re$$

for plotting on the C_D:Re graph.

Because the drag in the Stokes range is due to the "widespread deformation of the basic flow pattern," there is extensive viscous movement of the fluid normal to the ambient direction of flow. Such movement must be accompanied by a drop in pressure in the direction of flow and hence a drag on the particle due to a difference in pressure between the upstream and downstream sides of the particle. Also boundary shear on the particle contributes to the drop in pressure. In fact, Prandtl (4:74) has pointed out that theoretically one-third of the drag on a sphere is due to pressure difference and two-thirds is due to boundary shear. Furthermore, Prandtl has shown that in the direction of motion the sum of the shear and pressure difference is the same at all points. Because a circular disk has no boundary in the direction of flow, however, the viscous drag is due entirely to the pressure difference. It is remarkable that the drag coefficients for the two extreme cases of a sphere and a disk are so near the same value that it is difficult to plot the difference on a graph.

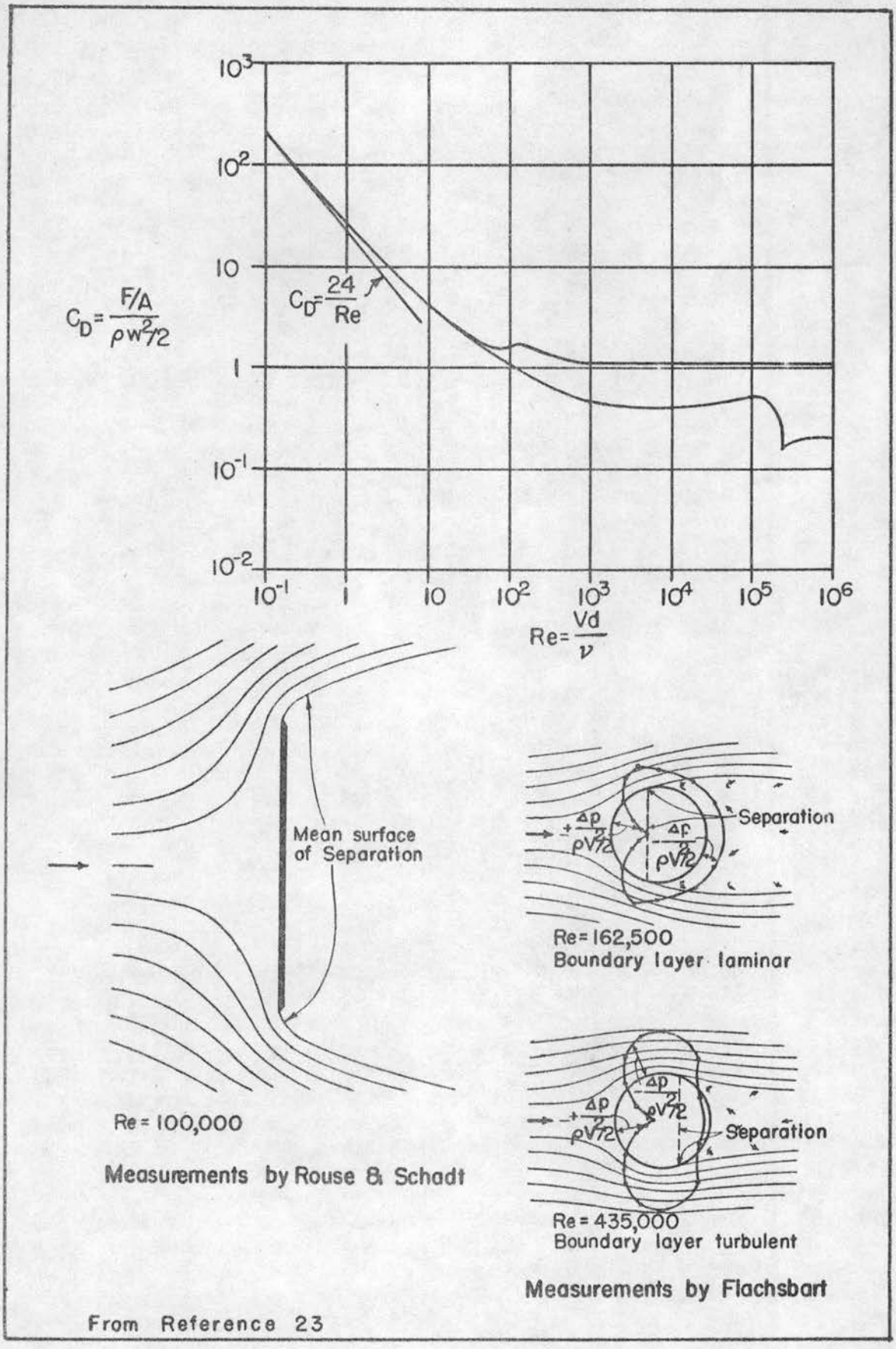
$C_D = \frac{F/A}{\rho w^2/2}$
$C_D = \frac{24}{Re}$
10^3
10^2
10
1
10^{-1}
10^{-2}
10^{-1} 1 10 10^2 10^3 10^4 10^5 10^6
$Re = \frac{Vd}{\nu}$
Mean surface of Separation
Re = 100,000
Measurements by Rouse & Schadt
$+\frac{\Delta p}{\rho V^2/2}$
$-\frac{\Delta p}{\rho V^2/2}$
Separation
Re = 162,500
Boundary layer laminar
Separation
Re = 435,000
Boundary layer turbulent
Measurements by Flachsbart
From Reference 23

Fig. 2

Evidently, then the drag coefficient in the viscous range is essentially independent of the thickness of the particle (provided the particle is not relatively long) and depends only upon the magnitude and shape of the projected area of the particle. Furthermore, because the resultant of the pressure and shear is the same at all points on the boundary there is no unbalanced force to create a torque which would rotate the particle. This confirms the experimental findings of McNown and Malaika (14:78) in which the falling particle did not rotate regardless of its initial orientation.

Intermediate Reynolds numbers:- As Reynolds number is increased to the range of $0.1 < Re < 1000$, the viscous flow pattern becomes unstable and the inertial forces gradually assume greater importance. The zone of viscous flow -- though still present -- becomes restricted to a relatively thin layer at the surface of the particle known as the laminar sublayer. Outside the laminar sublayer the inertial forces predominate and the flow is turbulent. The shape of the particle determines to a large extent the path taken by the fluid, as it flows about the particle, hence determines the radial and tangential accelerations necessary for the fluid to travel this path.

As a result of the instability of the laminar flow and the increased importance of the inertial forces (due to acceleration), a zone of separation is formed on the downstream side of the particle as shown in Fig. 2. This zone of separation has a poorly defined appearance at $Re = 3$ but gradually takes on a more clearly defined appearance as the Reynolds number is increased, until at $Re = 20$ the separation zone has a well-defined vortex pattern downstream from the particle (5:65) (5:551).

Separation occurs at the point where the flow is expanding (streamlines are spreading) and the local velocity in the boundary layer becomes zero. Any further expansion of the boundary layer causes flow near the boundary in the direction opposite to the ambient velocity v_o. The point of separation may occur at a number of positions along the boundary of the particle (as the case of the sphere) or the point of separation may be fixed always by a sudden change in the curvature of the boundary of the particle (as the case of the disk).

Thus in the Intermediate Range of Reynolds number the type of drag gradually changes from about half surface drag and half pressure drag ($Re = 0.5$) to almost exclusively pressure drag ($Re = 1000$) -- the surface drag (viscous effects) being negligible compared with the pressure drag.

Finally, because the inertia forces have become significant in this range of Reynolds number, there develops a single

stable orientation for each particle relative to the direction of motion.

High Reynolds numbers:- As the Reynolds number is increased further (Re > 1000) the influence of viscosity becomes of less and less importance until at Re = 500,000 for spheres and Re = 5000 for disks the flow pattern in general and the drag in particular becomes completely independent of Reynolds number.

Throughout this range the separation is well defined; but the point of its beginning upstream, and hence its size, varies with the nature and extent of the laminar sublayer surrounding the particle upstream from the point of separation. Complete destruction of the laminar sublayer occurs for smooth spheres at about Re = 200,000 and for disks at about Re = 5000. The sphere and the thin disk can be considered to be the extreme limits of shape for natural particles.

For high Reynolds numbers, the particles assume an orientation which is most stable. Because of the asymmetric formation of vortices in the separation zone, however, there develops an unsteady oscillating motion, the extent of which depends largely upon the shape of the projected area of the particle.

Dimensional analysis

Before any attempt is made to analyze the problem further, the variables will be organized into orderly dimensionless parameters using the principles of the Buckingham -Theorem (21:13).

The variables:- All the fundamental variables which affect the motion of the particle are tabulated together with their dimensions.

w - fall velocity - cm/sec (L/T),
ρ_f - density of the fluid - gm sec^2/cm^4 (FT^2/L^4),
ρ_p - density of the sediment - gm sec^2/cm^4 (FT^2/L^4),
μ - dynamic viscosity of the fluid - gm sec/cm^2 (FT/L^2),
b - intermediate axis of the particle (normal to a) - cm (L),
c - shortest axis of the particle (normal to ab) - cm (L),
a - longest axis of the particle - cm (L),
F - activating force; apparent weight of sediment particle in fluid - $(\rho_p - \rho_f)$ gV - gm (F),
k - A measure of surface roughness or surface irregularities (L).

Here a, b, and c are used to represent the geometry of the particle. It is doubtful that these are fully adequate to rigorously describe the geometry; however, they are simple and convenient and any more adequate system would be greatly complicated. The relationship between these variables may be expressed by the following equation:

$$\phi_1 (w, a, b, c, F, \rho_f, \rho_p, \mu, k) = 0 \qquad (1)$$

The variables can then be rearranged into dimensionless parameters by combining the repeating variables (w, b and ρ_f) successively with each of the remaining variables in Eq. 1. The following equation of parameters then results:

$$\phi_2 \left(\frac{wb\rho_f}{\mu}, \frac{F}{b^2\rho_f w^2}, \frac{\rho_p}{\rho_f}, \frac{a}{b}, \frac{c}{b}, \frac{k}{b} \right) = 0 \qquad (2)$$

As previously discussed the activating force F must be equal to the drag force D and $D = C_D A_f w^2/2$ (19:244). The expression for drag D can be solved for the drag coefficient C_D:

$$C_D = \frac{D}{A\rho_f w^2/2} \qquad (3)$$

where A refers to the projected area normal to the path of motion. Wilde (41:37) has shown that this projected area A can be approximated by the product ab provided the particle travels with its greatest projected area normal to the path of motion. Eq. 3 then becomes:

$$C_D \approx \frac{F}{ab\rho_f w^2/2} . \qquad (4)$$

Eq. 2 may be rearranged into the following dimensionless equation:

$$\phi_3 \left(\frac{w\sqrt{ab}\rho_f}{\mu}, \frac{F}{ab\rho_f w^2}, \frac{\rho_p}{\rho_f}, \frac{a}{b}, \frac{c}{\sqrt{ab}}, \frac{k}{\sqrt{ab}} \right) = 0 \qquad (5)$$

Each of the parameters in Eq. 5 is described as follows:

$\frac{w\sqrt{ab}\rho_f}{\mu}$ - a form of Reynolds number Re

$\frac{F}{ab\rho_f w^2}$ - a form of drag coefficient C_D

$\frac{\rho_p}{\rho_f} = \frac{\gamma_p/g}{\gamma_f/g}$ - specific gravity of the sediment particle SG

$\frac{a}{b}$ - disregarded for present

$\frac{c}{\sqrt{ab}}$ - Corey shape factor sf

$\frac{k}{\sqrt{ab}}$ - surface roughness coefficient ϵ .

Eq. 5 can then be rewritten:

$$\phi_4 (Re, C_D, sf, SG, \epsilon) = 0 \qquad (6)$$

Eq. 6 indicates the scope of the research program since the influence of the variation of each of the parameters must be studied in relation to the others. However, in the light of past research, some of the parameters may be disregarded until the more fundamental relationships have been established.

The C_D:Re equation:- If the specific gravity term SG and the surface angularity term are assumed to be constant or of secondary importance, Eq. 6 then can be written in the simplified form:

$$\phi_5 (Re, C_D, sf) = 0 \qquad (7)$$

or

$$C_D = \phi_6 (Re, sf) \qquad (8)$$

when the drag coefficient C_D is chosen as the dependent variable. Eq. 8 may be represented graphically as shown in Fig. 3 and is simply a minor elaboration on the C_D:Re graph. With this arrangement of the data, the drag coefficient and the Reynolds number are expressed in terms of lines of constant shape. This arrangement is the most convenient for obtaining a direct solution of the drag (or submerged weight) of the particle of given shape moving at a given velocity.

The C_D:C_s equation:- An arrangement of the data which will give the velocity at which a particle of known size, shape, and weight moves in a given fluid may be developed by reconsidering the variables in Eq. 1. Choosing variables b, ρ_f, and F as the repeating variables, the following equation results:

$$\phi_7 \left(\frac{F\rho_f}{\mu^2}, \frac{F}{b^2\rho_f w^2}, \frac{a}{b}, \frac{c}{b}, \frac{\rho_p}{\rho_f}, \frac{k}{b} \right) = 0 \qquad (9)$$

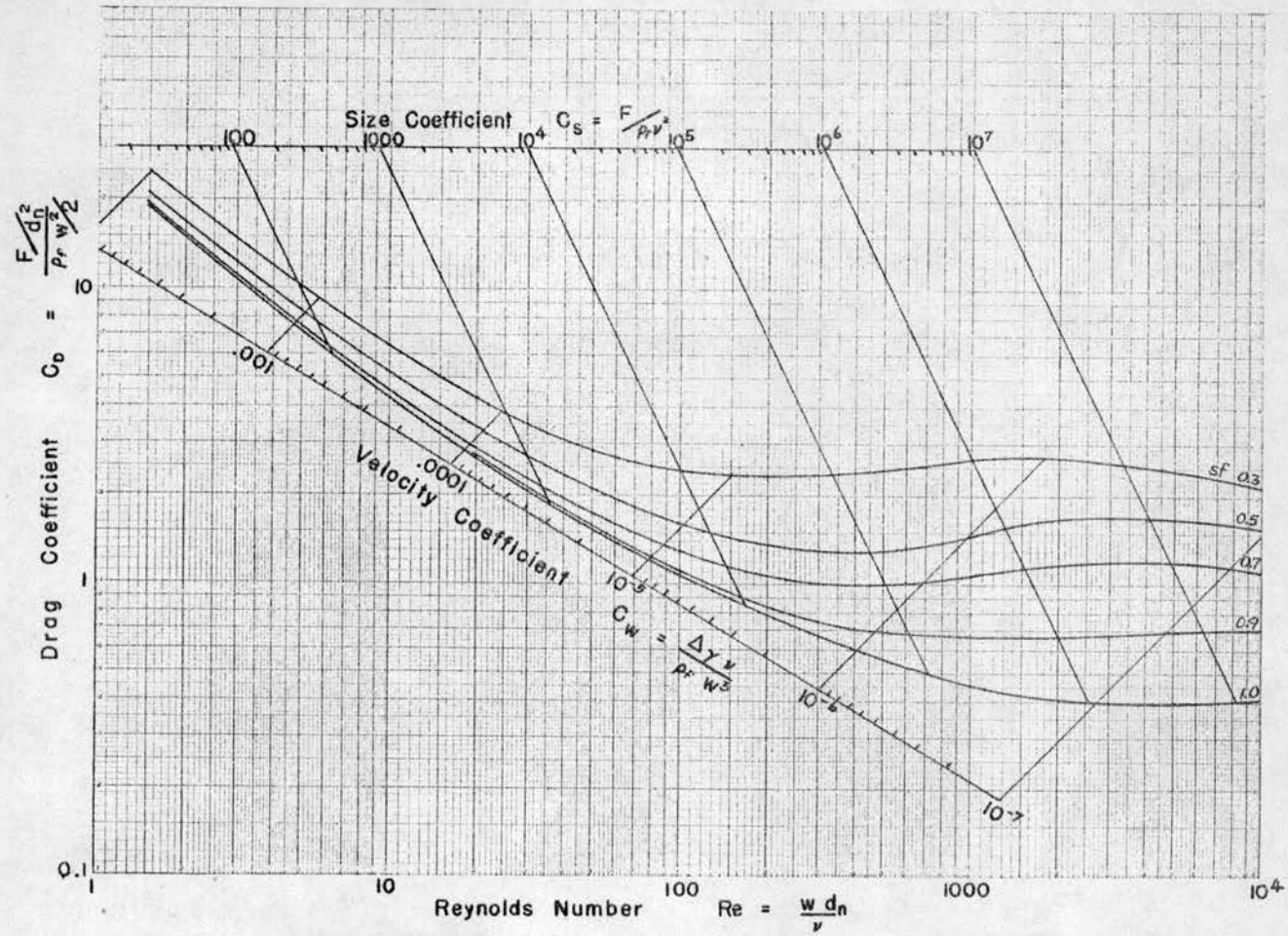

(a) C_D:Re Graph for Naturally Worn Sediments

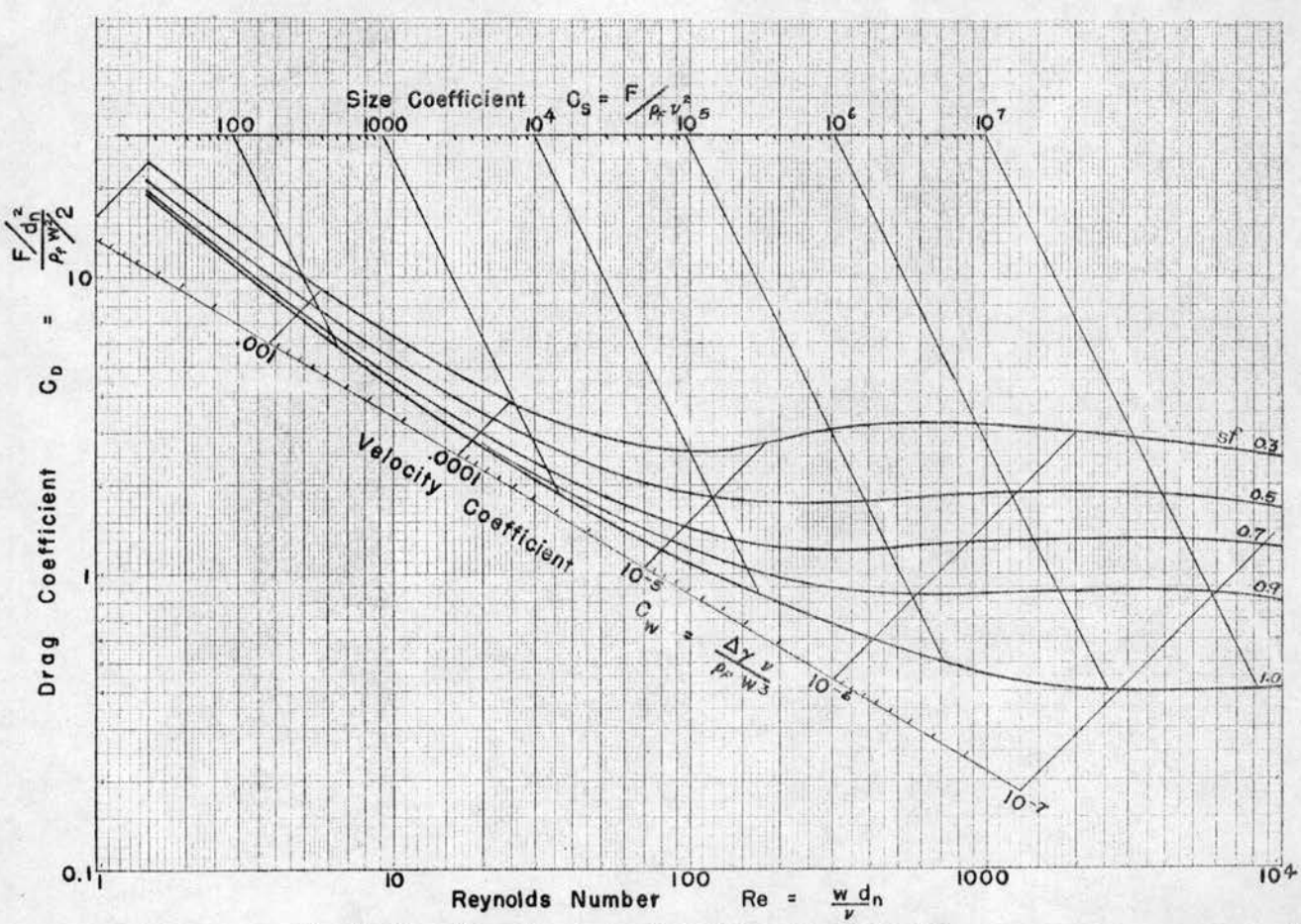

(b) C_D:Re Graph for Crusher Fragments

Fig. 3

When this equation is modified as previously described, the following simplified equation results:

$$\phi_8\left(\frac{F\rho_f}{\mu^2},\ C_D,\ sf\right) = 0 \qquad (10)$$

By choosing $C_s = \frac{F\rho_f}{\mu^2}$ as the dependent variable, Eq. 10 becomes:

$$C_s = \frac{F\rho_f}{\mu^2} = \frac{F}{\rho v^2} = \phi_9\ (C_D,\ sf) \qquad (11)$$

This arrangement is useful when the fall velocity w is unknown because in Eq. 11 w appears only in the drag coefficient C_D. Malaika (11:6) has shown that Eq. 11 plots as a series of straight lines of constant resistance (or constant size) at a slope of -2 and may be plotted on the C_D:Re graph by using an auxiliary scale. In making such a statement, however, and must also be considered to be constant. This is illustrated in Fig. 3.

The C_w:Re equation:- In a similar manner, lines of constant fall velocity (or constant sedimentation diameter) may be developed by again reconsidering Eq. 1 and choosing w, ρ_f, and μ as the repeating variables. The following equation results:

$$\phi_{10}\left(\frac{wb\rho_f}{\mu},\ \frac{F\mu}{w^3b^3\rho_f^2},\ \frac{\rho_p}{\rho_f},\ \frac{kw\rho_f}{\mu},\ \frac{aw\rho_f}{\mu},\ \frac{bw\rho_f}{\mu},\ \frac{cw\rho_f}{\mu}\right) = 0 \qquad (12)$$

Eq. 12 may be rewritten and simplified by the method previously described, resulting in:

$$\phi_{11}\left(Re,\ \frac{F\mu}{w^3b^3\rho_f^2},\ sf\right) = 0 \qquad (13)$$

or

$$\frac{F\mu}{w^3b^3\rho_f^2} = \frac{F\nu}{w^3dn^3\rho_f} \cong \frac{\Delta\gamma\nu}{w^3\rho_f} = \phi_{12}\ (Re,\ sf) \qquad (14)$$

When the nominal diameter (equivalent to b), fluid characteristics, and fall velocity are known, this arrangement is useful for a direct solution of size or relative weight ($\Delta\gamma$). Malaika (11:6) shows that Eq. 14 plots as a series of straight lines of constant fall velocity at a slope of +1 and may be plotted on the C_D:Re graph using a second auxiliary scale which is illustrated in Fig. 3.

Summary

In Summary, one should state that there are too many variables in the geometry of natural particles to make a

complete analysis by theoretical methods alone.

By dimensional analysis the fall velocity may be shown to be included in a functional relationship involving Reynolds number, drag coefficient and some parameter or parameters describing particle shape. The shape factor is generally considered to be a combination of length and area terms, the Reynolds number contains a length term, and the drag coefficient contains an area term. Although certain theoretical deductions can be made regarding the area and length terms in these parameters, it is necessary to determine experimentally the most significant form of each parameter.

Because of the many irregularities and odd shapes found in natural sediment it is highly improbable that a simple method can be devised which will completely describe shape. Based on the work of previous investigators and the theoretical considerations in this chapter, the shape factors which seem to be most easily measured are based on one or a combination of:

1. Maximum projected areas.
2. Lengths of mutually-perpendicular axes.
3. Nominal diameter.

Use of the mutually-perpendicular axes in the dimensional analysis results in three factors describing shape.

Chapter IV

EXPERIMENTAL EQUIPMENT AND PROCEDURE

Because this report has assembled the data from a number of different experiments, the materials studied, the equipment used, the experimental procedure and the results of each experimenter will be briefly described.

Krumbein

Materials:- Krumbein was concerned with the settling-velocity and flume-behavior of non-spherical particles. He made special particles from cement mortar. All particles were of the same volume and density. The shape was varied systematically. A total of 17 different particles were made and tested. The a, b, and c dimensions of each particle were measured.

Equipment and procedure:- The fall velocity was determined by dropping each of the 17 particles in a vertical lucite fall-column, 6 in. in diameter and 6 ft long filled with water at 20°C. Each particle was released in a random position at the surface and was timed with a stop-watch. A 2-ft distance was allowed for particle acceleration before velocity measurements were begun. The particles were timed over a distance of 4 ft. An average fall velocity for each particle was obtained from 10 to 20 observations on each shape.

The flume behavior was observed in a stream of running water in a flume 22 ft long, 0.44 ft wide, and 0.96 ft deep. Water was supplied to the flume from a constant-head tank through a stilling basin. The discharge was measured over a 90° V-notch weir. Observations were made in a 10-ft control section in which the depth was 0.43 ft being controlled by adjusting the discharge and the tail gate position.

Each particle was dropped into the stream upstream from the indicator which marked the beginning of the control section. The velocity of the particle through the 10-ft control section was measured with a stop watch.

Results:- Prior to Krumbein's work, two theories were advanced to explain the importance of shape in studying the fall velocity. Some writers thought the most important shape

consideration was the angularity of the corners and edges; other writers believed that the general form of the particles was more important than angularity. Krumbein's observations proved that the general form was a more important consideration than particle angularity.

Krumbein derived a dimensionless shape parameter based on the three mutually perpendicular axes, a, b, and c .

$$\Omega = \sqrt[3]{(b/a)^2 (c/b)} \qquad (15)$$

This equation was developed from Wadell's (37) concept of sphericity and the substitution of the a or b dimensions for the appropriate radii. Using this shape-parameter, Krumbein plotted a family of curves representing equal shape parameter on a dimensionless b/a:c/b graph. This curve served as a guide to the optimum particle dimensions for his particles. His particles were made with a complete range of variation of b/a, c/b, and Ω . Krumbein's data are shown in Appendix B. The data obtained by Krumbein varied from $3000 < Re < 10,000$.

Serr

Materials:- Under the direction of Dr. N. A. Christensen, Serr compared the sieve diameter with the sedimentation diameter of sand from 10 different sources. The sources were a fresh talus slope, sand dunes, a lake beach, a river bed, and standard Ottowa sand. The sand samples came from many geologic origins. Table 3 lists the types and sources of the sands studied by Serr.

Table 3

Types and Sources of the Sands Studied by Serr

Sample	Type	Source
1.	River bed material	Cache la Poudre River, Fort Collins, Colorado
2.	River bed material	Michigan River, Camp Pennock, Colorado
3.	Fine rock debris	Talus slide, Verdi, Nevada
4.	Dune sand	Small dunes, Fernley, Nevada
5.	River bed material	Truckee River, Truckee, California
6.	River bed material	South Fork, Yuba River, Cisco, California
7.	River bed material	Putah Creek, Davis, California
8.	Dune sand	Dunes near Great Salt Lake, Utah
9.	Lake beach material	Grand Lake, Colorado
10.	River bed material	Cache la Poudre River, Chamber Lake, Colorado
11.	Sedimentary deposit	Standard Ottawa sand

Equipment and procedure:- For dividing his samples into size groups or sieve fractions, Serr used Tyler Standard Sieves. Tyler Numbers 10, 14, 20, 28, 35, 48, 60, 65, 80 and 100 were used, with some exceptions (See Appendix C). About 500 gm of material were quartered from the oven dried and air cooled raw sample. This material was sieved through the series of sieves by shaking for 15 minutes in a Ro-tap Shaker. Each sieve fraction was weighed and retained for sedimentation analysis.

Fifty random particles were taken from each sieve fraction using a specially constructed microsplit as described by Otto (17). Each particle was timed through a fall of 50 cm in a glass fall-column filled with water. The time of fall was determined with a ten-second-sweep stop watch giving the time to the nearest 0.01 sec. The particles were allowed to fall 25 cm before the timing was begun to insure that the particle had attained terminal velocity.

The fall-column consisted of a large glass graduate 5.08 cm in diameter. The ratio of the particle diameter to the diameter of the tube was less than 0.06 in all cases. However, the boundary was close enough so that its influence should not be ignored. Based on a study reported by McNown et al (13), a 1% boundary correction factor should have been applied. A graph giving the correction to be applied is shown in Fig. 4.

It is necessary that the viscosity be constant throughout the fluid column so that the viscous stress on the particle will be constant after the particle has accelerated to terminal velocity. No attempt was made to control either the temperature of the water or the temperature of the air surrounding the fall column. The temperature of the water was measured at the center of the column and half-way down at the beginning and end of each group of runs. If these two temperatures differed by more than 1.0°F, the data were not used and the runs were repeated. The temperature just outside the tube was also kept within 1.0°F to insure that the transverse viscosity pattern in the tube was sufficiently uniform to insure the desired accuracy.

The average fall velocity of each sieve fraction was computed from the values obtained for the 50 random particles. The standard deviation of the fall velocities was computed for each sieve fraction.

The specific gravity of a 25 cc sample of each sieve fraction was determined by the standard method described in ASTM D 854-45T.

Results:- Serr used the data to compute the Reynolds number Re and the Drag Coefficient C_D for each sieve

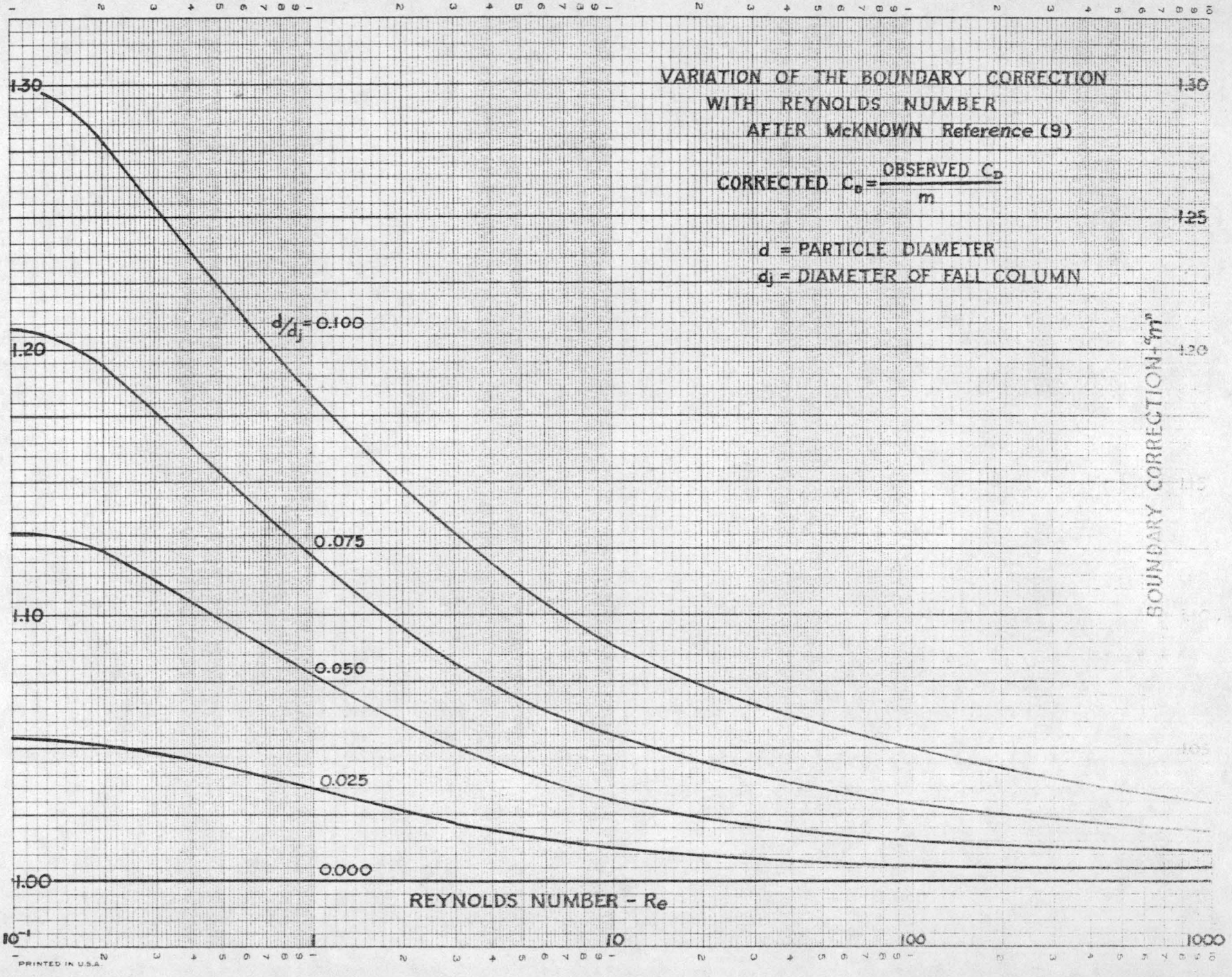

Fig. 4

fraction using these formulae:

$$Re = \frac{\rho_f \bar{w} \bar{d}_n}{\mu}$$

$$C_D = 4/3 \frac{(\rho_p - \rho_f) g \bar{d}_n}{\bar{w}^2 \rho_f}$$

These data for each sieve fraction and sample were plotted on the $Re:C_D$ graph. Lines of constant size (slope -2) were drawn through each group of experimental points representing each sieve fraction. These straight lines were extended to intersection with the line for spheres. This intersection gives values Re_o and C_{Do} for the mean sedimentation diameters of each sieve fraction. Serr stated that the ratio of C_{Do} at the intersection to C_D determined from the fall velocity data yields a ratio of sedimentation diameter d_o to the sieve diameter d_n for that particular sieve fraction[a]. From this ratio d_o/d_n the sedimentation diameter can easily be computed. Serr's analysis is slightly in error here. He spoke of lines of constant fall velocity, but used lines of slope -2 which Malaika pointed out are lines of constant size.

Malaika

Materials:- Under the direction of Dr. John S. McNown, Malaika conducted a series of experiments using 25 steel particles of 12 regular geometric shapes. With the exception of one steel ball bearing, all the particles were specially machined for the investigations. The different shapes and geometric ratios are tabulated in Table 4.

Table 4

List Of Particle Shapes Used by Malaika

Shape	Length - diameter ratio or Length - side ratio		
	1/4	1	4
Spheroids	1	1	1
Circular cylinders	1	1	1
Square prisms	1	1	1
Double-cones	1	1	1

[a]

$$\frac{C_{Do}}{C_D} = \frac{\frac{4(\rho_p - \rho_f) g \bar{d}_o}{3 \bar{w}_f}}{\frac{4(\rho_p - \rho_f) g \bar{d}_n}{3 \bar{w}_f}} = \frac{\bar{d}_o}{d_n}$$

Six different fluids were used consisting of two natural mineral oils furnished by Standard Oil Company of California, three synthetic oils furnished by the Standard Oil Company of Indiana and a mixture of two of the last three oils. These fluids exhibited a range of kinematic viscosity of from 0.00004 to 0.3 ft^2/sec at ordinary room temperature.

Equipment and procedure:- Each particle was dropped in each of the six different oils thereby producing a wide range of Reynolds number. The fall-column was set in a water bath and consisted of a lucite pipe 0.68 ft in diameter and 1.5 ft long. The water was heated by an immersion coil. Current to the heater was controlled by an electronic relay. A 13-in. by 13-in. by 21-in. tank was used for the water bath. This tank was made from glass supported in an angle iron frame and was insulated on the outside by 1/2-in. celotex. Openings were left in the insulation for photographic and lighting purposes.

Prior to dropping, the particles were held in the desired position just under the surface of the fluid by a point of an electromagnet. Position of the particle prior to dropping could be altered by changing the relative position of a small plastic ring surrounding the tip of the electromagnet.

The fall velocity of each particle was obtained from successive images on a photographic film. The experiment was set up in a darkened room. Photographs were obtained using an f-2.8 Robot or an f-2.7 Mercury II camera. The shutter of the camera was opened for the entire run and the particle was lighted for short intervals regularly spaced in time by a Strobolux driven by a Strobotac. Fall velocity computations were made by observing the number of time intervals (images of the particle) required for the particles to travel a known distance. This equipment was perfected by McPherson (15).

The two most viscous oils lacked sufficient transparency to use the photographic method of measuring the fall velocity. Therefore, a 10-second-sweep stop watch was used to measure the time required for the particle to travel a known distance. All measurements using this stop watch were repeated four times. The average of the four readings was recorded. The maximum deviation from the mean was less than 1% in all cases. The distance of fall was determined by a white-face steel tape placed at the line of fall of the particle and photographed. The particles were placed in an electro-magnetic release mechanism and a ten-minute period was allowed for all disturbances caused by placing the particle to be damped out.

The specific gravity of the particles was determined by weighing relatively large pieces of the stock in air and then

in distilled water at known temperature. Each individual particle was weighed to the nearest 0.0001 gm on a chain-o-matic balance.

The specific gravity of the oils was determined with a Mohr-Westphal balance hydrometer. The viscosity of the fluids was determined for a range of temperature of from 25 - 35°C using a Hoepler precision viscosimeter.

Results:- Malaika investigated extensively the stable falling position of the particles. These findings have been discussed in Chapter III.

The technique of changing the viscosity of the oil resulted in data covering a large range of Reynolds number ($0.0001 < Re < 1400$). Malaika's data are given in Appendix E.

Corey

Materials:- Corey obtained data from four samples of sand. The sources of the materials are tabulated in Table 5.

Table 5

Sources of Sand Samples Used by Corey

Sample	Type	Source
1.	River bed material	Cache la Poudre River near Bellvue, Colorado
2.	River bed material	Middle Loup River at Dunning, Nebraska
3.	Rock crusher fragments	Rock crusher near Bellvue, Colorado
4.	Wind blown sand	Dune at LaPorte, Colorado

Corey limited his observations to the sand grains between the Tyler Number 4 and 14 sieves (5 mm to 1.2 mm). He also chose only particles of quartz and feldspar. Photographs of Corey's samples are shown in Fig. 26.

Equipment and procedure:- Corey used Tyler Standard Sieve Numbers 4, 8, 9, 10, and 14 to divide his samples into size groups. Each sample was sieved for 15 minutes in a Ro-tap Shaker. Ten particles were chosen from each sieve fraction. The a, b, and c dimensions of these particles were measured using an ocular micrometer. Particles were placed on a glass slide using a pair of tweezers. The long (a) and intermediate (b) axes were measured by orienting the glass slide parallel to the micrometer scale. The shortest axis (c) was then measured by grasping the particle with a pair of

tweezers and turning 90° on edge and then measured with the micrometer.

Each particle was weighed to the nearest 0.1 milligram on a chain-o-matic balance. Since only quartz or feldspar particles were used, the specific gravity of the particles was assumed to be the average published value for these minerals - 2.65.

The temperature of the fluid (water) was measured before and after each run. It varied not more than 1°F. during the entire experiment. Since the investigation was carried out in the furnace room in the basement of the Hydraulics Laboratory where the air temperature was nearly constant at 69°F, the constant-temperature water bath designed by McPherson and later used by Malaika was not necessary.

The fall-column consisted of a rectangular tank 10 in. by 11 in. by 21 in. high. Three sides and the bottom were made of plywood painted flat black. The fourth side was made of polished plate glass. Glass and plywood were cemented to a welded angle-iron frame.

The fall velocity was measured by obtaining successive images of the particles on photographic film as they settled through the water. A 3 1/4 x 2 1/4 Speedographic press-type camera was used. The experiments were conducted in a darkened room and the particles were lighted at regular intervals for an instant by a Strobolux powered by a Strobotac. In general the apparatus was similar to that designed by McPherson. Corey experienced difficulty in obtaining satisfactory photographs for the smaller particles (1.5mm) which he studied because the light reflected from the particles was insufficient to expose properly even Dupont High Speed Pan Type 428 (ASA exposure index 200) at a lens opening f-3.5.

Corey also reported difficulty from oscillation of the particles about the straight falling path. Since the camera had a very limited depth-of-field when the lens was set at f-3.5, and 22 in. from the expected fall path, the particles moved in and out of the range where a sharp image could be obtained. This oscillation also caused some error in the distance measurements.

The particles were placed between the points of a pair of tweezers fixed at the surface of the water. The particles were handled with a second pair of tweezers. Each of the particles was placed in the fixed tweezers with the greatest cross section in the horizontal plane. The larger particles were released just above the surface of the water while the smaller ones had to be released below the surface because the

surface tension was great enough to hold the particles on the surface. All particles dropped about 12 cm before they entered the field of the camera. Acceleration to terminal velocity was accomplished in this distance.

Results:- Corey was concerned about the particles which traveled in an irregular path as they settled through the water. Tests were repeated on several particles to obtain an estimate of the degree of error to be expected in the measurements of fall velocity. These findings are tabulated in Table 6.

Table 6

Estimated Error Caused by Particles not Falling in a Straight Line

Type of particles and motion	Percent deviation
Small particles falling in a straight line	0.6%
Irregular particles falling continuously within depth of field	5%
Irregular particles falling partly outside focused range of camera	10%

In interpreting his results, Corey found that best correlation of the shape factor parameter ($c/\sqrt{ab}$) existed when the drag coefficient and Reynolds number were defined as

$$C_D = \frac{F/d_n^2}{\rho_f w^2/2}$$

and

$$Re = \frac{wdn}{\nu} .$$

He first attempted to use

$$C_D = \frac{F/ab}{\rho_f w^2/2}$$

and

$$Re = \frac{wb}{\nu} .$$

The data obtained by Corey for natural quartz and feldspar particles covered a range of Reynolds number from 200 to 2500 and shape factor from 0.21 to 0.95. Corey's data are presented in Appendix D.

Wilde

Materials:- Recognizing the limited range of Reynolds number investigated by Corey, Wilde studied the behavior of the larger, gravel-sized particles falling with a Reynolds number greater than 2,500. He obtained gravel particles from three sources. Table 7 lists the types and sources of the gravel particles studied by Wilde. Photographs of these samples appear in Fig. 27.

Table 7

Types and Sources of Gravel Studied by Wilde

Sample	Type	Source
1.	Gravel stock pile	A selected sample to obtain extreme shapes
2.	River bed material	Cache la Poudre River near Fort Collins, Colorado
3.	Rock crusher fragments	Rock crusher near Fort Collins, Colorado
4.	Lateral moraine	Rocky Mountain National Park, Colorado

Equipment and procedure:- Wilde's samples were divided by sieving into size groups using Tyler Standard Sieves Size 1 in., 3/4 in., 1/2 in., 3/8 in., No. 4 and No. 6. The samples were sieved in a Ro-tap Shaker. A representative sample of 10 particles was chosen from each sieve fraction by a method of pure chance.

The three mutually perpendicular axes were measured using a vernier micrometer. Because of the irregular shape of many particles, the longest dimension was often not obvious. To make all measurements in directions which were mutually perpendicular was also rather difficult. For these reasons, duplicate measurements of the shape of a particular particle varied sometimes as much as 5% from the mean. Wilde also measured the maximum projected area. This was accomplished by placing the particle in a pair of tweezers in such a position that the shadow of the particle fell on a cross-ruled translucent screen. The area was measured by counting the squares within the shadow area. The position of the particle for maximum area was determined by visual observation.

Each particle was weighed to the nearest milligram on an analytical balance. The specific gravity of each particle was obtained by weighing the particles submerged in distilled water while suspending them with a fine wire. It was found necessary to stabilize the action of surface tension on the suspension wire by adding a trace of detergent to the water. Before the detergent was added to the water, the surface tension caused erratic and severe damping of the balance and made accurate weighing impossible.

Wilde's fall-column consisted of a lucite tube 10 in. in diameter and 10 ft long. During the latter part of the experiments, a glass tube made of the glass bowls from salvaged old-fashioned gasoline pumps was substituted for the lucite tube. Initially the fall-column was filled with Fort Collins City water and later filled with oil. A fall-column which is round in cross section was to be desired because the round fluid column acted as a lens and magnified the particle in the horizontal plane to aid in observing the particles.

For measuring the fall velocity, Wilde used a variation of the photographic method suggested by McPherson and used by Malaika and Corey. Since Corey had difficulty with particles passing in and out of focus if they travelled an irregular fall path, Wilde devised a method of overcoming this difficulty. He used a smaller lens opening (f-4) and set his camera at a greater distance (7 ft) from the expected fall path. This gave him sufficient depth of field, and also a somewhat larger field of vision, which permitted the particle to be timed for a longer period than Corey or Malaika. He used a Kodak 35 camera and Plus-X film (ASA exposure index 50). Illumination was provided by a No. 4 photo flood lamp placed above the fall-column. The beam of light was concentrated by a "liquid" lens made by filling a convex dish of lucite with water and placing between the light and the fall-column. To obtain periodic exposures of the falling particle, a revolving desk with four equally spaced slots was placed directly in front of the camera. The revolving disk was made by gluing a circular piece of cardboard onto a phonograph turntable which was placed on edge. The speed of the revolving disk was checked several times and was found to vary not more than 1%. The shutter was opened only during the interval in which the particle was in the field of view of the camera. This reduced the exposure of the field in general and produced sharper and more clearly defined pictures. The photograph was identified by a card bearing the particle number in the photograph during the test run.

A graduated scale was placed beside the tube so that it was photographed with each falling particle. The scale was made slightly distorted to exactly compensate for refraction

when the particle fell in the center of the tube. A mirror was also placed alongside the tube so that the position of the particle relative to the center of the tube at any point of its descent could be observed and the velocity corrected accordingly. When the particle fell at the extreme front of the fall-column the observed velocity was reduced by four percent. Similarily, an increase of four percent was required when the particle fell at the rear. A general view of the apparatus except for the camera is shown in Fig. 5.

The average temperature over the section of the tube in which velocity measurements were taken was recorded to the nearest 0.5 degree F for each run. This was done by suspending a thermometer in the tube, near one side and in the center of the camera field of view. At first, temperatures were taken along the entire length of the test section but, when it was found there was little variation, this practice was discontinued. Heating of the fluid at the top by the photo-flood light was prevented by the "liquid" lens.

When the film had been developed the negatives were placed in a standard photographic enlarger and measurements were made directly on the projected image. With this method accurate measurements were obtainable and the cost was less than five cents per negative. A sample of the type of results obtained by this method is presented in Fig. 27.

When all the particles had been dropped two or three times in water, the water was removed, and the tube was shortened to about seven feet and filled with oil. The oil used was a light, colorless, pure mineral oil designated by the Texas Oil Company as Texaco White Oil A and had an S.A.E. rating of approximately five.

For the series of tests in which the particles were dropped in oil, no dropping mechanism or camera was used. Instead, the particles were released by hand and timed with a stop watch. Experience showed that when flat particles were dropped with the dropping mechanism they entered the oil edgewise and as a result tended to oscillate during the first two or three feet of fall before they became stable with their projected areas perpendicular to the direction of motion. For this reason the dropping mechanism was discarded in favor of hand placing the particles in their most stable position.

The velocity of most of the particles was sufficiently low to accurately measure, with a stop watch, the time required for them to travel 100 cm. Since the stop-watch method is much faster than the photographic method it was used exclusively for the oil phase of the experiment. However, some of the larger particles tested fell faster in the oil

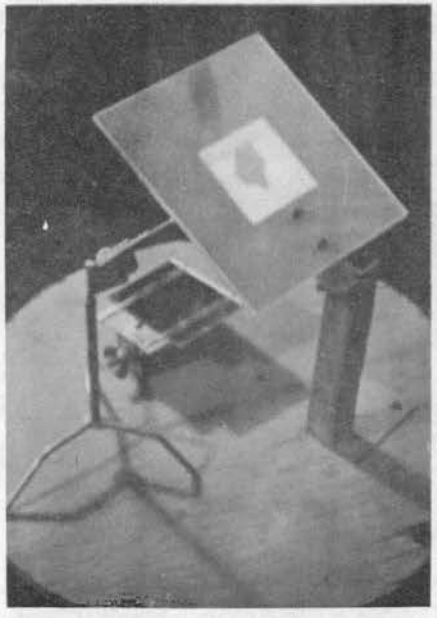

Equipment used for measuring the projected area of the particle.

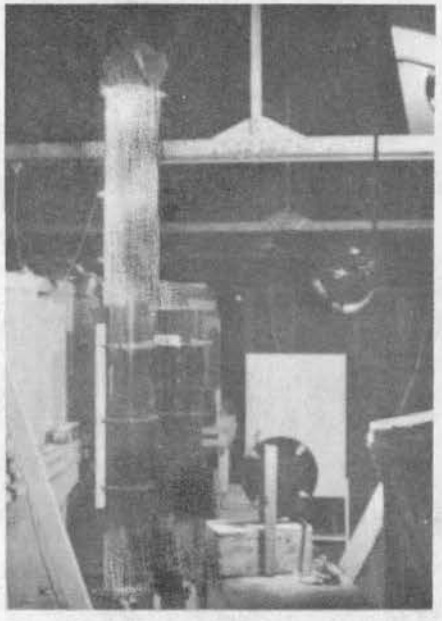

10 inch lucite fall-column.

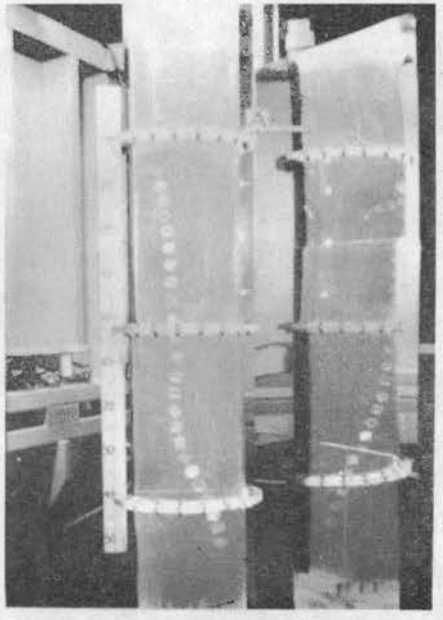

Photograph of falling lucite cube including view from right (Mirrors at right.)

PHOTOGRAPH OF WILDE'S EXPERIMENTAL EQUIPMENT

Fig. 5.

than in water and the velocity data for them is probably subject to considerable error, because the error in measuring the fall velocity of particles moving fast is greater than for the particles moving slowly. Particles would move faster in oil if the drag coefficient for the particle in oil was less than for the same particle in water. Some of Wilde's data occurred in the range where this was true.

The standard published data for the viscosity of the water were used (See Fig. 1). The viscosity of the oil was measured using a Saybolt Viscosimeter.

At higher Reynolds numbers, many of the particles struck the sides of the tube, in all cases these data were discarded.

Results:- Wilde obtained data for the gravel particles falling in water between Reynolds number 1000 and 25,000 and for the gravel particles in oil between Reynolds number 4 and 200. At the higher Reynolds number the fall-path was erratic and deviated greatly from the basic assumption that the motion must be only in the vertical direction. This erratic nature was due in part to the eddies formed in the wake of the particles and the turbulence associated therewith. The degree of error under these conditions is doubtless considerable.

Wilde found that the rock crusher fragments gave significantly higher drag coefficients for a given shape factor than the other samples. The probable reason for this difference was the fact that the crusher fragments were rough and angular while the other samples were smoother and rounded, having been worn and polished by the abrasive action of the stream. Therefore, angularity and possibly surface roughness have an important influence on fall velocity which the shape factor does not take into account.

Schulz

Materials:- A majority of the sediments causing problems in hydraulic engineering today occur in the smaller size ranges. Therefore, Schulz set out to study the shape characteristics of the small size natural sediments (1/5 mm to 1.5 mm). This is in the range of Reynolds number 1 to 300. A sample of spherical glass beads was tested as a standard and a number of sediments from natural deposits was used to represent natural material. These sediments are tabulated in Table 8. Photo-micrographs of these samples are shown in Fig. 28.

Table 8

Types and Sources of Sand Studied by Schulz

Sample	Type	Source
1.	Glass spheres/1	
2.	Crusher fragments/1	Rock crusher near Fort Collins, Colorado
3.	River bed material	Wolf Creek below Fort Supply Dam, Oklahoma
4.	River bed material/2	Arkansas River at Lamar, Colorado
5.	River bed material/2	Loup River near Dunning, Nebraska
6.	River bed material/2	Cache la Poudre River near Fort Collins, Colorado
7.	River bed material/2	Alder Creek in Yosemite National Park, California
8.	River bed material/2	Colorado River at Yuma, Arizona

/1 Incomplete size range.
/2 Data obtained only on shape factor and mineral type.

These sands originate from widely separated geologic and geographic origins. No attempt was made to choose only certain mineral types; therefore, the data can be used to study the distribution of the mineral types in these sediments.

Equipment and procedure:- Schulz sieved his samples through Tyler Standard Sieve Numbers 12, 14, 16, 20, 24, 28, 32, 35, 42, 48, 60, and 65 in order to establish size-groups. Oven-dried and air-cooled samples were sieved for 15 minutes in a Ro-tap Shaker.

The three mutually perpendicular axes were measured using a specially-constructed microscope. The particles are placed on a piece of glass 3 in. wide and 36 in. long and moved about by sliding with a pointed brass rod. Since a great deal of hazard of losing was involved in handling the particles needlessly, the microscope was adapted to move on a ball-bearing carriage over the glass sorting table. The glass table was carefully adjusted until in the same plane as the carriage rails. A microscope was made from a discarded Leitz tube, a 32 mm Bausch Lomb objective lens, and a 10x Bausch Lomb eyepiece fitted with a biological eyepiece micrometer. The eyepiece micrometer was calibrated after the apparatus had been assembled using a standard stage micrometer. The microscope was also fitted with a Starrett dial indicator reading to 0.0001 in. This was used to measure the

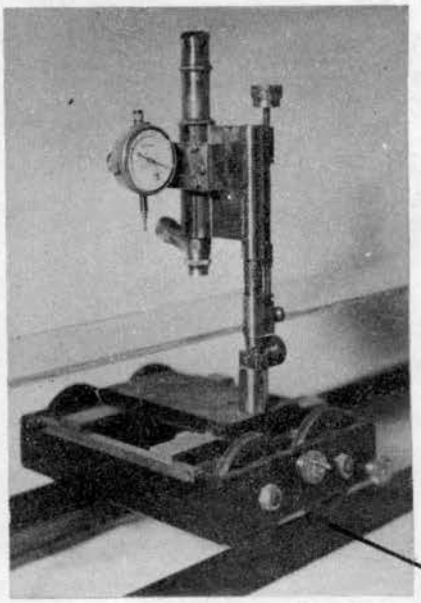

Detail of Microscope & Carriage

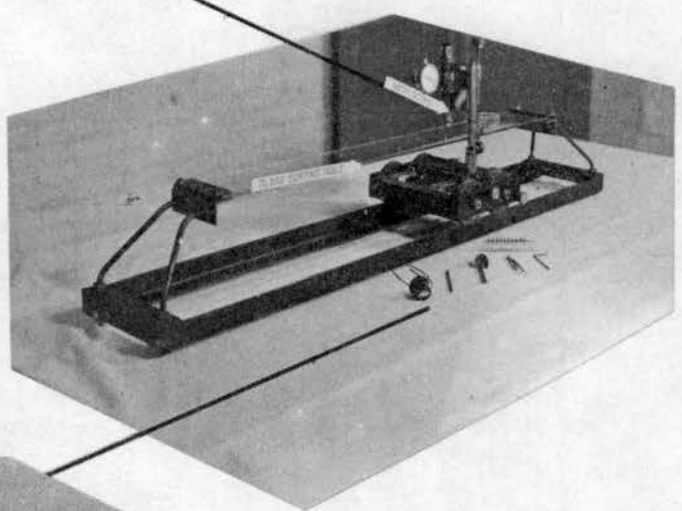

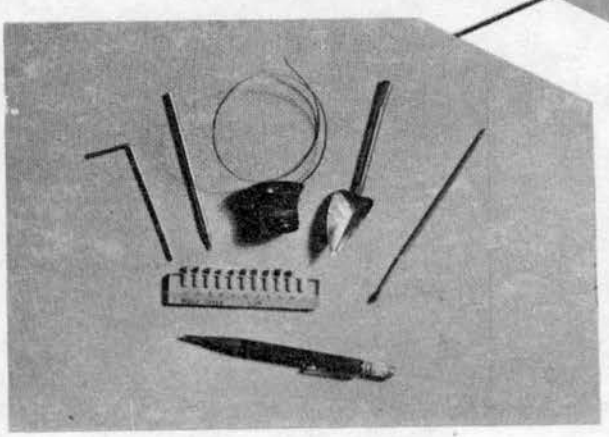

Detail of Equipment Used
For Handling Particles

MICROSCOPIC MICROMETER & RELATED EQUIPMENT

Fig. 6

thickness or "c"-axis. Fig. 6 is a photograph of this microscopic micrometer. The procedure for measuring the shape was as follows:

1. The sieve fraction was reduced to about 500 particles by quartering.

2. The remaining part was placed in a single line on the sorting table.

3. The sample was further reduced by choosing every fifth (or some other convenient number) particle until the sample was reduced to 10 representative paeticles from the entire sieve fraction.

4. The ten particles were oriented to their most stable position by tapping the table several times.

5. The microscope was moved over the particles and the eyepiece rotated until the major axis of a particle was parallel to one set of the coordinates of the micrometer grid.

6. The a and b axes were measured.

7. The carriage was then moved until the stem of the dial indicator could be brought down carefully on the sand grain. In this manner the remaining "c" axis was measured.

8. The particle was carefully swept into a small brass scoop with a camel's hair brush and stored for further processing.

The fall-column was constructed of cast lucite 6 in. in diameter and 72 in. long. The bottom was a sloping sheet of lucite. A small drain was located at the bottom of this slope. As the particles reached the bottom of the tube, they could easily be sluiced out with about one ounce of water.

The particle-release mechanism consisted of a series of 1/4 in. diameter glass tubes 4 in. long which were "drawn out" to smaller tip openings. The tip openings were approximately 3/4 mm, 1 mm, 1.5 mm and 2.5 mm. The size used was controlled by the "a" axis of the particle to be dropped. This dropping tube was held by a spring loaded clip in such a manner that the small opening was just below the surface of the water in the fall-column. The opening of the tip was closed off by a round steel wire approximately 1 mm diameter whose axis was normal to the longitudinal axis of the dropping tube. For releasing the particle this wire was

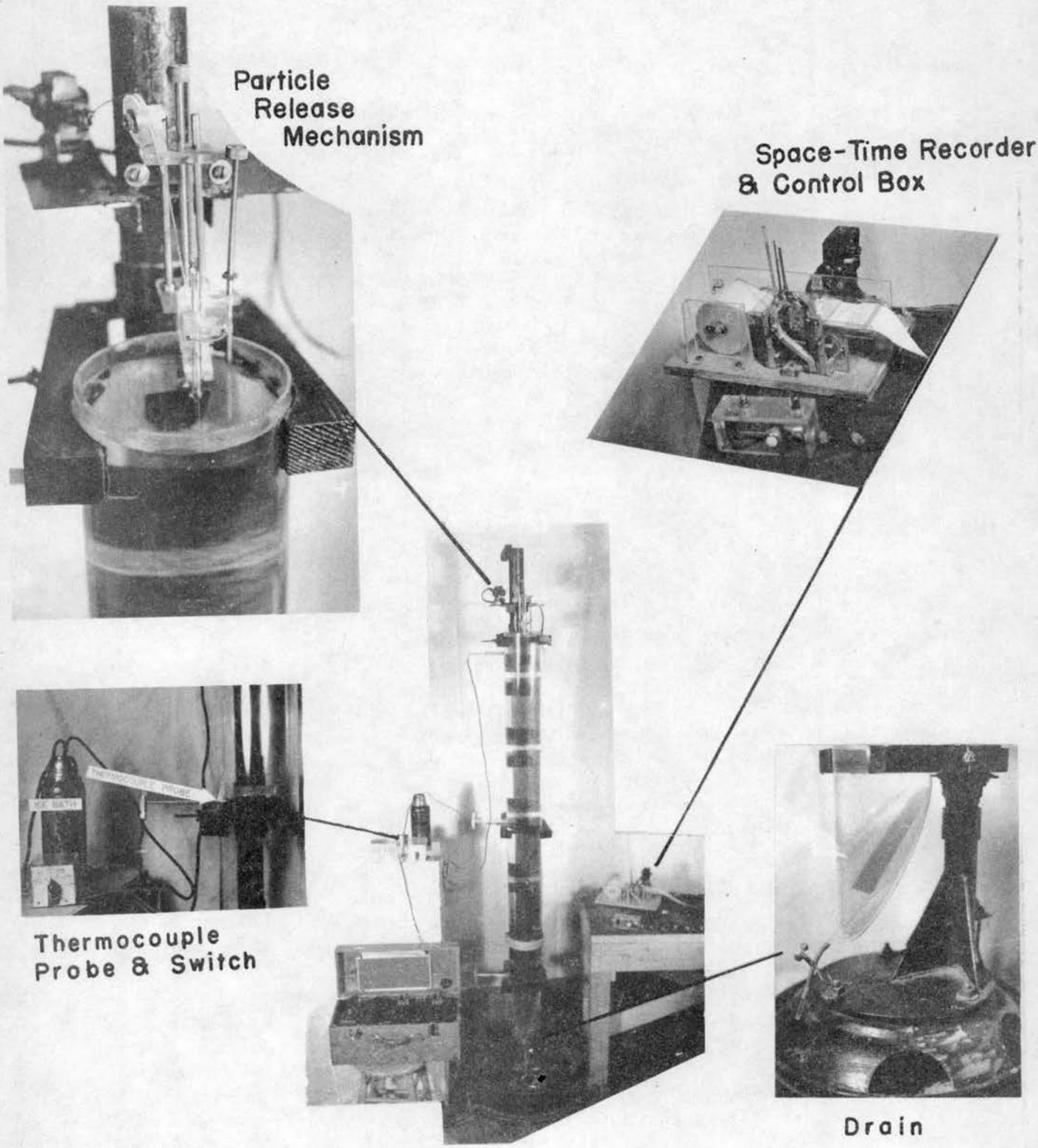

FALL COLUMN & RELATED EQUIPMENT

Fig. 7

moved first down and then to the side allowing the particle to settle in the fluid. The wire was operated by an electric solenoid.

No attempt was made to control the temperature of the water. Copper-constantan thermocouples made from B and S No. 30 wire and mounted on a 1/4-in. diameter round lucite rod were located approximately 12, 36, and 55 in. from the top of the fall-column. The round lucite rod was set in the side of the fall-column through a water-tight seal and the probe could be moved into the water column to measure the transverse temperature variation which was never greater than 0.5°C.

Illumination of the column was provided by a 200-watt spot-bulb located outside the room and about 2 ft directly above the fall-column. Light was admitted into the room through a glass-covered hole in the ceiling.

The column was divided into five 30-cm measuring courses and one 15 cm accelerating course at the top. These positions were marked on the surface of the tube by scribing a fine line in front of the tube. This scribed line was filled with green paint and a mirror was fastened to the back of the tube opposite these lines. The time when the particle crossed the plane of each line and its reflected image in the mirror was observed visually and transmitted to the space-time recorder by closing an electrical contact. Sufficient accuracy was obtained because the fall velocity of these smaller particles was never greater than 17 cm/sec. A specially designed space-time recorder was used to record the data. Date were recorded on ordinary adding-machine tape drawn through the recorder by two rollers driven by a phonograph motor. The tape speed could be varied from approximately 3/8 in. to 2 in. per second by adjusting the governor. Normally a tape speed of 1/2 in. per sec was used.

Data were fed into the recorder as electrical signals which operated any one of three electrical solenoids. The solenoids each moved a ball-point pen causing a break in a normally straight line. One of the pens received a time signal every second from a clock. A second pen received a position signal from the position switch-button which was on the small control box in the hand of the operator. A third pen was operated by the run-cancelling, switch-button which was also on the control box. This button was depressed whenever the run or part of the data were to be discarded. Such occasions were when the particle oscillated badly or when the particle touched the side of the tube. In this manner poor data were clearly marked and there was no danger of such data being used by mistake.

Switches for operating the particle-release mechanism and the space-time recorder were also mounted on the control box. This was necessary so that the operator could easily control the entire run while giving his undivided attention to the falling particle and its behavior.

Each particle was weighed to the nearest 0.0001 gm using an Ainsworth semi-micro balance. It was necessary to know the weight of the particle in order to compute F in the drag coefficient.

The volume of each particle was determined by dropping the particles one at a time in a serological pipette, which was partially filled with water, and observing the rise of the water surface. Two pipettes were used depending on the length of the b-axis of the particle. One pipette had a uniform bore of 1 mm and the other 2 mm. The fluid used in the pipette was water to which 5% Aerosol and 5% fluorescein dye had been added in order to nullify the effects of surface tension and make the fluid more visible. A small amount of the fluid was drawn into the pipette and the pipette closed with a rubber tube and pinch-cock as shown in Fig. 8. The pipette was mounted in a clamp on a ring stand and the water surface in the pipette was observed with the microscope previously described. The particle was introduced at the top of the pipette and pushed to the water surface with a fine wire. This was necessary because the inside surface of the pipette and the particle was always wet and caused the particle to stick. The volume of the particle was computed from the rise of the water surface caused by introduction of the particle in the water. This method of volume determination was unreliable when the rise of the water surface was very small (about 0.1 of a scale unit on the micrometer.)

Results:- Schulz was handicapped in the interpretation of his data. While the fall velocity and shape factor data were obtained with satisfactory precision, the reliability of the drag coefficient depends upon the accuracy of the particle weight and volume determinations.

Since the particle volume was probably known with a higher degree of accuracy, it was decided to use this particle volume and an assumed specific gravity. Because the specific gravity of the glass spheres could not be assumed with any degree of certainty (because of inclusion of minute air bubbles), the data for the glass spheres were not used. For the natural minerals, the apparent weight of each particle was computed using the measured volume and the regularly published value of the specific gravity for that particular mineral. These data have been tabulated in Appendix G, Table 14.

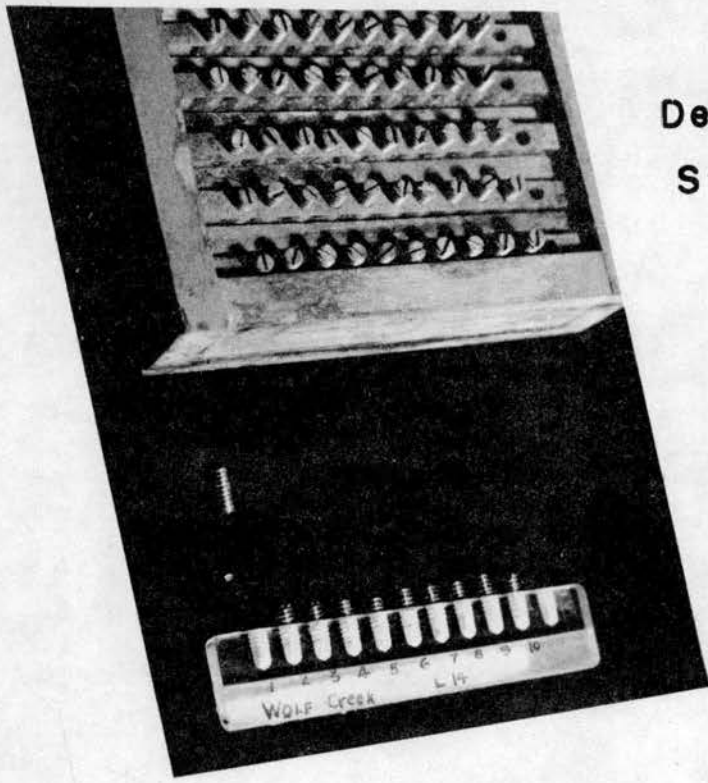

Detail of Particle Storage Facility

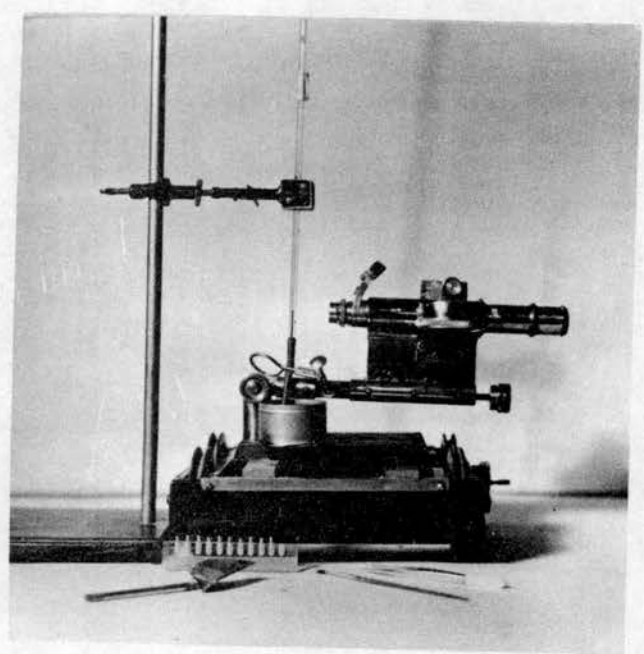

VOLUME MEASURING EQUIPMENT

Fig. 8

The data on the shape factor were used to study the variation of shape factor with sieve size and mineral type. Some correlation between shape and sieve size was observed when the average shape factor for a given sieve size was used. The average shape factor for all the particles from a particular sieve fraction was plotted on a graph (Fig. 18) against the sieve diameter. Also shown is an average curve for all sieve fractions from all sources.

Chapter V

DISCUSSION OF RESULTS

Scope of experiments

These experiments have presented considerable data supporting the use of some form of shape parameter. The primary purpose of this report is to consider the adequacy of the Corey shape factor $c/\sqrt{ab}$ and to use the shape factor to relate sieve diameter and sedimentation diameter. Also the report has collected considerable additional information regarding the extent of variation of the shape factor in natural sediments.

Choice of the shape factor parameter

Since the standard procedure in fluid mechanics is to use projected area for the term A in the drag coefficient $2F/A\rho_f V^2$, Fig. 9 was plotted on that basis. The shape factor used as the third variable in this plot was the dimensionless area ratio, $\pi d_n^2/4A$. The lines of average shape factor were drawn in by eye as the best fit to the data. The second trial for correlation between shape and fall velocity is represented in Fig. 10 in which the shape factor is $c/\sqrt{ab}$, ab is used for A in the drag coefficient, and c as the length measure in Reynolds number in place of d_n.

Comparison of Figs. 9 and 10 reveals that they are very similar in all respects. As was stated, the average shape factor lines were drawn in as the best fit to the points. However, there are many points on both figures which do not fit. For example, in Fig. 9 two different particles, each having a shape factor of 0.77, have values of drag coefficient of 0.66 and 1.19 respectively at Reynolds number between 4×10^3 and 9×10^3. The difference in the drag coefficient represents 50 percent of the complete range at that Reynolds number.

The data shown in Figs. 9 and 10 indicate that at high Reynolds numbers low values of shape factor tend to be associated with high values for the drag coefficient which is as would be expected. For Reynolds numbers below 100, the lines of constant shape factor all tend to converge to the line for spheres.

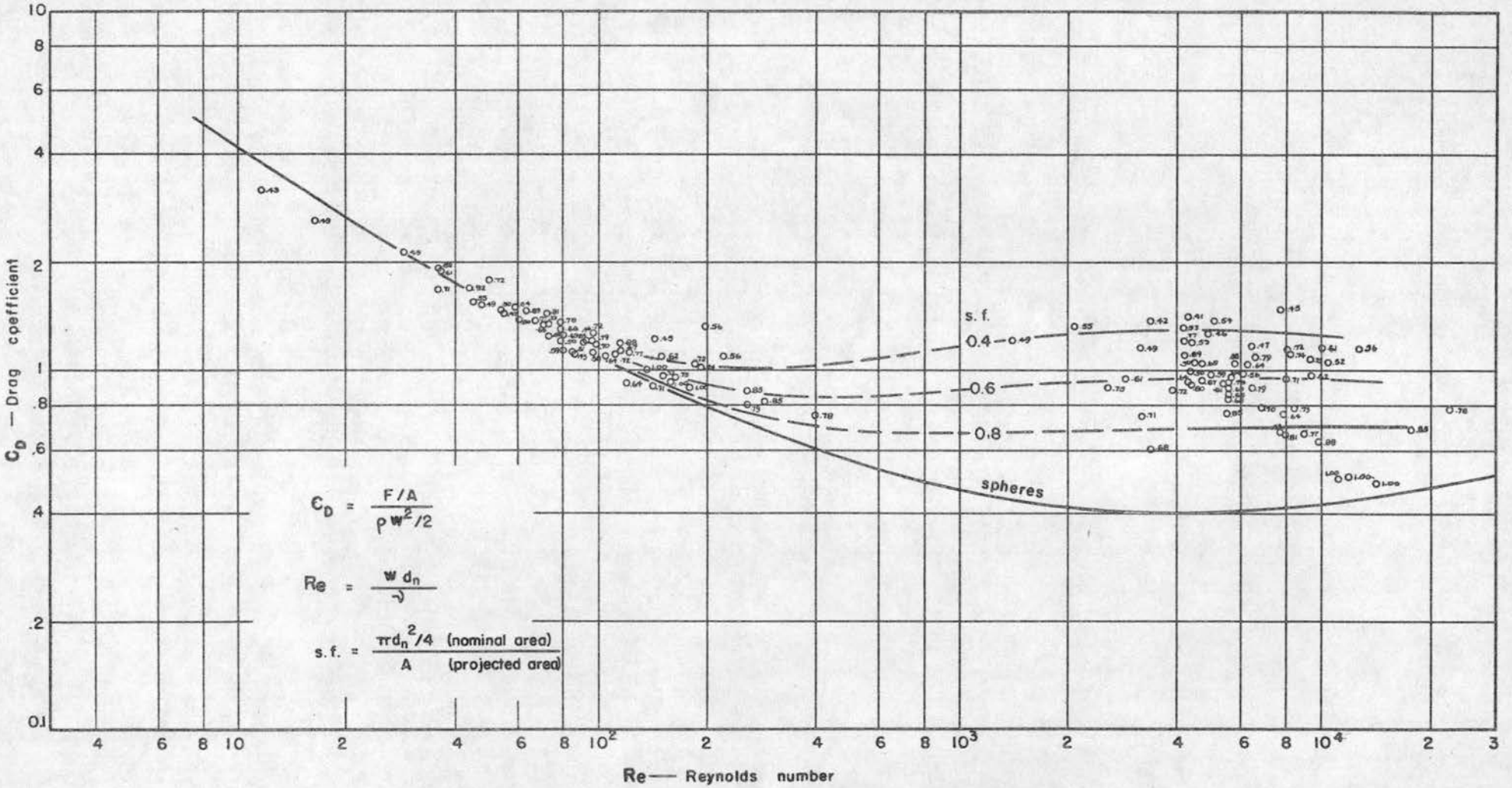

Influence of Shape on Drag Coefficient for Random Sample

Fig. 9

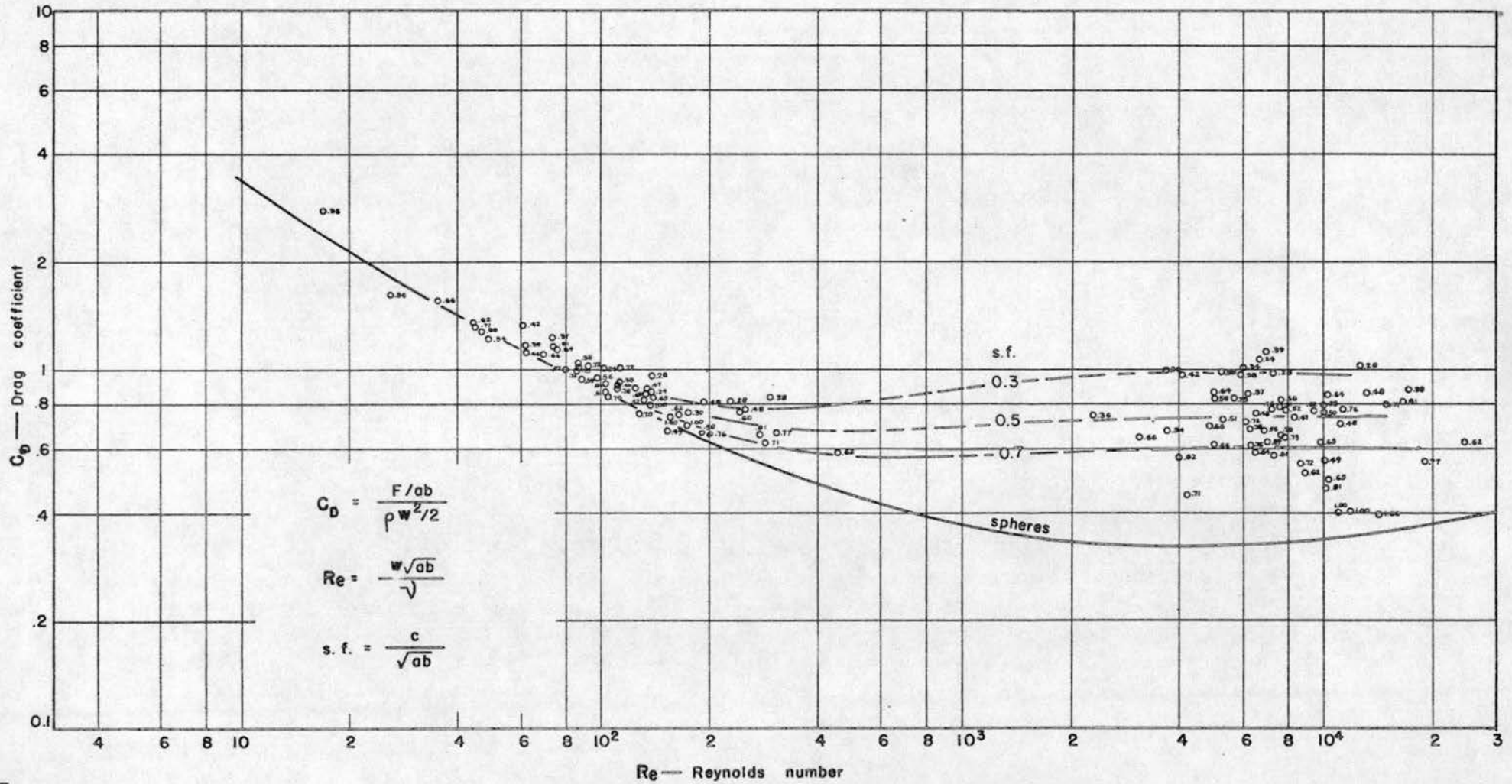

Fig. 10

Influence of Shape on Drag Coefficient for Random Sample

After this fact was indicated by the plots of the data, careful consideration and a more thorough review of the literature revealed the probable reason. The numerator of the drag coefficient is the ratio between submerged weight and projected area. Submerged weight is a function of particle volume. Knowing projected area, the approximate value of particle thickness to give the actual particle volume can be computed. In other words, the numerator of the drag coefficient is in itself a measure of particle flatness or a shape factor. Therefore, the effect of shape is largely already taken into account by the drag coefficient and a second shape factor has little significance at low Reynolds numbers.

At high Reynolds numbers there is a second factor influencing the drag coefficient -- namely, fluid separation in the wake of the particle. The degree of separation, and hence the influence on the drag coefficient, depends again on particle shape. Therefore, as a result of the phenomenon of fluid separation the shape factor has some significance at high values of Reynolds number but little significance at low values of that number.

Evaluation of shape factor:- At this point a choice was made between the two shape factors investigated. The time required to measure the mutually-perpendicular axes of the particles was considerably less than that required for measurement of projected area using the present technique. This matter of time required to make measurements is a very important consideration if the shape factor is to be practical. The product ab is a good indication of projected area. More information about the particle is obtained by measurement of the axes lengths than by a measure of projected area -- for example, the length to width ratio may be important. Since both showed about the same degree of correlation with drag coefficient, one could not be chosen as more significant than the other. Because of the other advantages obtained by measurement of the axes lengths compared with the measurement of the projected area, the shape factor $c/\sqrt{ab}$ was considered the more practical of the two and therefore was used in the remainder of the investigation.

Malaika (8) and Corey (3) suggested the use of the square of the nominal diameter in the drag coefficient to replace projected area. Fig. 11 is similar to Figs. 9 and 10 except that nominal diameter was used to compute drag coefficient. The use of nominal diameter had the effect of widening the range of values of drag coefficient covered by the data. Errors in individual points then became less noticeable. Also, the numerator of the drag coefficient was then the ratio of two factors based entirely on particle

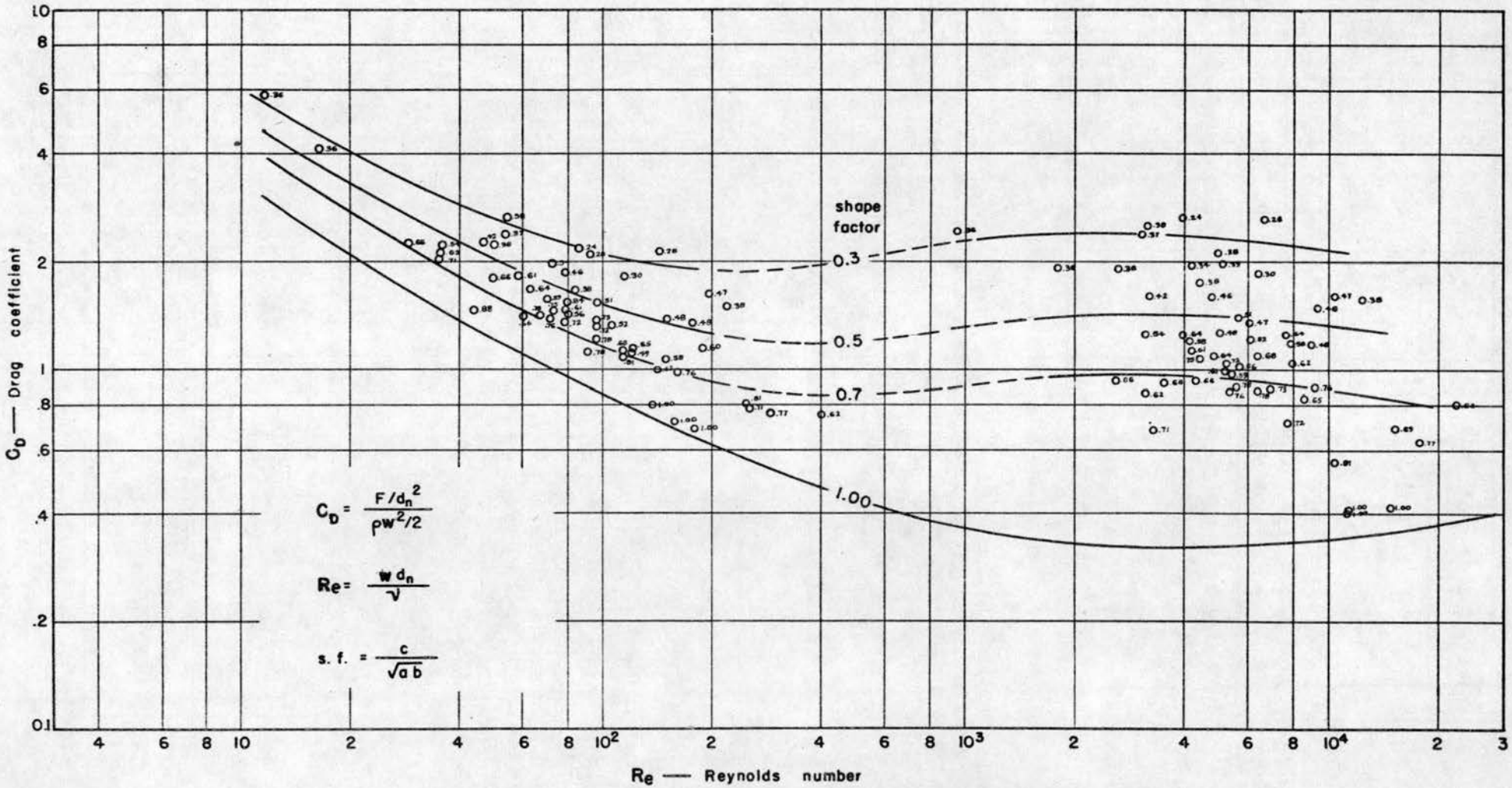

Influence of Shape on Drag Coefficient for Random Sample

Fig. 11

volume with the result that the drag coefficient did not include particle shape. This single fact greatly increased the significance of the shape factor at low Reynolds number.

Even at high Reynolds numbers the use of nominal diameter improved the correlation between drag coefficient and shape factor. For example, the data for two particles which had a shape factor of 0.48 were analyzed. When plotted with drag coefficient based on ab the values of the coefficient were 0.73 and 0.88. In the range of Reynolds number in which the above points lie, the complete range of drag coefficient was from 0.31 to 1.10 which includes a range in shape factor from 0.24 to 1.00. Thus, in this case the variation in the drag coefficient for two particles having the same shape factor was 19 percent of the total range of the coefficient when ab was used in the drag coefficient. When nominal diameter was used, however, the same data resulted in values of 1.23 and 1.52 in a region where the total range of drag coefficient was from 0.31 to 2.81. This amounts to a variation of 11.6 percent of the complete range of drag coefficient which is less than in the preceding case. For these reasons nominal diameter appeared to be the best dimension to use in the drag coefficient and further studies were made on this basis.

Study of Fig. 11 indicated that the drag coefficient remained nearly a constant in the range of Reynolds number between 10^3 and 10^5. As was pointed out in Chapter III and also by McNown and Malaika (10), the ratio a/b may be an important factor in describing shape. To study the importance of the a/b ratio, a graph of C_D:sf was made with a/b as the third variable (see Fig. 12). There was a lack of any trend in the data so that no definite conclusions could be drawn. However, in the lower portion of the curve there was an indication that higher values of the ratio a/b tend to result in an increased drag coefficient for particles with the same shape factor. Unfortunately, this type of plot may be made only in the comparatively narrow range in which the influence of Reynolds number is insignificant and for that reason the practical significance of a/b is questionable.

Two other factors describing shape, namely angularity and surface roughness were discussed in the theoretical analysis and discarded with the hope that for natural particles these factors would be essentially a constant value and could be neglected. A comparison of the results obtained by Wilde is shown in Fig. 13 where one may note that the drag coefficients for the crusher plant sample are larger than for the other samples. The photograph, Fig. 27, indicates the probable reason. The crusher-plant sample fragments were very rough and angular. Hence, one may infer that the two factors--angularity and roughness -- are of importance. However, the

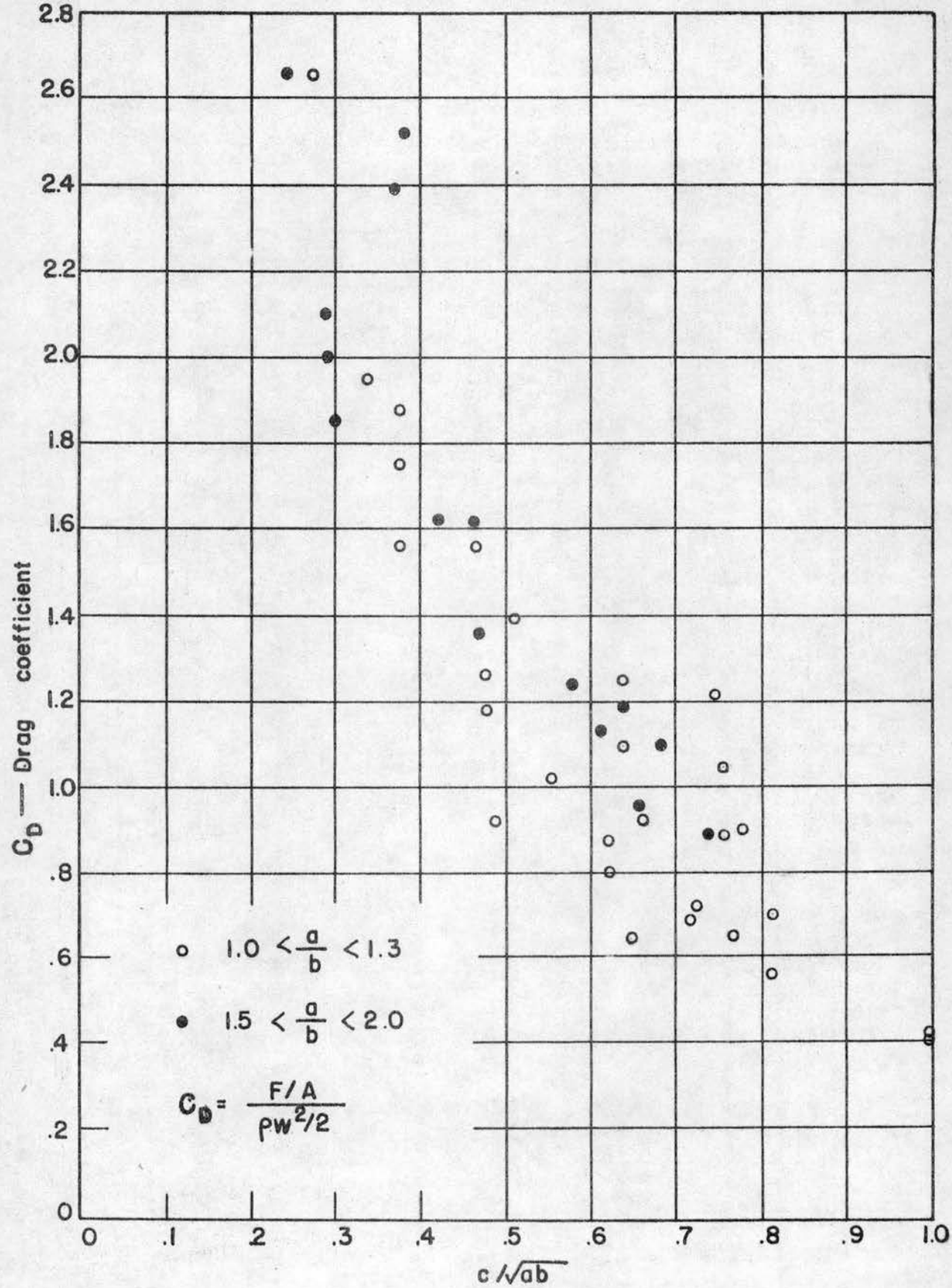

Effect of particle length on C_D.

Fig. 12

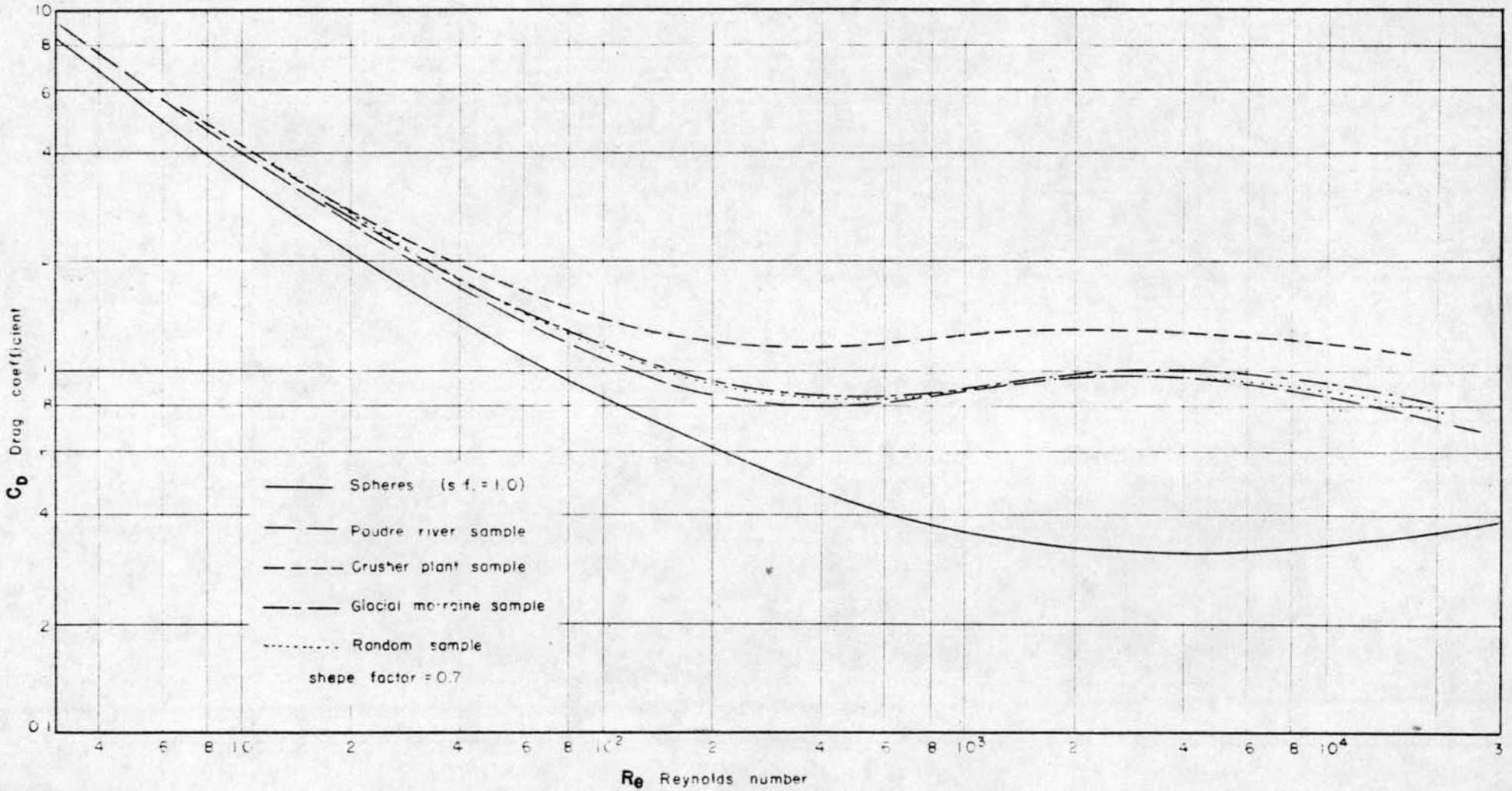

COMPARISON OF DRAG COEFFICIENT OF SAMPLES STUDIED BY WILDE

Fig. 13

other samples which were composed of natural particles (not modified by crushing) did produce results exactly comparable as is indicated by the rather small spread between the curves of Fig. 13. Therefore, in practice, the two factors, angularity and roughness, probably could be neglected except when those characteristics were very noticeable. In that case a small over-all correction could be applied to the measured shape factor to give results more nearly correct. A sample of the natural sediment in question may be compared with the photographs of the samples. The crusher fragments probably represent the extreme condition of angularity and roughness. Natural particles would range between the value of zero angularity (or roughness represented by smooth spheres) and the condition represented by crusher fragments.

The C_D:Re graph for natural particles

The data here presented indicate that the Corey shape factor can be employed to explain a significant part of the variation of the drag coefficient for a particular Reynolds number. All of the available data were reduced to the parameters of drag coefficient, Reynolds number, and Corey shape factor. The data were plotted on two composite C_D:Re graphs as shown on Figs. 14 and 15. Fig. 14 represents the composite graph for the rounded particles and sediments that have been well worn. The crusher fragments and angular particles have been plotted separately on Fig. 15, because Wilde has shown on Fig. 13 that this segregation is desirable.

The Corey shape factor also was computed for the particles used by Krumbein and Malaika. Because Malaika's particles were geometric shapes made from steel, the particle angularity could be varied over an extreme range for a particular shape factor. For example the shape factor of 1.0 could be for a sphere or for a double cone. Examination of the data discloses that the double cone whose shape factor is 1.0 behaves more like a natural particle of shape factor 0.6. For this reason Malaika's particles were further identified on Figs. 14 and 15. The four basic shapes were spheroids S, cylinders C, prisms P, and double-cones D (in order of increasing angularity). Because some of Malaika's particles were rounded and others were angular, all of his data were plotted on both Figs. 14 and 15. Lines of constant shape factor were drawn through the data giving careful consideration to the particle angularity and the general principles of laminar and turbulent flow. The undulations in each shape factor line in the range $500 < Re < 10{,}500$ can be explained as the migration of the line of separation on the surface of the particle. Characteristic of this range of Re is the wide scatter of the data which is typical of the turbulent conditions in the boundary layer around the particle and the

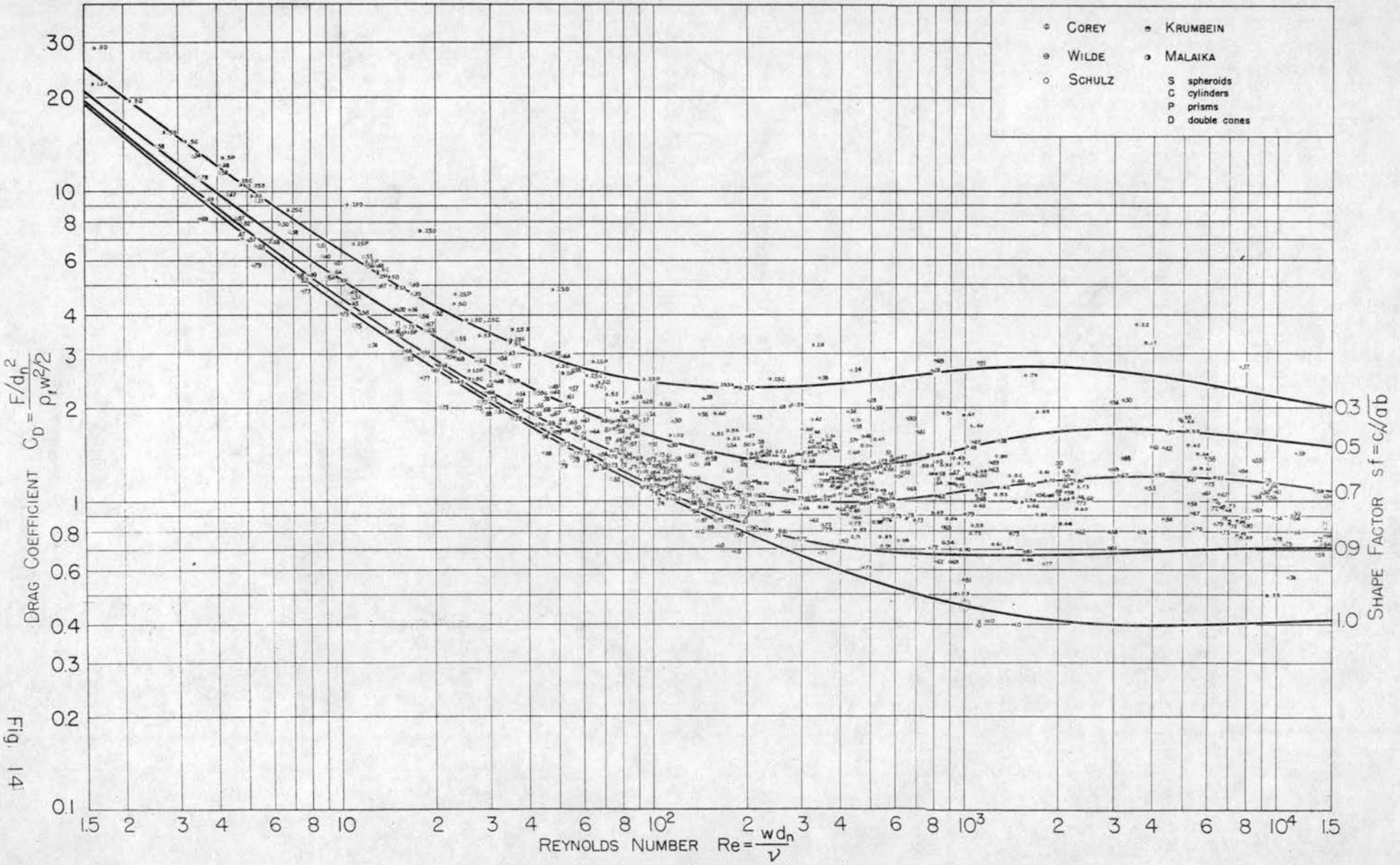

Fig. 14

C_D : Re GRAPH FOR NATURALLY WORN SEDIMENTS

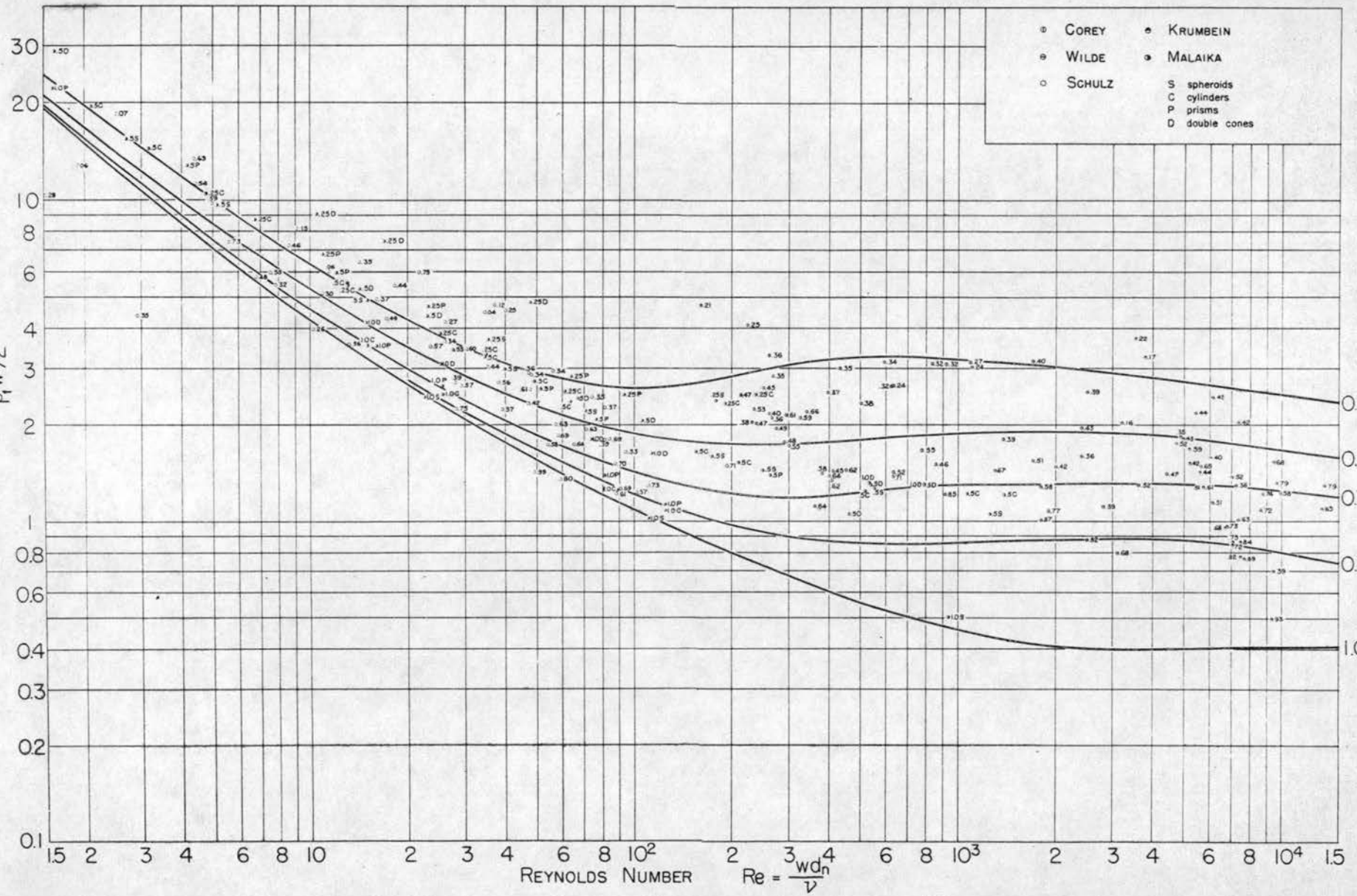

Fig. 15

C_D : Re Graph for Crusher Fragments and Angular Particles

large scale eddies in the wake of the particle.

The shape factor lines from Figs. 14 and 15 have been plotted on Fig. 3 and tables giving the drag coefficient for a particular shape factor, Reynolds number, and sample source are given in Appendix G.

It is interesting to note all of Krumbein's data fall generally on a line of slope -2 because all of Krumbein's particles were of constant size. This verified Malaika's statements about these lines and repudiates Serr's assumption that these lines of slope -2 should be used to determine the sedimentation diameter.

Variation in fall velocity of a particle

Because of the possibility of a single particle falling with different orientations, and hence different velocities, several runs were made to determine what variations existed with respect to the fall velocity of a single particle when it was dropped a large number of times. Several selected gravel-sized particles were dropped in both oil and water. The particles were selected to give a wide range of shape and surface roughness.

Results of this study revealed only small fluctuations in fall velocity for Reynolds numbers less than approximately 100. The data for Reynolds numbers less than 100 were obtained by dropping the particles in oil. For Reynolds numbers increasingly greater than 100, the variations in fall velocity from one run to another rapidly increased. Associated with this difference is the fact that $Re = 100$ is approximately the point where the orientation of the particles becomes unstable and oscillations develop. It was found that the stability of a particle depended upon the shape factor and Reynolds number. In some cases where the particles were unsymmetrical but had large shape factors, there was no stable position for Reynolds numbers greater than 100. These particles while falling would change their orientation frequently and continuously. Other particles having small values of the shape factor but an approximately symmetrical shape, were stable up to relatively high Reynolds numbers ($Re = 10,000$).

It is quite probable that the variation of the fall velocity could account for a large part of the scatter displayed by some particles on Fig. 14 and Fig. 15. The data used to compute the drag coefficient and the Reynolds number on Fig. 14 and Fig. 15 were based on single observations of the fall velocity. Time and resources were not available to conduct an adequate statistical investigation of the variation of the fall velocity of each particle.

Relation of fall velocity to shape factor and weight

A graph showing the correlation between fall velocity and the shape factor was used by Corey in his report. The requirement for this graph is that the viscosity must remain constant. All the available data for water temperature 69.5°F (20.8°C); ν = 0.0098 cm^2/sec were plotted on Fig. 16. Lines of constant shape factor can easily be drawn on this graph of fall velocity versus particle weight. The importance of shape factor in the fall velocity problem is apparent by considering the extent of the variation of the fall velocity. For example, assume a particle weight of 200 mg, the fall velocity of a sphere (sf = 1.0) would be more than 300% greater than the fall velocity of a particle whose shape factor is 0.35. For this same weight a particle whose shape factor is 0.85 would fall at twice the velocity of the particle whose shape factor is 0.35. In using Fig. 16, certain limitations should be kept in mind:

1. The graph is for a water temperature of 69.5°F only. If a similar diagram is desired for some other temperature, a new curve for the desired temperature must be computed using the dimensionless C_D:Re graph.

2. This graph is not valid for particles which fall at high velocities (greater than 30 cm/sec) and the secondary irregularities are important. If the particles are extremely rough (note the photographs of these samples), the C_D:Re graph for the crusher fragments must be used to construct a separate graph of fall velocity vs. particle weight.

Relation of shape factor to volume

If the product abc is an accurate measure of particle volume, the necessity of weighing each individual particle

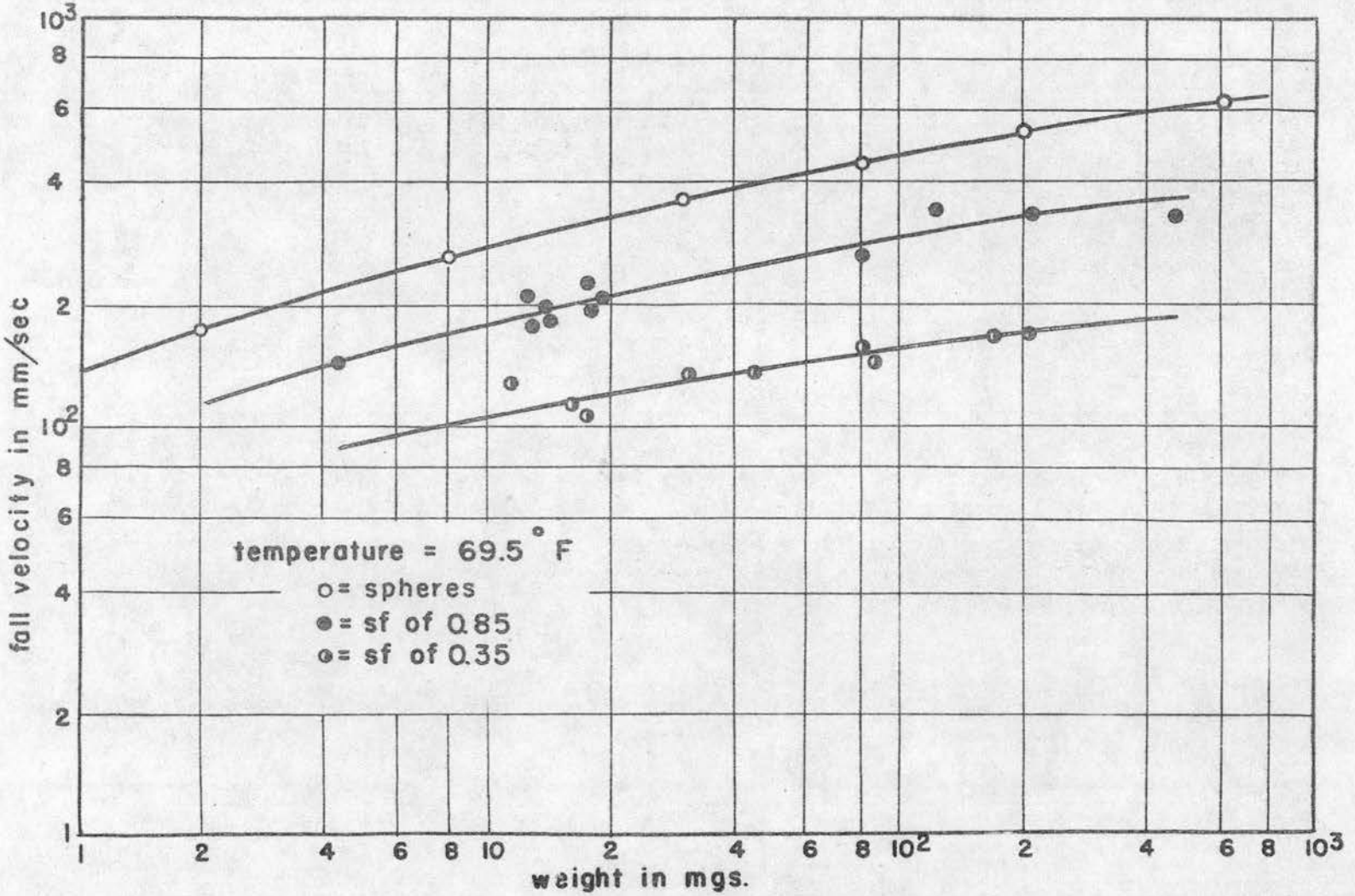

Fall velocity as a function of weight

Fig. 16

could be eliminated. Wilde and Schulz investigated this relationship from their data. A graph of abc vs volume for natural particles was prepared and is shown in Fig. 17. Two lines representing cubes and spheres were also added to this graph. The average value of the ratio of the volume to abc (volume/abc) for the natural particles was 0.49 and the average deviation was 15.8 percent. This large variation was considered too great to justify using abc as a measure of volume. For comparison purposes the theoretical lines for cubes and spheres were also drawn on the graph -- the cubes from the equation volume equals abc, and the spheres from the equation volume equals $\pi abc/6$. The curve for cubes is the extreme case in which volume equals abc and is obtained only by particles which are rectangular in three dimensions. The ratio between volume and abc for spheres is $\pi/6$ or 0.52 which, once again, is a close approximation of the data for natural particles.

Relation of shape factor to source of material

Serr reasoned that the most angular material produced in nature would be that material which was newly formed and for his investigations he chose material from a fresh talus slope. Corey, Wilde, and Schulz used rock crusher fragments as examples of the extremely rough case of natural material. It may be reasoned that as these newly formed materials are carried by water, wind or glaciers, they are constantly worn down -- becoming rounder and smoother. Therefore, a relatively "old" sediment should have a smooth appearance and the shape factor should tend toward a spherical particle (maximum volume for a given surface area).

Another example explaining this theory is mica. The mica particles are formed from laminae of mica scaling from the parent deposits. The thickness of these mica flakes is a characteristic of the parent deposit. At the formation of these mica flakes, the shape factor would be quite low because the particle is very thin. It may be reasoned further that after the particle undergoes the action of sedimentation the relatively large particle is divided into smaller ones but still maintaining its original thickness; therefore, the shape factor must be increasing during this wearing down process. Examination of Schulz's data yields some verification of this logical deduction concerning the mica.

Examination of the mineral types from the various sources disclosed the fact that mica is a small percent of the total (usually less than 10%); however, when it is present, the average shape factor is somewhat less for both the sample as a whole and for any particular sieve fraction. On the one hand, no mica was found in the Loup River sample and the

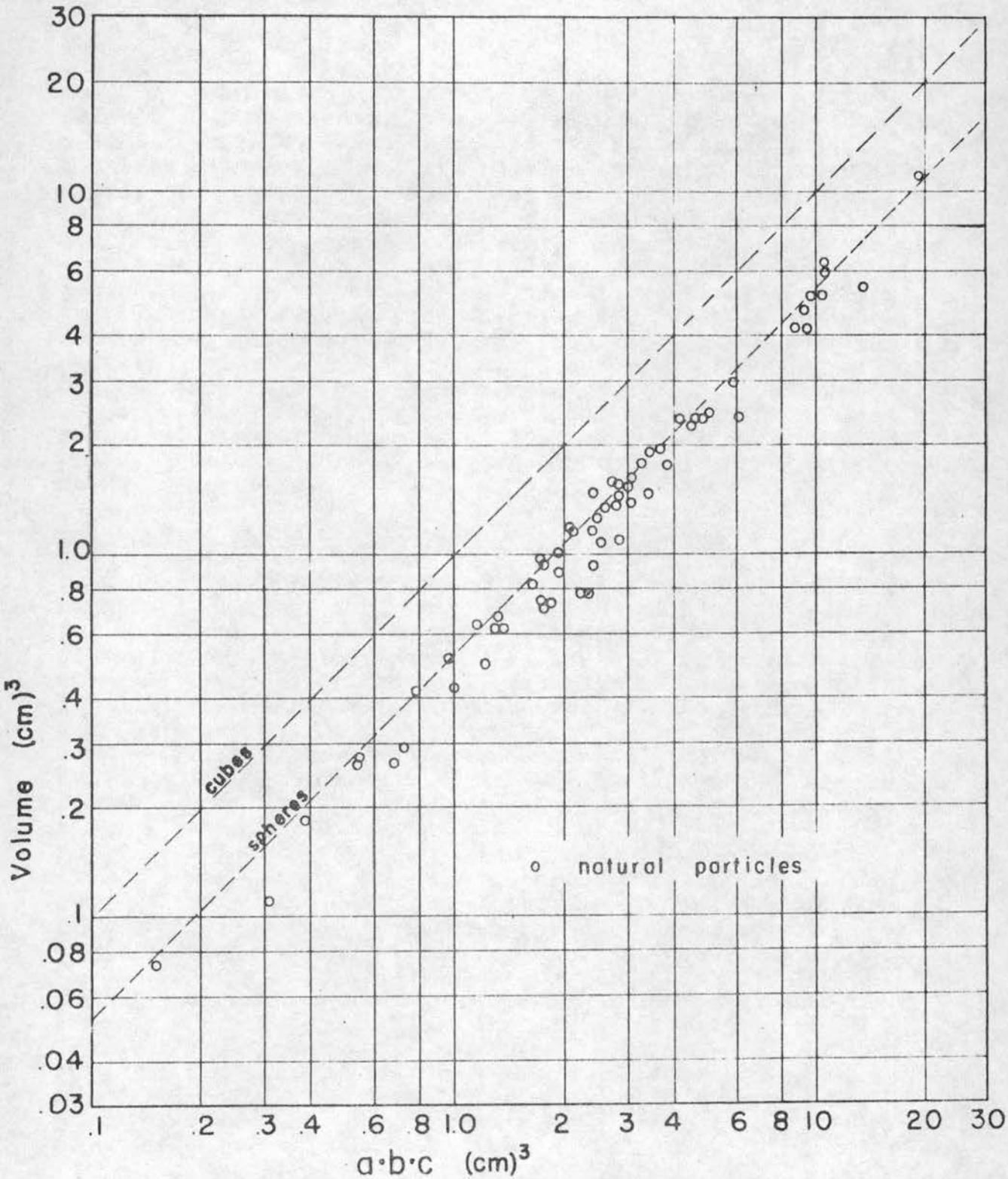

Relationship between volume and a·b·c

Fig. 17

average shape factor for the entire sample was 0.66. On the other hand, about 12% mica was found in the Alder Creek sample and the average shape factor for the entire sample was 0.56.

The data showing the distribution of mineral types, and average shape factor of the particles for each sample and sieve fraction are shown in Table 14 in Appendix G. A graph showing the average shape factor for each sieve fraction in each sample is shown in Fig. 18.

In this report the sieve fractions are always identified with the sieve on which they were retained. On the other hand the sieve diameter for a given sieve fraction is the size of the sieve opening of the passing sieve (the one preceding the retained sieve). A graph showing the intermediate axis as a function of the sieve diameter for the crusher fragments is shown on Fig. 19. Examination of this graph discloses that the intermediate axis is nearly always larger than the sieve opening. Since the sieve opening is a square, the largest possible sieve opening is not the diameter of the largest sphere which would go through the opening, but the diagonal distance across the opening. If the particles are very thin, the length of the intermediate axis could then be $\sqrt{2}$ times the sieve opening. This line is also plotted on Fig. 19.

Most of the points lie between the two lines $b = d_{sv}$ and $b = \sqrt{2}\, d_{sv}$. The points occurring to the right of the $b = \sqrt{2}\, d_{sv}$ line can be explained as errors in measuring the true "b" axis, a sieve which is "leaking" at the edge, a sieve having larger openings than specified, or poor sieving technique.

Relation of sieve diameter to nominal diameter

A graph giving the relation of the sieve diameter to the nominal diameter for the rock crusher samples studied by Corey, Wilde and Schulz is also shown on Fig. 19. Examination of this graph shows that a line of slope +1 ($d_{sv} = d_n$) could be assumed to represent the data. A majority of the data are enveloped by two lines -- $d_{sv} = 1.2 d_n$ and $d_{sv} = 0.8 d_n$. It is interesting to note that for the larger sieve sizes ($d_{sv} > 2$ mm) most of the data seem to fall to the left of the $d_{sv} = d_n$ line; whereas, for the smaller sieve sizes ($d_{sv} < 1.5$ mm) most of the data fall to the right side of the $d_{sv} = d_n$ line. Some of this might be explained as personal error since the data at the two extreme ends of this curve were obtained by different investigators.

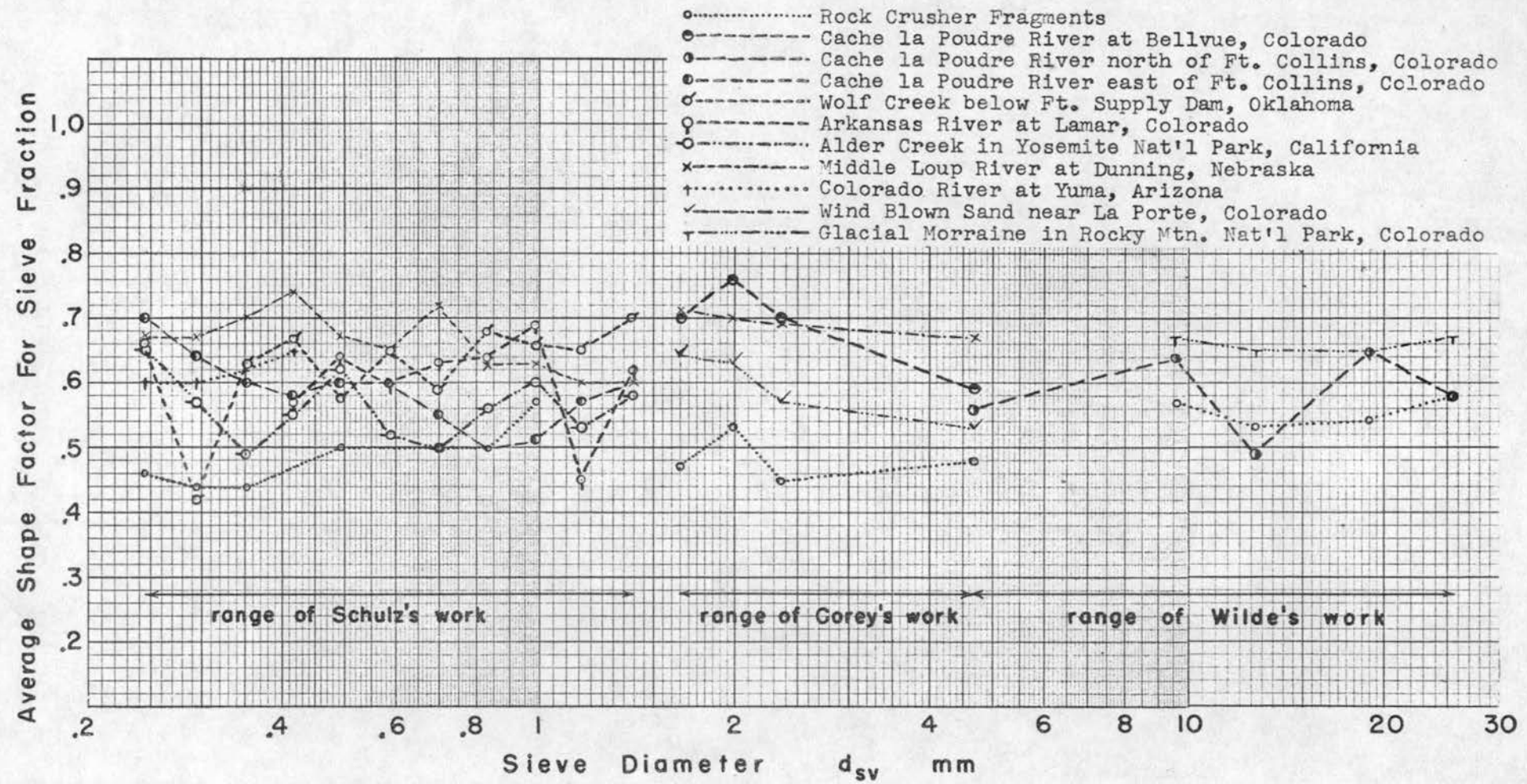

VARIATION OF SHAPE FACTOR WITH SIEVE SIZE

Fig. 18

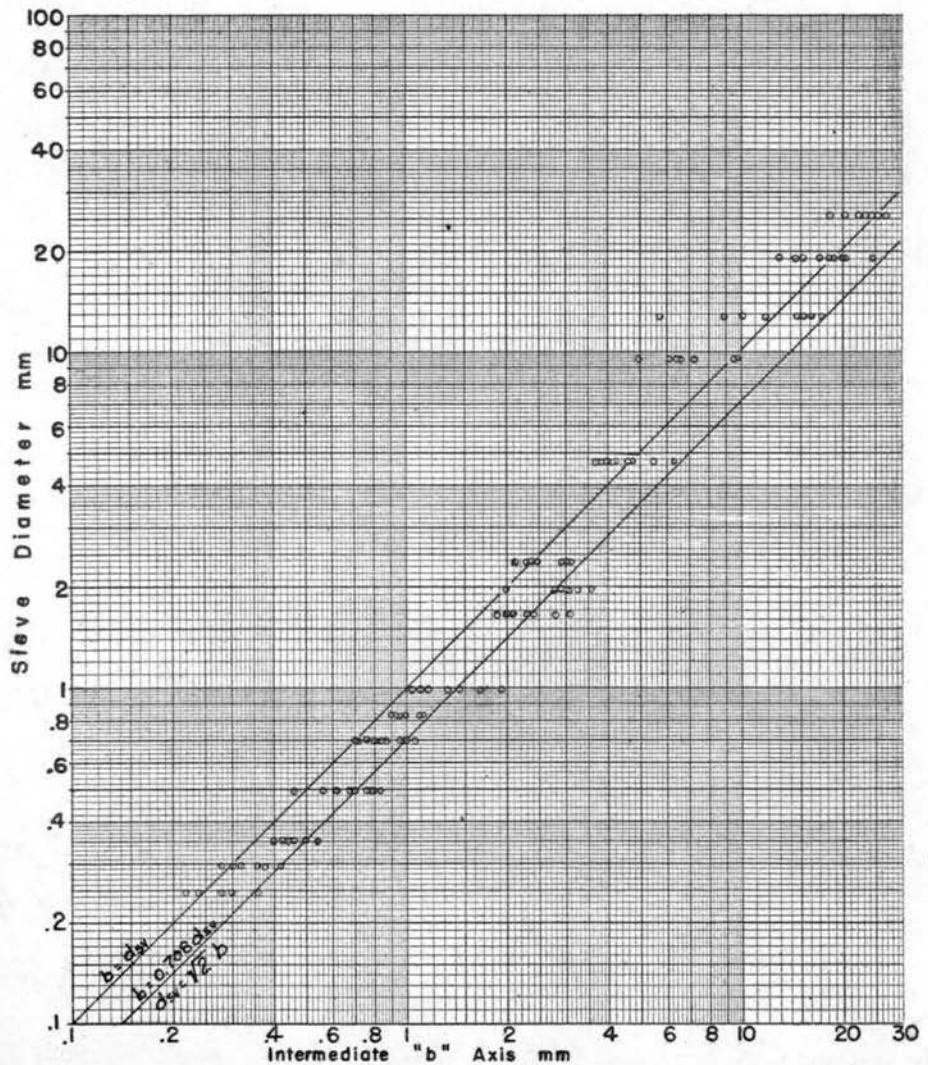

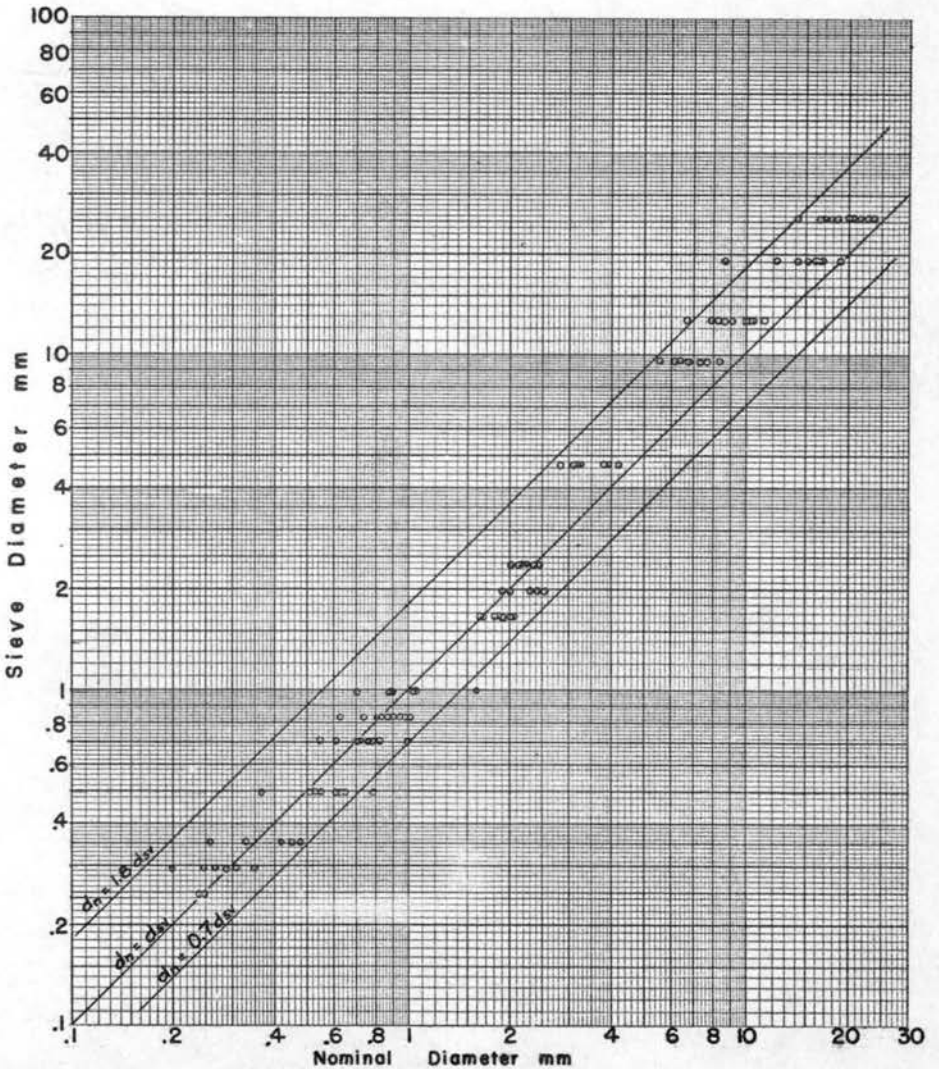

COMPARISON OF SIEVE DIAMETER WITH INTERMEDIATE AXIS AND NOMINAL DIAMETER

Fig. 19

The C_D:C_S graph for natural particles

It has been illustrated in Chapter III how lines of constant size at a slope of -2 could be superimposed on the C_D:Re graph. Each of these lines represents a constant value of the size coefficient:

$$C_S = F/\rho_f w^2.$$

This arrangement of the variables is useful in engineering problems where the fall velocity is unknown and to be determined. An example of this type problem is the determination of the critical scour velocity for certain bed material. To make this graph more useful, the C_D, C_S, and sf parameters have been transposed from Fig. 3, p 24 to Figs. 20 and 21. Since it has been necessary to differentiate between the rounded particles and the rough and angular particles on the C_D:Re graph, it is also necessary to make two graphs of C_D vs. C_S. Examples of the use of these graphs are in Chapter VII and tabular values are given in Table 17, Appendix G.

The C_w:Re graph for natural particles

Lines of constant fall velocity at a slope of +1 are superimposed on the C_D:Re graph (Fig. 3). This family of lines can be defined as

$$\frac{F\mu}{w^3 d_n \rho_f^2} = \frac{6\Delta\gamma\nu}{w^3\rho_f}.$$

The lines on Fig. 3 have been displaced by the constant $6/\pi$ and plotted as $\frac{\Delta\gamma\nu}{w^3\rho_f}$.

This arrangement of the variables is useful where the nominal diameter is unknown because the nominal diameter appears only in the Re parameter. To make this graph more useful, the C_w, Re, and sf parameters have been transposed from Fig. 3, p 24 to Figs. 22 and 23. Again it has been necessary to have two graphs -- one for rounded particles and one for angular particles. Tabular values of Figs. 22 and 23 appear in Table 18, Appendix G.

Relation of sieve diameter to sedimentation diameter

Sediment engineers have recognized a need for a method of relating sieve diameter to sedimentation diameter without actually having to measure the fall velocity, weight and volume of the particle. This has been made possible through

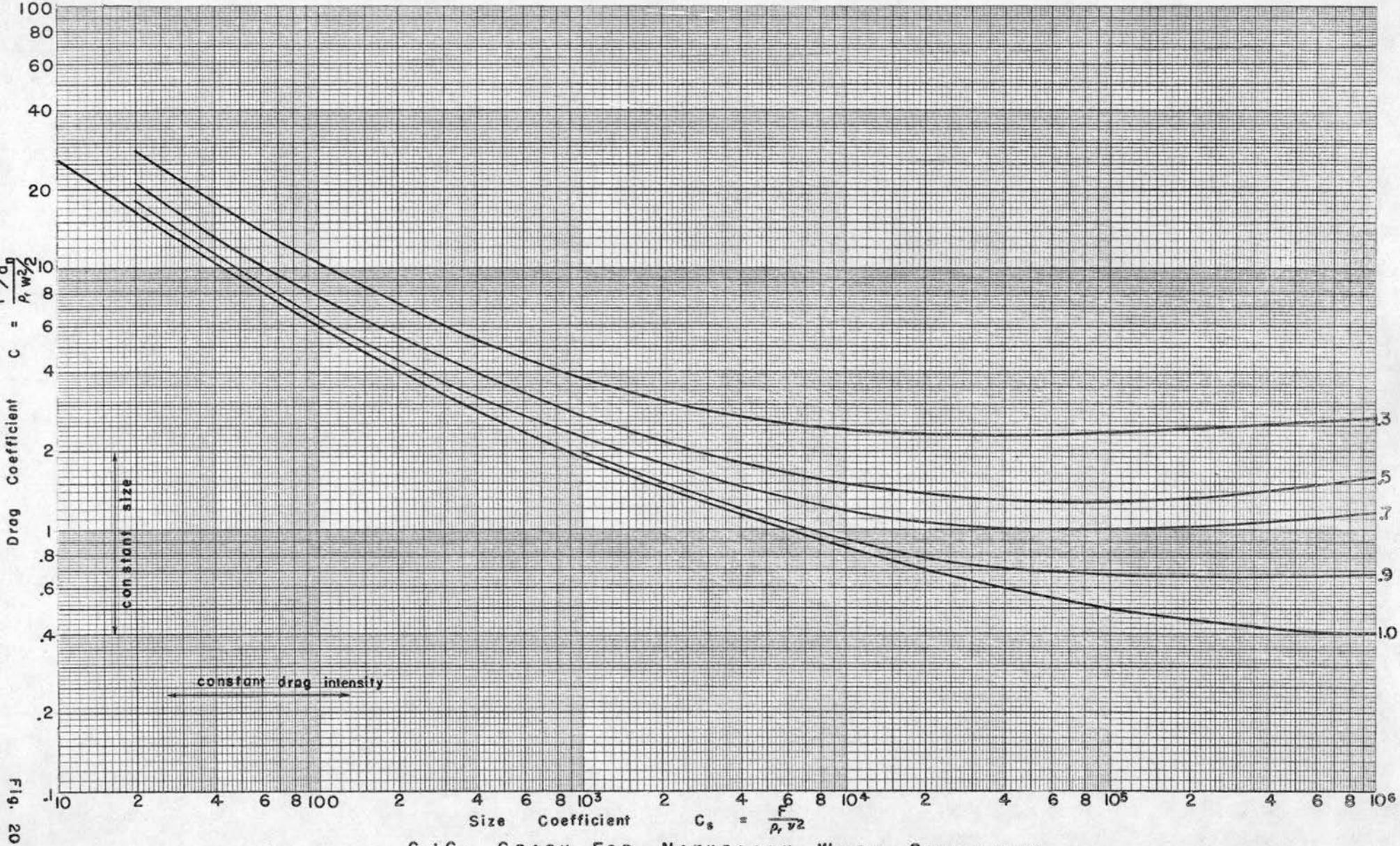

Fig. 20

$C_D : C_S$ GRAPH FOR NATURALLY WORN SEDIMENTS

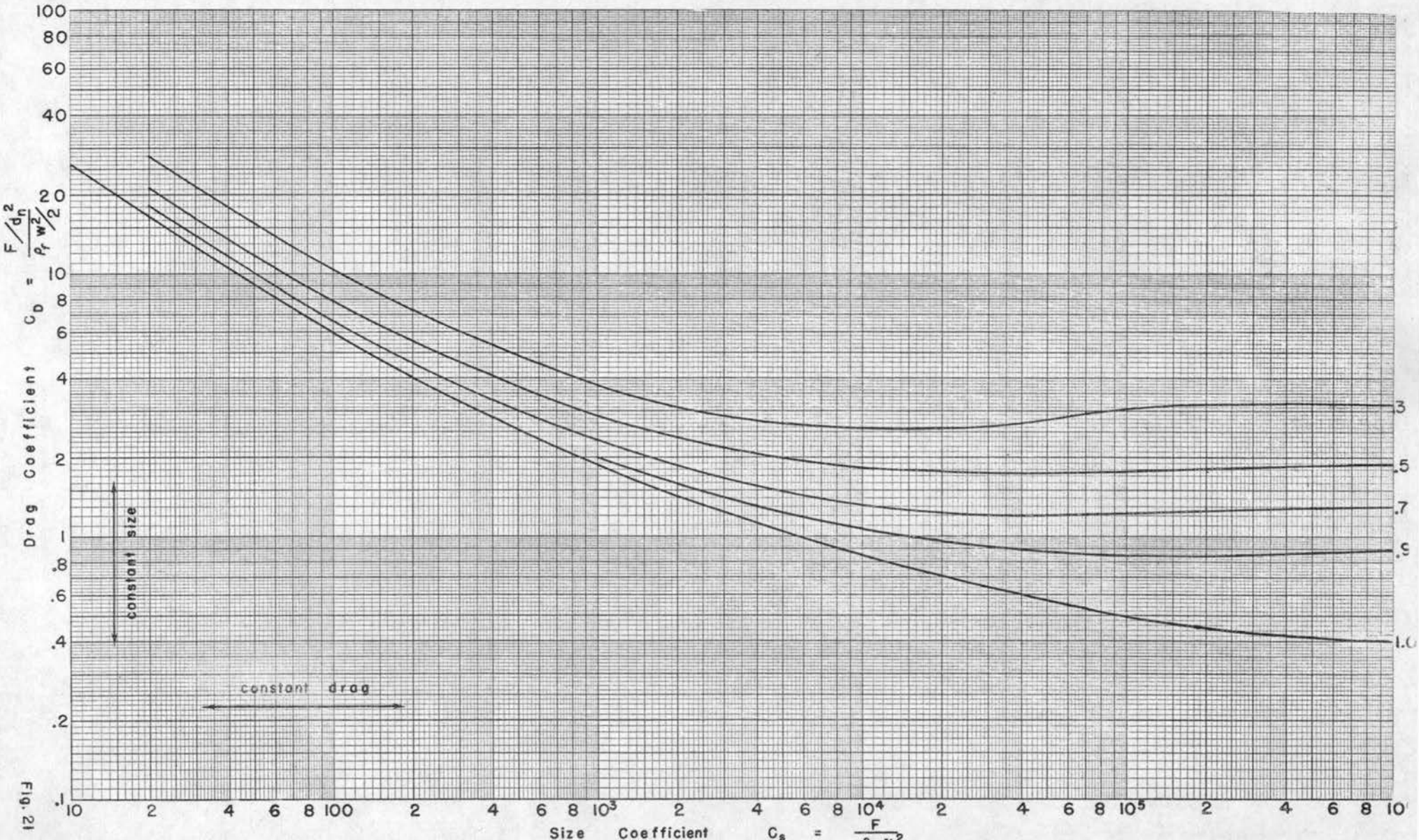

Fig. 21

$C_D : C_S$ GRAPH FOR CRUSHER FRAGMENTS

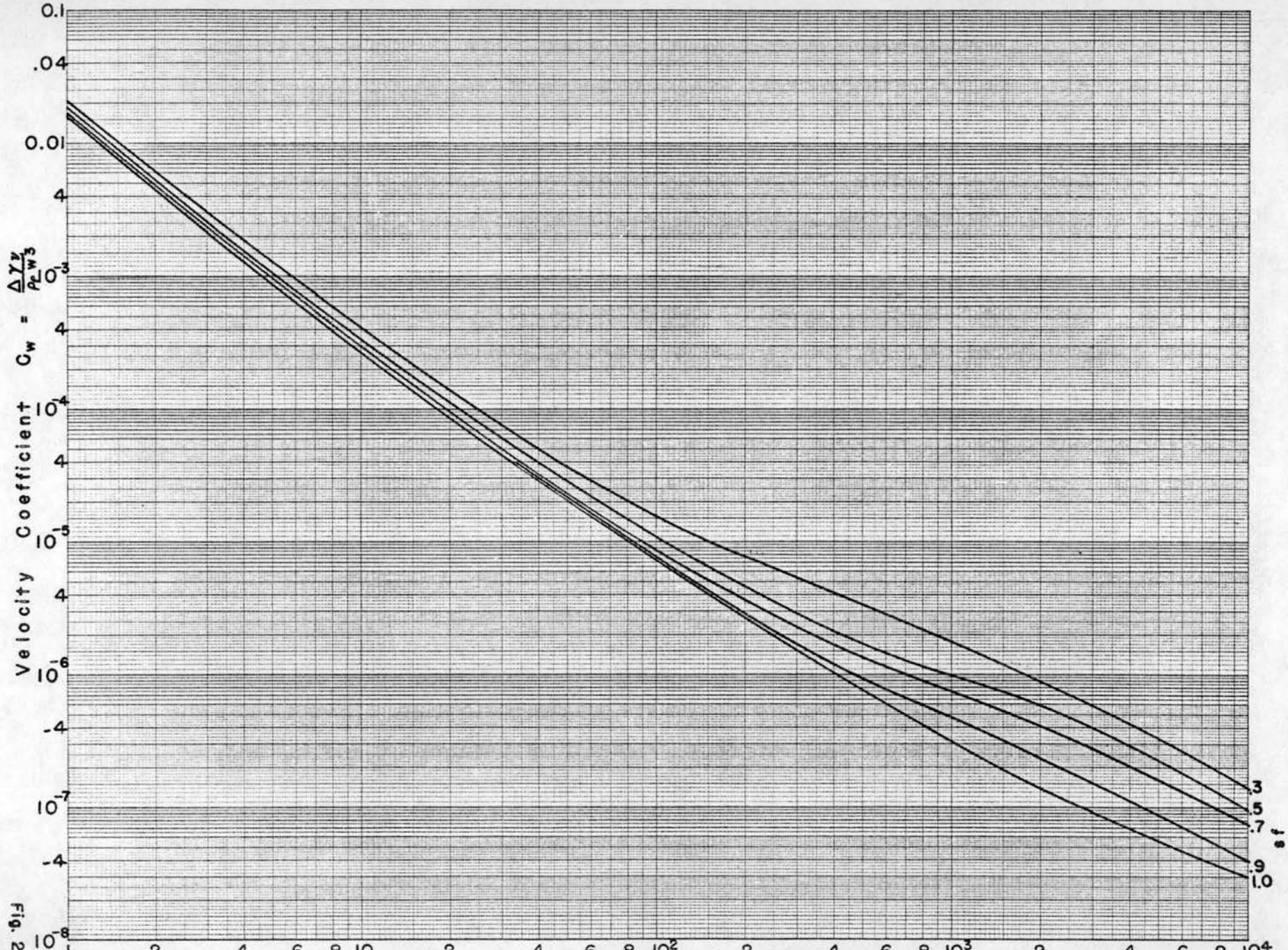

Fig. 22

C_w : Re GRAPH FOR NATURALLY WORN SEDIMENTS

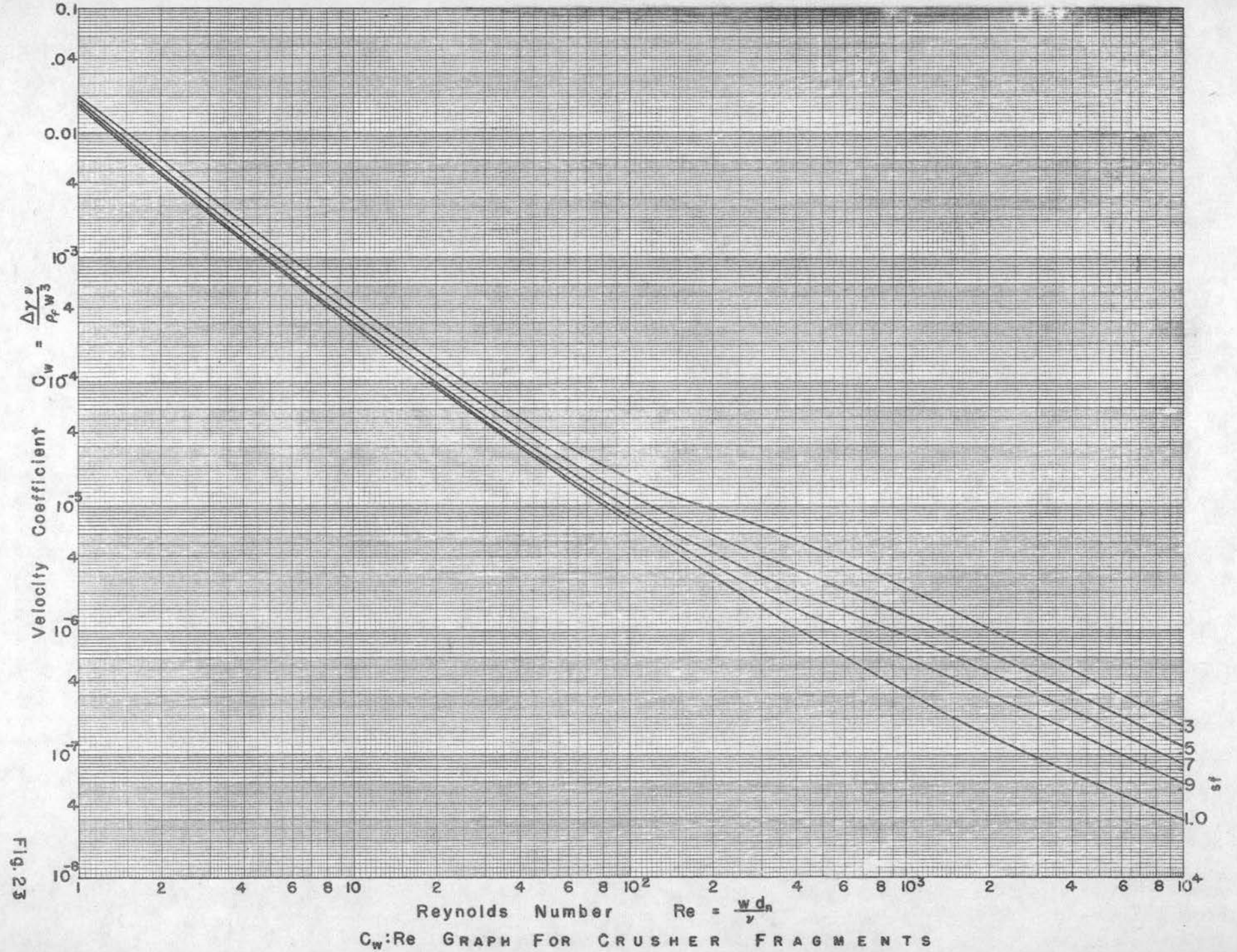

Fig. 23

C_w:Re Graph For Crusher Fragments

the medium of the shape factor. The sedimentation diameter for each particle that was dropped can be determined using the method suggested by Serr. This is based on two facts:

1. The nominal diameter, sieve diameter and sedimentation diameter are all equivalent for a sphere.

2. On the C_D:Re graph lines of constant fall velocity occur at +1.

The sedimentation diameter coefficient K_w has been computed from a ratio of the Reynolds number of the particle to the Reynolds number of a sphere of the same fall velocity.

$$K_w = \frac{Re_p}{Re_s} = \frac{\frac{w_p\ d_{n_p}}{\nu}}{\frac{w_s\ d_{n_s}}{\nu}} = \frac{d_{n_p}}{d_{n_s}} = d_n/d_s.$$

The sedimentation diameter for any particle can be determined from a ratio of the Reynolds number of the particle to a ratio of the Reynolds number of the particle projected along a line of slope +1 to the C_D:Re line for spheres (sf = 1.0). Because the nominal diameter is assumed to be equivalent to the sedimentation diameter for a sphere and because all of the particles falling on a line of slope +1 have equal fall velocities, a simple ratio of these two Reynolds numbers results in a ratio of the nominal diameter of the particle to the sedimentation diameter of the particle. Since the sieve diameter and the nominal diameter for each of the particles is known, the ratio of the sieve diameter to the sedimentation diameter can easily be obtained by multiplying the sedimentation diameter coefficient K_w by the ratio d_{sv}/d_n. The resulting ratio is called the diameter coefficient, d.

$$K_d = K_w\ (d_{sv}/d_n) = (d_n/d_s)(d_{sv}/d_n) = d_{sv}/d_s.$$

The diameter coefficient d has been computed for the naturally worn stream sediment samples and is shown on Fig. 24. The Reynolds number on Fig. 24 is based on d_{sv} instead of d_{nv}. The lines of constant shape factor have been drawn on this graph. This graph is now in a practical form and can be used to solve for the sedimentation diameter, d_s, if the sieve diameter d_{sv}, shape factor sf, the fall velocity w, and the kinematic viscosity ν are all known.

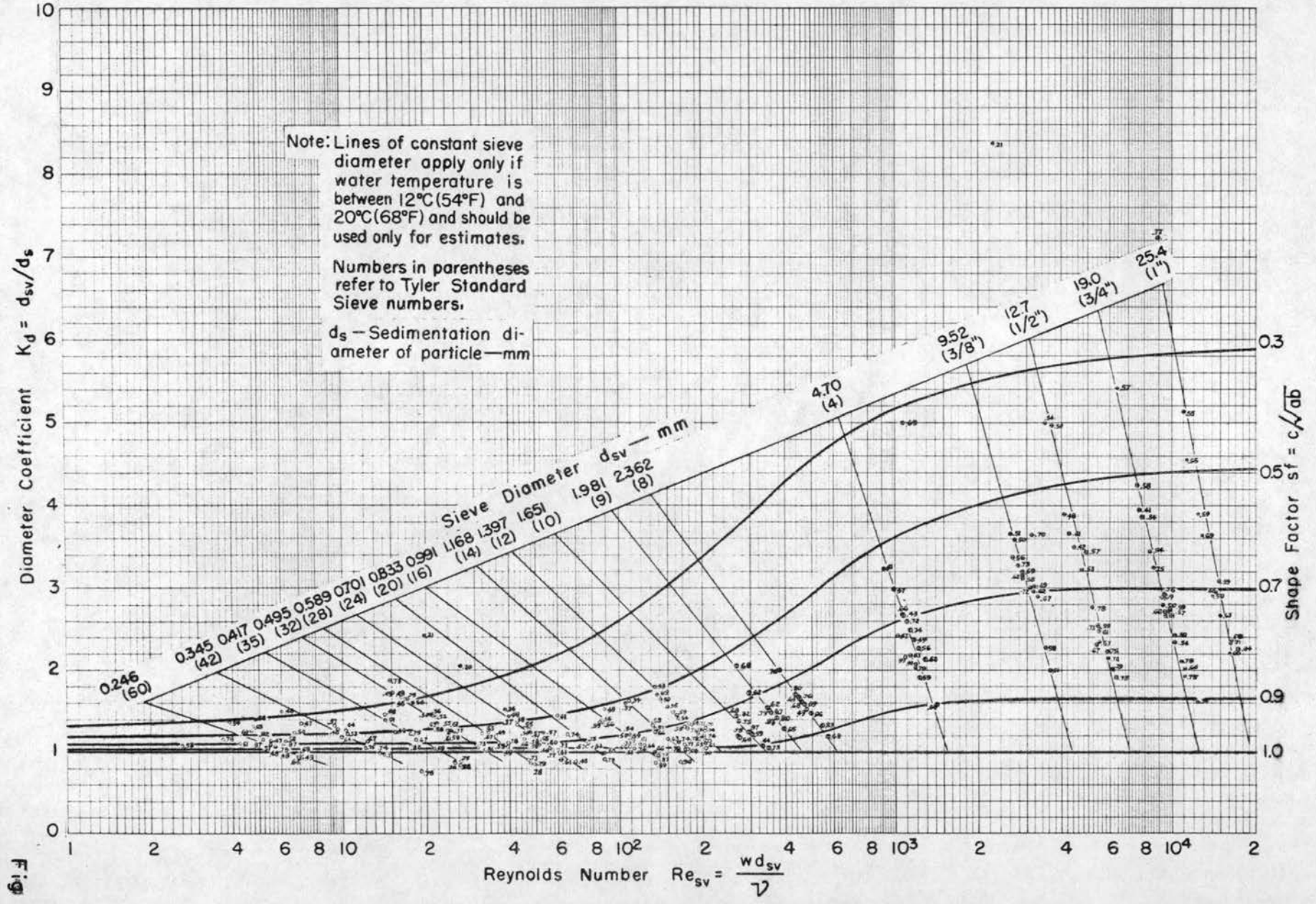

Fig 24

Variation of Diameter Coefficient with Reynolds Number

The procedure outlined for using this graph is given in the following listed steps:

1. Determine the kinematic viscosity ν from Fig. 3 using the water temperature which must be either known or assumed.

2. Estimate the fall velocity of the particle in question using Fig. 25. Assume the nominal diameter to be equal to the sieve diameter of particle.

3. Compute Reynolds number using this equation and the quantities determined in Step 1 and Step 2:

$$Re = \frac{w\, d_{sv}}{\nu}.$$

4. Using Fig. 24, determine K_d using the Reynolds number from Step 3 and the known shape factor.

5. Compute the sedimentation diameter

$$d_s = \frac{d_{sv}}{K_d} = \frac{d_{sv}}{d_{sv}/d_s}$$

If only a rough estimate of the ratio of sieve diameter to sedimentation diameter is desired, the lines of constant sieve diameter drawn on this graph may be used. It must be pointed out, however, that these lines resulted from data in which the temperature of the water (and hence its viscosity) varied, and therefore the lines could be expected to drift considerably for wide variations in water temperature. The temperature of the water varied from 12°C(54°F approx.) to 20°C (68°F approx.) during the experiments. These curves of constant sieve diameter should not be used unless the water temperature falls within the experimental range.

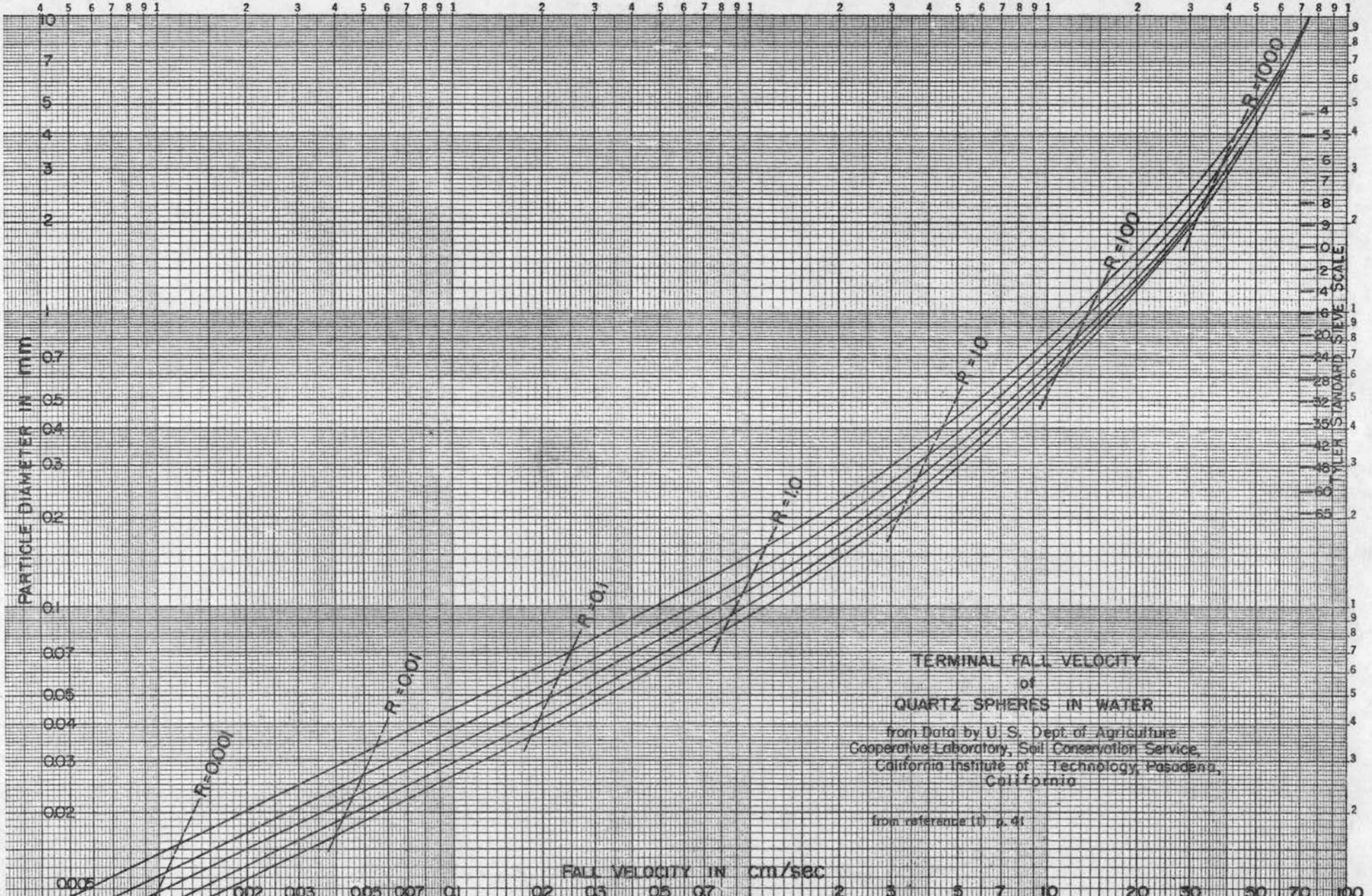
PARTICLE DIAMETER IN mm
FALL VELOCITY IN cm/sec
TYLER STANDARD SIEVE SCALE
R=0.001
R=0.01
R=0.1
R=1.0
R=10
R=100
R=1000
TERMINAL FALL VELOCITY
of
QUARTZ SPHERES IN WATER
from Data by U. S. Dept. of Agriculture
Cooperative Laboratory, Soil Conservation Service,
California Institute of Technology, Pasadena,
California
from reference (1) p. 41

Fig. 25

Fig.

Chapter VI

CONCLUSIONS

The C_D:Re graph for natural particles

All the data available have been plotted on two C_D:Re graphs (Figs. 14 and 15) and lines of constant shape factor have been drawn through the data. These shape factor lines may seem to contradict the data at certain points; however, they have been drawn carefully giving proper consideration to the data as a whole and with due consideration of the principles of fluid mechanics herein discussed. If Figs. 14 and 15 are used, the possibility of large errors must be recognized; however, the errors involved in using the shape factor lines are reduced considerably over what they would have been if the original sphere line (sf = 1.0) had been used.

If it is not possible to perform the necessary shape factor measurements, an estimate of average shape factor can be obtained from Fig. 19 or by comparing the natural sediment with the photographs of the samples appearing in this report. Because the two C_D:Re graphs have been used as a basis for Figs. 3, 20, 21, 22, 23 and 24, these graphs also must be used with the same discretion as Figs. 14 and 15.

By repeating fall velocity measurements on a number of selected particles, the variation of fall velocity was found to be of relatively minor importance at Re less than 100 but of increasing importance at Re greater than 100. Principal reason for the fluctuation of fall velocity seemed to be instability of orientation. The instability of orientation was associated with low values of the shape factor, lack of symmetry of the particles, and high values of the Reynolds number.

Relation of fall velocity to shape factor

If the temperature of the water can be fixed, then a graph of fall velocity as a function of weight, similar to Fig. 16, can be constructed from either Fig. 14 or 15 (depending on the particle roughness or angularity). As has been pointed out, by using the shape factor, a difference in fall velocity of as much as 300 percent can be explained. This fact serves to illustrate the necessity for considering the shape of the particle.

Relation of shape factor to sieve diameter

If the sieving process is thorough, the sieve diameter is proportional to the b-axis of the particle. The average shape factor for all the particles measured from all the samples has been converted to a graph of average sf vs. sieve size and is shown in Fig. 18. This curve was obtained from average data and should be used only to obtain an estimate. It is apparent from this graph that the average shape factor for all samples is approximately 0.60; although the angular crusher fragments exhibit generally a higher shape factor than the naturally worn stream sediments. In some cases the smaller sediments seem to have a higher shape factor than the larger sizes.

Variation of drag coefficient with size coefficient

Figs. 20 and 21 are especially useful for determining the drag coefficient for a particular size when the shape factor is known. If the size coefficient and shape factor for a particular particle are known, the drag coefficient for a sphere of the same size (or weight) can be obtained from the intersection of the given C_s and the sf = 1.0 line. The drag coefficient can in turn be used to solve for the fall velocity. All the errors inherent in the original C_D:Re graph are also inherent in Figs. 20 and 21.

Variation of the velocity coefficient with Reynolds number

Many times it is desirable to know the size of some other particle having the same fall velocity, but a different shape than the particle under study. The determination of the sedimentation diameter is a special case of this type of problem. Figs. 22 and 23 have been constructed to aid in the solution of these types of problems. All particles having the same fall velocity will plot as horizontal lines on these two graphs. Examination of Figs. 22 and 23 will indicate that all particles having the same fall velocity but of shape factor less than one will be larger in size and fall with a higher Reynolds number than a sphere (sf = 1.0).

Relation of nominal diameter and sieve diameter

The nominal diameter and sieve diameter for the rock crusher samples have been compared on Fig. 19. The data have been enveloped by two lines having the equations:

$$d_n = 1.8\ d_{sv}$$

$$d_n = 0.7\ d_{sv}\ .$$

As an approximation the nominal diameter can be assumed equal to the sieve diameter ($d_n = d_{sv}$).

Relation of sieve diameter to sedimentation diameter

The ratio of the sieve diameter to the sedimentation diameter ($K_d = d_{sv}/d_s$) was determined and is shown on Fig. 24 for all naturally worn stream sediments. This graph gives the diameter coefficient as a function of a Reynolds number with shape factor as the third variable. The length term in the Reynolds number is the sieve diameter. The substitution of the sieve diameter for the nominal diameter was made as an aid for the use of Fig. 24 when the nominal diameter is not known. It is expected that Fig. 24 is the most useful to sediment engineers from the practical point of view.

Chapter VII

EXAMPLES

Examples have been included in this report as reference material to guide the reader in the use of the information herein presented.

Photographs showing a representative sample of sediment from each source have been included. Corey's samples have been enlarged approximately 1 1/3 times. A 25-cent coin (approximately 24 mm diameter) appears in each of the photographs taken by Wilde. The photomicrographs taken by Schulz show the sand grains enlarged approximately 2 1/2 times.

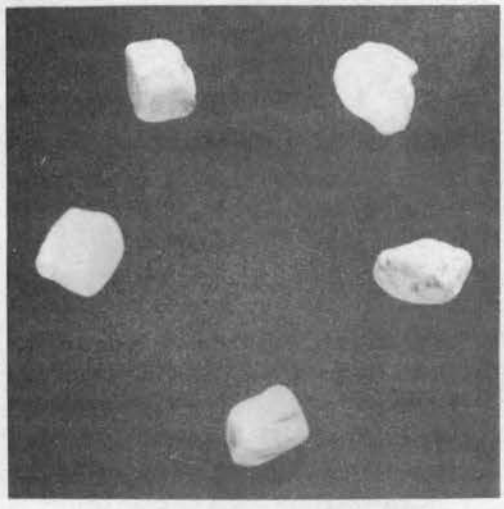

a) Sample of sand grains from Cache Le Poudre River near Bellvue, Colorado.
Ave. S. F. - 0.59 to 0.76.

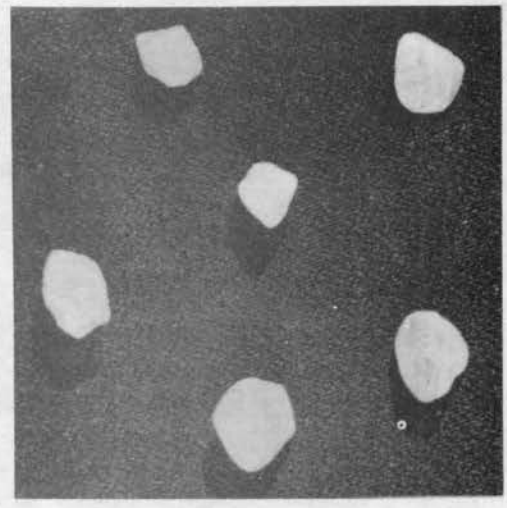

b) Sample of sand grains from the Middle Loup River at Dunning, Nebraska.
Ave. S. F. - 0.67 to 0.71.

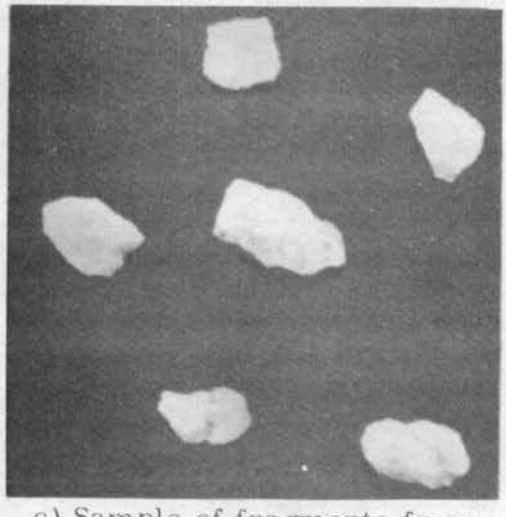

c) Sample of fragments from rock crusher at Bellvue, Colorado.
Ave. S. F. - 0.45 to 0.53

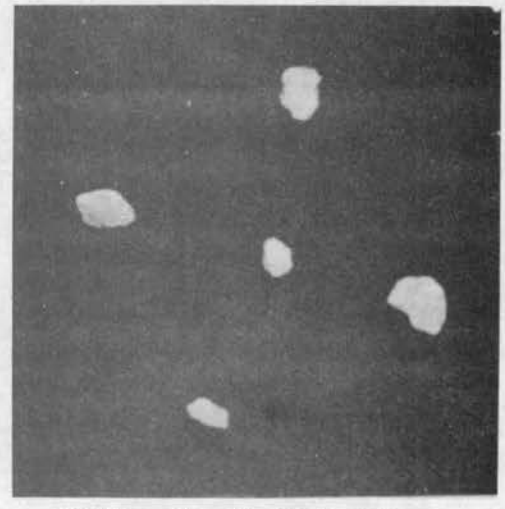

d) Sample of wind -blown sand grains from Laporte, Colorado.
Ave. S. F. - 0.53 to 0.64.

(Note: Enlarged 1 1/3 times natural size.)

PHOTOGRAPHS OF SAMPLES STUDIED BY COREY

Fig. 26.

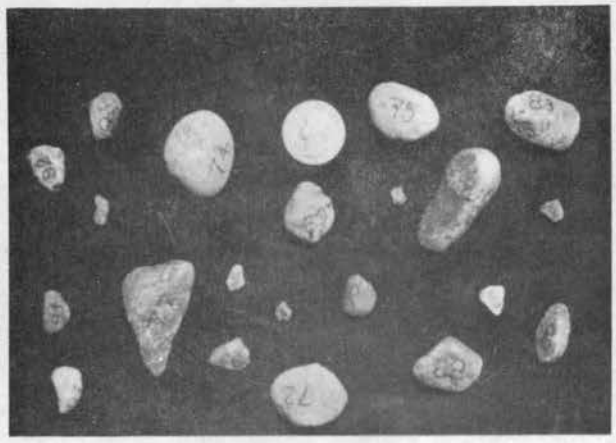

Sample from Cache La Poudre River north of Fort Collins, Colorado.
Ave. S.F. - 0.49 to 0.65.

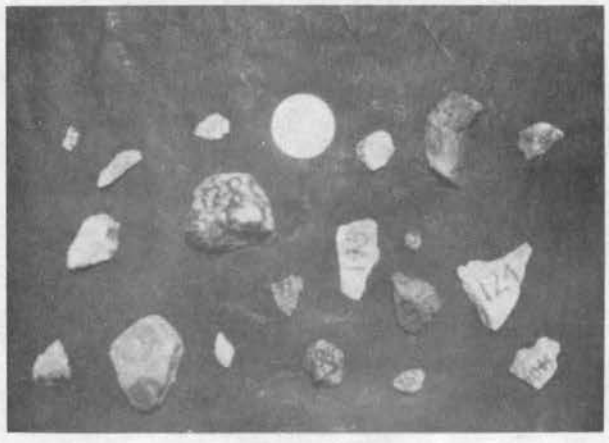

Sample from crusher plant near Fort Collins, Colorado.
Ave. S.F. - 0.53 to 0.57.

Sample from glacial morraine in Rocky Mountain National Park, Colorado.
Ave. S.F. - 0.65 to 0.67.

(Note: 25-cent piece in each photograph indicates size.)

PHOTOGRAPHS OF SAMPLES STUDIED BY WILDE

Fig. 27

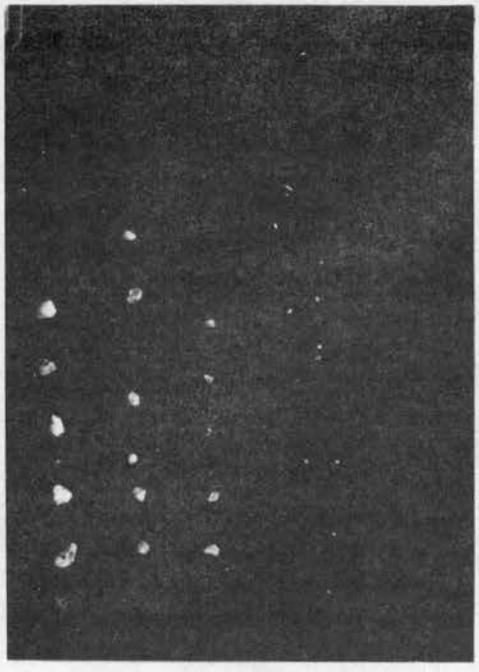

a) Sample of sand grains from Cache La Poudre River east of Fort Collins, Colorado.
Ave. S. F. - 0.50 to 0.70.

b) Sample of sand grains from Wolf Creek below Ft. Supply Dam, Oklahoma.
Ave. S. F. - 0.42 to 0.70.

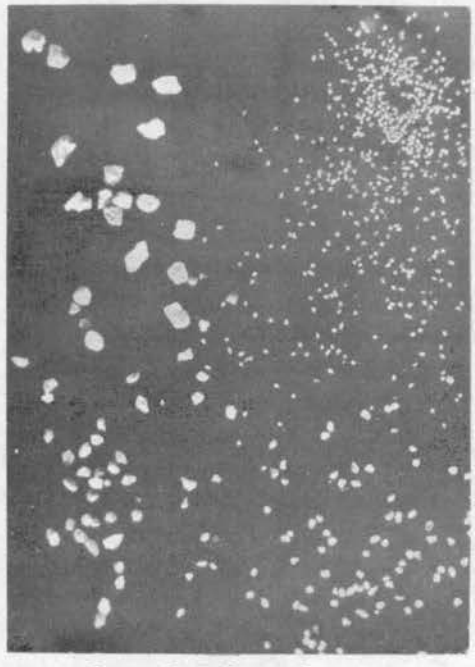

c) Sample of sand grains from Arkansas River at Lamar, Colorado.
Ave. S. F. - 0.45 to 0.69.

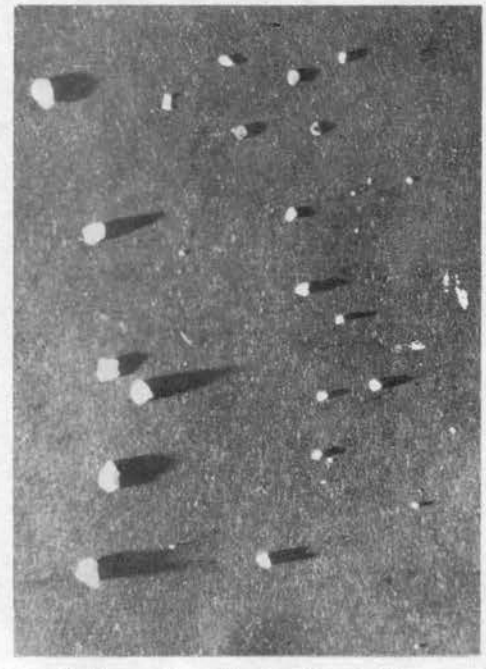

d) Sample of sand grains from Alder Creek in Yosemite Nat'l Park, California.
Ave. S. F. - 0.49 to 0.65.

PHOTOGRAPHS OF SAMPLES STUDIED BY SCHULZ.

Fig. 28.

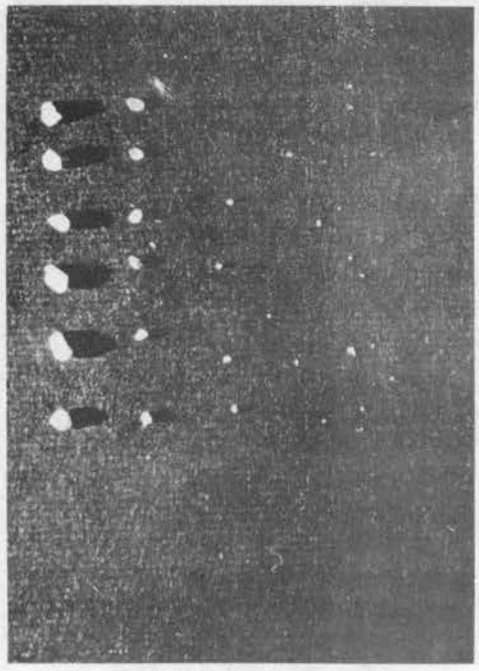

a) Sample of sand grains from Middle Loup River at Dunning, Nebraska.
Ave. S. F. - 0.60 to 0.74.

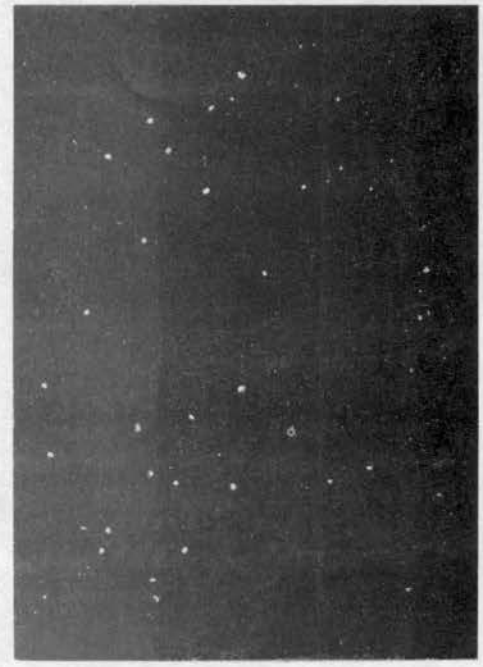

b) Sample of sand grains from Colorado River at Yuma, Arizona.
Ave. S. F. - 0.60 to 0.75.

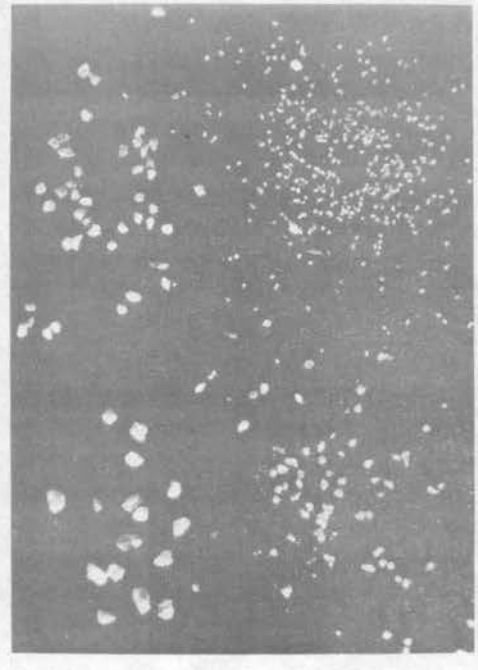

fragments.
Ave. S. F. - 0.44 to 0.67.

PHOTOGRAPHS OF SAMPLES STUDIED BY SCHULZ.

Fig. 29

Example Problem No. 1

A well rounded particle of the following properties was dropped in water at 20°C. It was found that the fall velocity was 8.0 cm/sec and that

a = 1.2 mm
b = 0.9 mm
c = 0.5 mm
weight = 0.00132 gm
volume = 0.0005 cc.

To find the sedimentation diameter of this particle the following computations are necessary.

Solution:

$$sf = c/\sqrt{ab} = \frac{0.5}{\sqrt{1.2\ (.9)}} = 0.49$$

for water at 20°C $\nu = 0.01011$ cm^2/sec (from Fig. 1)

$$d_n^3 = \frac{(6)(\text{Volume})}{\pi};\ d_n = 0.0998 \text{ cm}$$

$$Re = \frac{wd_n}{\nu} = \frac{8.0(.0998)}{.01011} = 79$$

From Fig. 22 at Re = 79 and sf = 0.5, $C_w = 1.5 \times 10^{-5}$. Move to the point where sf = 1.0 and $C_w = 1.5 \times 10^{-5}$. At this point Re = 61.

$$d_{sphere} = d_s = \frac{61}{79}\ (.0998) = 0.077 \text{ cm.}$$

Example Problem No. 2

Find the fall velocity of an extremely angular particle having the same nominal diameter as the known particle but having a shape factor of 0.3 falling in water at 20°C. The properties of the known particle are as follows:

a = 0.5 mm
b = 0.3 mm
c = 0.26 mm
F = 0.00006 gm

Solution:

$$sf = \frac{0.26}{\sqrt{.5(.3)}} = 0.67$$

$\nu = 0.01012$ cm^2/sec (from Fig. 1)

$\rho_f = 0.9982$ gm/cc.

$$C_s = \frac{F}{\rho_f \nu^2/g} = \frac{0.00006}{.9982(.01012)^2/980} = 578$$

Use Fig. 21 for crusher fragments (because the particle is extremely rough) to find C_D. At sf = 0.67 and $C_s = 578$, $C_D = 3.8$. Move upward from this point to the point where sf = 0.3 and $C_s = 578$. $C_D = 4.6$ at this new point. Assume the specific gravity to be 2.65 then

$$F = (\Delta\gamma)(\text{Volume}) = (\Delta\gamma)\left(\frac{\pi d_n^3}{6}\right),$$

$$d_n^3 = \frac{6F}{\Delta\gamma} = \frac{6\,(.00006)}{(2.65-1)} = .000069,$$

$$d_n = 0.041 \text{ mm},$$

but $$C_D = 4.6 = \frac{F/d_n^2}{\rho_f w^2/2g},$$

$$w^2 = \frac{F/d_n^2}{4.6\rho_f/2g} = \frac{.00006/(.041)(.041)}{4.6(.998^2)/2(980)} = 1.52,$$

$w = 1.24$ cm/sec .

Example Problem No. 3

Determine the sedimentation diameter of a particle when the sieve diameter is 0.35 mm and the shape factor is 0.7. The temperature of the water is 20°C.

Solution:

Fig. 24 is used for the solution of this problem. One method of solution is as follows:

1. Use lines of constant sieve size and constant shape factor to determine the diameter coefficient, K_d .
2. Solve for the sedimentation diameter.

Another solution uses both Fig. 24 and Fig. 25.

at 20°C = 0.01012 (from Fig. 1)

w at 20°C and d = 0.35 mm = 5 cm/sec (from Fig. 25).

$$Re_{sv} = \frac{w d_{sv}}{\nu} = \frac{5(.035)}{.01012} = 17.3,$$

$K_d = 1.15$ at sf = 0.7 and $Re_{sv} = 17.3$,

$$d_s = \frac{d_{sv}}{K_d} = \frac{0.35}{1.15} = 0.3 \text{ mm}.$$

BIBLIOGRAPHY

1. Cooperative Federal Interagency Project. Methods of analyzing sediment samples. Report No. 4. St. Paul U. S. Engineer District Sub-Office, Hydraulic Laboratory, University of Iowa, Iowa City, Iowa, 1941. 203p.

2. Cooperative Federal Interagency Project. A study of new methods for size analysis of suspended sediment samples. Report No. 7. St. Paul U. S. Engineer District Sub-Office, Hydraulic Laboratory, State University of Iowa, Iowa City, Iowa, 1943. 102p.

3. Corey, A. T. Influence of shape on the fall velocity of sand grains. Master's thesis, 1949. Colorado A & M College. 102p.ms.

4. Durand, W. F., ed. Aerodynamic theory, vol. III. Pasadena, California Institute of Technology, 1943. 354p.

5. Goldstein, S., ed. Modern developments in fluid dynamics. London, Oxford University Press, 1938. 2 volumes, 702p.

6. Heywood, H. Measurement of the fineness of powdered materials. Institute of Mechanical Engineers. Proceedings, 140:257-347, 1938.

7. Krumbein, W. C. Measurement and geological significance of shape and roundness of sedimentary particles. Journal of sedimentary petrology, 11:64-72, 1941.

8. Krumbein, W. C. Settling velocities and flume behavior of non-spherical particles. American Geophysical Union. Transactions, 1942:621-33.

9. Lamb, Horace. Hydrodynamics. New York, Dover Publications, 1932. 738p.

10. Linsley, R. K., Kohler, M. A. and Paulhus, J. L. H. Applied hydrology. New York, McGraw-Hill Book Company, 1949. 689p.

11. Malaika, Jamil. Particle shape and settling velocity. Ph.D. dissertation, 1949. State University of Iowa. 64p.ms.

12. McNown, J. S. Particles in slow motion. La Houille Blanche, 6:5:701-722, Sept.-Oct. 1951.

13. McNown, J. S., Lee, H. M., McPherson, M. B., and Engez, S. M. Influence of boundary proximity on the drag of spheres. Seventh International Congress of Applied Mechanics. Proceedings, London, England, Sept. 1948.

14. McNown, John S. and Malaika, Jamil. Effects of particle shape on settling velocity at low Reynolds numbers. American Geophysical Union. Transactions, 1950:31:74-82.

15. McPherson, Murray B. Boundary influence on the fall velocity of spheres at Reynolds numbers beyond the Stokes range. Master's thesis, 1947. State University of Iowa. 39p.ms.

16. O'Brien, M. P. Review of the theory of turbulent flow and its relation to sediment-transportation. American Geophysical Union. Transactions, 1933:487-491.

17. Otto, G. H. Comparative tests of several methods of sampling heavy mineral concentrates. Journal of sedimentary petrology, 3:30-39, April 1935.

18. Pernolet, V. A l'etude des preparations mecaniques des minerais, on experiences propres a etablir la theorie des different systemes usites on possibles. Annales des Mines, 4ME Serie XX, 390, 1851.

19. Rouse, H. Elementary mechanics of fluids. New York, John Wiley and Sons, 1946. 365p.

20. Rouse, H. Experiments on the mechanics of sediment suspension. Proc. 5th International Congress of Applied Mechanics, Cambridge, 1939.

21. Rouse, H. Fluid mechanics for hydraulic engineers. New York, McGraw-Hill and Co., 1938. 411p.

22. Rouse, H. Nomogram for settling-velocity of spheres. Ann. Report, Committee on Sedimentation, National Research Council, 57-64, 1937.

23. Rouse, H., ed. Engineering hydraulics. New York, John Wiley and Sons, 1950. 1039p.

24. Richards, R. H. Velocity of galena and quartz falling in water. American Institute of Mining Engineers. Transactions, 38:210-235, 1908.

25. Richards, R. H., Locke, C. E. and Berry, J. L. Ore dressing. 1925:127.

26. Rubey, W. W. Settling velocities of gravel, sand and silt particles. American Journal of Science, 25:325-328, April 1933.

27. Schiller, L. Fallversuche mit kugelin and scheiben. Handbook der Experimentalphysik, v. 4, Pt. 2, 1932.

28. Schmiedel, J. Experimentelle untersuchungen uber die fallbewegung von kugeln und scheiben in reibenden flussigkeiten. Physikalische Zeitschrift, Bd XXIX, 1928, p 593-610.

29. Schulz, E. F. Effect of shape on the fall velocity of sand particles. Master's thesis in progress. Colorado A & M College.

30. Schulz, P. Nene bestimmungen der konstanten der fallgesetze in der nassen aufbereitung mit bilfe der kinematographic und betracktungen uber dos gleichfalligkeitsgesitz. Doktor-Ingenieurs Dissertation, V. K. Sachs. Technischen Hochschule zu Dresden in verbindung mit der K. Sachs, Bergakademie zu Freiberg, 1914.

31. Serr, E. F. A comparison of the sedimentation diameter and the sieve diameter for various types of natural sands. Master's thesis, 1948. Colorado A & M College. 82p.ms.

32. Shields, A. Anwendung der aehnlichkeitsmechanik und der turbulenzforschung auf die geschiebeoewegung, Mitt Preuss. Versuchs. Wasserbaw u. Schiffbau, v. 26, Berlin, 1936.

33. Stanley, J. W. A method for relating sieve analysis and sedimentation analyses. Unpublished manuscript.

34. Wadell, H. Shape determinations of large sedimental rock fragments. Pan-American Geology, 61:187-220, 1934.

35. Wadell, H. Some new sedimentation formulas. Physics, 5:281-291, 1934.

36. Wadell, H. Sphericity and roundness of rock particles. Journal of Geology, 41:310-331, 1933.

37. Wadell, H. The coefficient of resistance as a function of Reynolds number for solids of various shapes. J. Franklin Institute, 217:No. 4:459-490, 1934.

38. Wadell, H. Volume, shape, and roundness of rock particles. Journal of Geology, 40:443-451, 1932.

39. White, C. M. The drag of cylinders in fluids at slow speeds. Proceedings, Royal Society, A, 1946:188.

40. Wieselsberger, C., Betz, A., and Prandtl, L. Ergebnisse der aerodynamischen versuchsanstalt zu Gottingen, Lief 2, p. 29, 1923.

41. Wilde, R. H. Effect of shape on the fall-velocity of gravel-sized particles. Master's thesis, 1952. Colorado A & M College. 86p.ms.

42. Zegrzda, A. P. Settling of gravel and sand in calm water. Leningrad. Scientific Research Institute of Hydrotechnics. Transactions, 12:30-54, 1934.

APPENDIX

FALLING OF GRAINS OF SAND AND GRAVEL IN CALM WATER

By A. P. Zegrzda, Eng.

1. The study of existing experimental data has shown that the descent of particles of the same kind in various liquids and of particles of various materials in the same liquid, proceeds according to laws which differ to a certain extent from one another.

As it seems this circumstance cannot be attributed to the difference in physical properties of the liquid or of the particles' material, but must be due to the influence of the shapes of falling particles.

2. The experimental data on the descent of sand-grains in water published in technical literature differ somewhat from one another and, if plotted, form two curves nearly parallel to each other.

This discrepancy may be explained, in our opinion, also by the difference in the shape, which, on the average, characterized the particles used in various experiments.

3. The fact that experimental data may be plotted and form smooth curves, indicates that in this case (uniform motion of particles of irregular shape) the relationship is also maintained between the coefficient of resistance and the Reynolds' number, if the latter characteristics be regarded as composed by average values (of velocities, dimensions, etc).

4. Existing formulae based in a majority of cases on experiments with balls, give naturally, such results which do not coincide with experimental data as obtained with sand-grains falling in water.

5. Practical formulae must be of such a nature as to satisfy conditions illustrated by both series of points (obtained by experiments).

This condition involves certain fluctuations in the values of parameters included into the formulae.

The formulae given below contain extreme values of such parameters, corresponding to the highest and lowest situation of test points on the diagram.

For each group of formulae, the extreme values of Reynolds' number are given, limiting the domain of application of this group; corresponding diameters of particles for the temperature of water equal to 10--15° are also given.

I. Streamline stage:

$Re < 1.0$ ($d < 0.125$ mm).

Stokes' formula: $$P = 4.50 \frac{1}{Re} \qquad (1)$$

II. Intermediary stage:

A) $1.0 < Re < 20$.

Allens' formula: $$P = 2.66 \frac{1}{Re} \qquad (2)$$

$$P = 4.50 \frac{1}{Re} \qquad (2')$$

B) $20 < Re < 150$ (0.60 mm $< d <$ 2.0 mm).

$$P = 0.90 \left(\frac{1}{Re}\right)^{0.120} \qquad (3)$$

$$P = 2.10 \left(\frac{1}{Re}\right)^{0.235} \qquad (3')$$

III. Turbulent stage:

$$Re > 150 \quad (d > 2.0 \text{ mm})$$

$$P = 0.45 \tag{4}$$

Richards' formula: $P = 0.65$ (4')

Note. Dimensionless characteristics P and Re are computed from average values of quantities characterizing the descent of a particle, using for this purpose the following formulae:

$$P = \frac{\quad}{\quad} \tag{5}$$

$$Re = \frac{\quad}{\quad} \tag{6}$$

where:

= the average velocity of descent,

= the average radius of a sand-grain,

= the acceleration of gravity,

= the density of the sand-grain,

= the density of the liquid,

= the kinematic coefficient of viscosity.

6. Except the equations mentioned above, the nomographic interpretation of the formulae, proposed by Prof. M. A. Velikanov and A. P. Zegrzda, may also be used.

In this case it is necessary to substitute into the formula the radius of the equivalent sphere, that is, such a sphere which, being of the same density as the sand-grain, has the same velocity of descent (at the same temperature) in water.

The radius of the equivalent sphere ( ) and the average radius of the sand-grain ( ) may be expressed as functions

of one another, as follows:

I. Streamline flow (d ' 0.125 mm)

= (7)

II. d ' 0.20 mm:

= 0.525 · (8)

= 0.66 · (8')

Experiments show that for particles having diameters from 0.125 mm to 0.20 mm, the relation between and , is rather uncertain.

7. It is recommended not to use the Krey's formula, which has acquired some popularity among hydraulic engineers.

This formula is based on data which are not sufficiently accurate.

Beside this, an analysis of experimental data published by Krey makes us believe that he selected an incorrect value for the coefficient in the formula for the turbulent flow (d > 1.5 -- 2.0 mm). For this stage the corresponding Krey's formula gives too low a value of resistance or, which is the same, -- too high a value of velocity of descent for a given size of grains.

Table 9

Physical and Hydraulic Properties
of
Particles Studied by Zegrzda

Particle Number	Average Radius - mm	Temperature °C	Fall Velocity v - cm/sec	Particle Density	Fluid Density	Kinematic Viscosity	P	$\frac{1}{Re}$	Radius of equivalent sphere - mm
1	0.278	18.0	8.46	2.67	1.00	0.0106	0.653	0.0436	0.276
2	0.425	12.0	10.98	2.67	1.00	0.0124	0.586	0.0258	0.391
3	0.750	10.0	15.62	2.67	1.00	0.0131	0.497	0.0112	0.594
4	1.25	12.0	20.80	2.67	1.00	0.0124	0.468	0.00477	0.796
5	1.25	18.0	20.70	2.67	1.00	0.0106	0.471	0.00410	0.712
6	1.75	18.5	25.00	2.67	1.00	0.0105	0.453	0.00240	0.850
7	0.278	7.5	7.82	2.67	1.00	0.0141	0.828	0.0626	0.308
8	0.425	8.2	10.85	2.67	1.00	0.0139	0.600	0.0292	0.415
9	0.750	12.0	15.00	2.67	1.00	0.0124	0.540	0.0110	0.555
10	1.25	10.0	20.10	2.67	1.00	0.0131	0.504	0.00522	0.759
11	1.75	7.5	25.90	2.67	1.00	0.0141	0.423	0.00265	1.125
12	2.25	8.2	28.10	2.67	1.00	0.0139	0.461	0.00220	1.190
13	0.425	14.4	3.27	2.67	0.880	0.167	8.00	1.17	0.398
14	0.750	13.7	5.79	2.67	0.880	0.173	4.39	0.398	0.596
15	1.25	12.3	9.84	2.67	0.880	0.186	2.53	0.151	0.892
16	1.75	13.7	15.80	2.67	0.880	0.173	1.37	0.0626	1.260
17	2.25	14.4	21.60	2.67	0.880	0.167	0.945	0.0344	1.620
18	3.00	13.9	29.10	2.67	0.880	0.171	0.694	0.0196	2.180
19	0.278	12.2	1.61	2.67	0.880	0.187	21.8	4.88	0.279
20	0.425	9.4	2.44	2.67	0.880	0.231	14.4	2.16	0.390
21	1.25	11.9	9.25	2.67	0.880	0.190	2.86	0.164	0.860
22	1.75	13.0	16.10	2.67	0.880	0.179	1.32	0.0635	1.280
23	2.25	12.3	20.50	2.67	0.880	0.181	1.05	0.0392	1.590
24	3.00	12.1	28.30	2.67	0.880	0.188	0.734	0.0221	2.180
25	0.278	15.2	2.86	2.67	0.880	0.057	6.96	0.691	0.225
26	0.425	12.0	3.84	2.67	0.880	0.094	5.88	0.560	0.343
27	0.750	14.3	7.75	2.67	0.880	0.067	2.48	0.115	0.484
28	1.25	16.6	13.15	2.67	0.880	0.045	1.43	0.0274	0.671
29	1.75	13.3	17.95	2.67	0.880	0.078	1.03	0.0248	1.02
30	2.25	13.2	25.45	2.67	0.880	0.080	0.688	0.0140	1.48

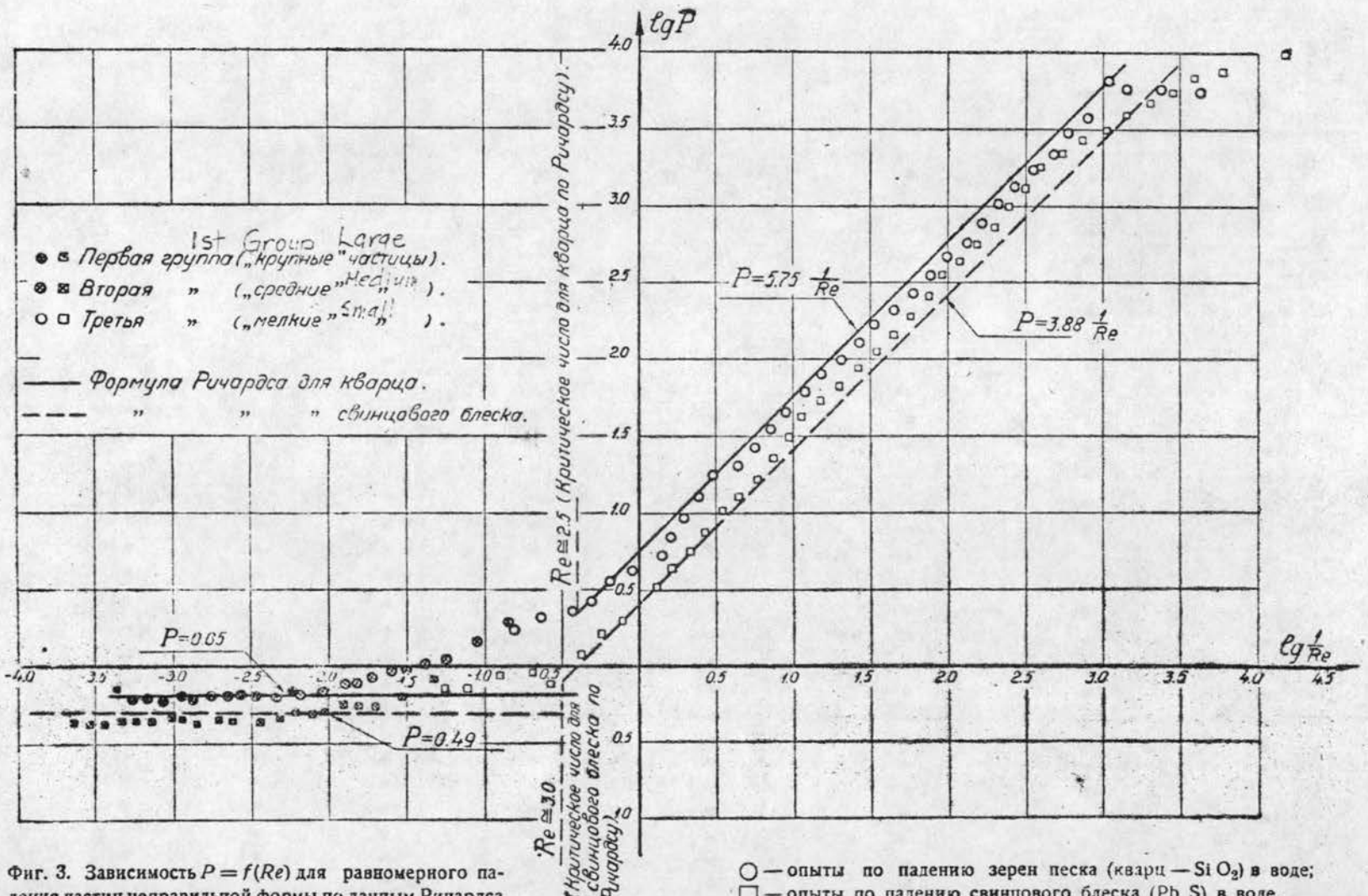

Фиг. 3. Зависимость $P = f(Re)$ для равномерного падения частиц неправильной формы по данным Ричардса

○ — опыты по падению зерен песка (кварц — $Si\,O_2$) в воде;
□ — опыты по падению свинцового блеска (Pb S) в воде.

Table 10

Physical and Hydraulic Properties
of
Particles Studied by Krumbein
(Table 1, p. 624 from Krumbein's paper)

Form	Symbol	Density	Nominal diameter	Sphericity	Approx. roundness, P	$\frac{sf}{ab}$ /1 c	Critical Froude No., F_c /2	(v/V) for F=0.5, d/y=0.11	Settling velocity	Reynolds No., R	Coeff. resistance, C_D	Form-coeff. (V_1/V_3)
		gm/cc	cm						cm/sec			
"Spheres"	S	2.06	1.47	0.96	0.95	0.93	0.13	0.68	63.4	9300	0.50	0.91
Rollers 1	R1	2.14	1.44	0.85	0.90	0.89	0.15	0.64	53.0	7640	0.77	0.75
Rollers 2	R2	2.11	1.44	0.68	0.85	0.75	0.20	0.58	48.8	7030	0.87	0.69
Rollers 3	R3	2.02	1.46	0.52	0.80	0.61	0.35	0.50	39.1	5700	1.28	0.56
Disks 1	D1	2.12	1.43	0.93	0.95	0.82	0.16	0.61	51.8	7410	0.78	0.73
Disks 2	D2	2.03	1.45	0.75	0.95	0.42	0.37	0.52	35.7	5170	1.53	0.51
Disks 3	D3	2.13	1.46	0.61	0.95	0.22	0.42	0.38	24.1	3520	3.72	0.35
Blades 1	B1	2.09	1.43	0.80	0.85	0.72	0.20	0.59	49.1	7020	0.85	0.69
Blades 2	B2	2.07	1.44	0.68	0.80	0.51	0.33	0.54	39.7	5710	1.28	0.56
Blades 3	B3	2.15	1.43	0.52	0.75	0.43	0.41	0.46	34.5	4960	1.82	0.49
Cubes	C	2.14	1.45	0.82	0.25	0.73	0.31	0.56	46.7	6750	0.97	0.66
Fragments	f	2.08	1.45	0.85	0.20	0.68	0.26	0.54	46.0	6680	0.96	0.65
"Bricks"	b	2.10	1.44	0.65	0.25	0.35	0.40	0.39	33.6	4840	1.84	0.47
Rollers 4	R4	2.24	1.44	0.82	0.30	0.84	0.18	0.62	51.6	7430	0.87	0.73
Rollers 5	R5	2.23	1.41	0.54	0.30	0.59	0.38	0.52	36.6	5160	1.69	0.51
Disks 4	D4	2.17	1.44	0.81	0.95	0.44	0.32	0.50	38.4	5540	1.46	0.53
Disks 5	D5	2.20	1.43	0.57	0.95	0.17	0.35	0.50	26.4	3760	3.26	0.37

/1 Computed from Krumbein's data.
/2 Froude Number not important in this case -- see Kalinske's discussion.

Serr's photographs
have not been included

Table 11

Physical and Hydraulic Properties
of
Particles Studied by Corey
(Combined from Tables 1, 3, & 4, pp. 75-99 from Corey's Thesis)[1]

Particle Number	Axis (mm) a	b	c	sf $c/\sqrt{ab}$	Particle Weight (mg)	Nominal Diameter (mm)	With nominal dimensions $\frac{wdn}{\nu}$	$\frac{Fld_n^2}{w/2^2}$	With projected dimensions $\frac{wb}{\nu}$	$\frac{F/ab}{w/2^2}$
Sample of sand from Cache la Poudre River at Bellvue, Colorado Retained on 4-mesh sieve										
1	9.1	7.8	5.3	0.63	446	6.85	1700	1.95	1930	1.28
2	6.4	5.0	4.5	0.80	190	5.08	1430	1.17	1410	0.95
3	8.3	7.4	5.7	0.73	471	7.00	2310	1.12	2440	0.90
4	9.9	8.8	4.0	0.43	399	6.60	2220	1.03	2950	0.52
5	5.5	5.0	4.3	0.80	175	5.01	1260	1.40	1250	1.25
6	10.1	6.8	6.3	0.76	493	7.07	1560	2.56	3150	1.82
7	8.2	6.8	5.7	0.76	444	6.83	2070	1.26	2100	1.05
8	6.4	5.3	4.9	0.84	209	5.32	1700	0.91	1700	0.76
9	8.3	6.4	4.4	0.60	388	6.54	2280	0.95	2220	0.76
10	9.6	6.4	3.1	0.40	---	----	----	----	1900	----
Retained on 8-mesh sieve										
1	7.8	5.3	3.0	0.47	147.0	4.73	990	1.90	1110	1.05
2	5.9	4.0	2.9	9.59	91.8	4.04	1060	0.84	1050	0.70
3	5.9	3.6	3.4	0.74	77.6	3.82	925	1.14	865	0.79
4	5.4	3.8	3.0	0.66	64.1	3.58	810	1.23	860	0.79
5	6.5	4.8	2.4	0.43	92.2	4.05	920	1.38	1090	0.73
6	5.4	3.7	2.5	0.56	54.1	3.38	875	0.88	960	0.50
7	6.4	4.7	3.4	0.62	143.0	4.68	1280	1.11	1280	0.81
8	5.8	3.7	3.3	0.72	96.2	4.10	956	1.33	860	1.07
9	5.9	4.8	3.4	0.64	121.0	4.43	1330	0.71	1440	0.60
10	7.3	4.8	2.9	0.49	118.0	4.39	1090	1.25	1190	0.69

(Continued on next page)

[1] All particles either feldspar or quartz -- Specific Gravity assumed to be 2.65

Table 11
(Continued)

Particle Number	Axis (mm) a	b	c	sf $c/\sqrt{ab}$	Particle Weight (mg)	Nominal Diameter (mm)	With nominal dimensions $\frac{wdn}{''}$	$\frac{Fld_n^2}{w/2^2}$	With projected dimensions $\frac{wb}{''}$	$\frac{F/ab}{w/2^2}$
Retained on 9-mesh sieve										
1	4.3	3.0	2.4	0.66	24.2	2.59	547	1.02	635	0.53
2	4.0	2.8	2.3	0.68	22.4	2.53	612	0.75	665	0.44
3	3.1	2.9	2.5	0.83	17.4	2.32	534	0.77	662	0.46
4	5.3	2.5	2.5	0.69	39.3	3.04	601	1.37	495	0.96
5	4.3	3.1	2.5	0.69	20.6	2.46	465	1.20	590	0.55
6	4.1	2.6	2.6	0.80	22.1	2.51	467	1.28	484	0.75
7	3.5	2.5	2.3	0.76	15.9	2.25	362	1.53	400	0.89
8	3.1	3.0	2.1	0.68	17.6	2.33	452	1.08	581	0.60
9	4.9	2.6	1.8	0.49	23.7	2.57	521	0.09	535	0.57
10	4.1	2.4	2.4	0.76	18.6	2.38	455	1.13	455	0.66
Retained on 10-mesh sieve										
1	2.4	2.5	1.9	0.65	13.9	2.15	430	0.94	501	0.51
2	3.8	2.1	1.8	0.62	12.7	2.09	360	1.23	366	0.67
3	3.0	2.4	1.9	0.75	13.8	2.15	---	----	---	----
4	3.3	2.4	1.9	0.68	12.1	2.06	275	2.03	317	1.12
5	4.3	2.5	2.0	0.62	13.3	2.12	320	1.63	380	0.69
6	3.0	2.8	2.5	0.87	12.9	2.10	375	1.15	491	0.62
7	3.4	2.1	2.1	0.80	16.6	2.29	430	1.13	400	0.82
8	2.5	2.4	2.4	0.98	8.7	1.84	---	----	---	----
9	3.1	2.6	2.3	0.79	14.7	2.20	390	1.24	461	0.73
10	3.1	2.4	2.3	0.83	14.1	2.17	400	1.13	435	0.74
Retained on 14-mesh sieve										
1	3.4	2.5	1.3	0.44	12.6	2.09	420	0.91	500	0.48
2	2.1	1.8	1.6	0.82	3.4	1.82	290	1.29	286	1.19

(Continued on next page)

Table 11
(Continued)

Particle Number	Axis (mm) a	b	c	sf $c/\sqrt{ab}$	Particle Weight (mg)	Nominal Diameter (mm)	With nominal dimensions $\frac{wdn}{F}$	$\frac{Fld_n^2}{w/2^2}$	With projected dimensions $\frac{wb}{F}$	$\frac{F/ab}{w/2^2}$
3	2.4	1.9	1.3	0.63	5.7	1.60	---	----	---	----
4	2.5	2.2	1.9	0.59	9.6	1.90	345	1.01	398	0.67
5	2.6	2.2	1.9	0.78	11.7	2.04	330	1.13	350	0.99
6	2.7	2.0	1.6	0.68	9.7	1.91	313	1.03	326	0.85
7	2.3	2.1	1.6	0.73	12.5	2.08	430	0.85	445	0.75
8	2.2	2.1	1.6	0.68	10.0	1.93	306	1.35	340	0.70
9	2.2	2.1	2.1	0.97	8.6	1.83	326	1.01	369	0.75
10	2.3	1.9	1.5	0.73	6.2	1.64	270	1.08	310	0.70

Table 12

Physical and Hydraulic Properties
of
Particles Studied by Malaika
(Tables III, IV, V, VI, VII & VIII pp. 54 to 64 from Malaika's Thesis)

Summary of Results with Oil No. 15967, Standard Oil Company of Illinois

Particle	Nominal Diameter D ft	Velocity v ft/sec	Reynolds Number R	Particle Density s Slugs/cu.ft.	Computed Drag Coef. C_D	Boundary Correction m	Corrected Drag Coef. C_D
1. At 27.15°C., oil density 1.702 slugs per cu. ft., kinematic viscosity 0.2060 sq. ft. per sec., jar diameter 0.675 ft.							
C-4	0.02264	0.02440	0.002662	15.30	13,090	1.107	11,810
C-4	0.01907	0.01770	0.001640	15.18	20,600	1.085	18,990
C-4	0.01183	0.00704	0.0004045	15.18	81,100	1.050	77,200
P-4	0.02295	0.02478	0.002756	15.30	12,820	1.098	11,690
P-1/4	0.01551	0.01151	0.000868	15.30	40,100	1.080	37,120
D-1	0.01233	0.009345	0.000559	15.30	48,400	1.049	46,200
D-1/4	0.01713	0.01193	0.000992	15.30	41,200	1.133	36,380
D-1/4	0.01280	0.00709	0.000441	15.30	87,100	1.098	79,400
S-1	0.01301	0.01173	0.000743	15.10	33,200	1.040	31,900
2. At 27.90°C, oil density 1.701 slugs per cu. ft., kinematic viscosity 0.1930 sq. ft. per sec., jar diameter 0.675 ft.							
C-1/4	0.01182	0.00705	0.000432	15.18	80,600	1.051	76,600
C-1/4	0.00885	0.00411	0.000189	15.30	178,200	1.040	171,500
C-1/4	0.00752	0.00302	0.0001178	15.18	280,000	1.031	271,500
P-1/4	0.01131	0.00613	0.000359	15.30	103,100	1.051	98,100
D-4	0.01233	0.00814	0.000521	15.30	64,300	1.049	61,000
S-4	0.01242	0.00863	0.000556	15.30	57,200	1.048	54,700
S-4	0.00766	0.00342	0.0001359	15.30	223,600	1.030	217,000

(Continued on next page)

Table 12
(Continued)

Particle	Nominal Diameter D ft	Velocity v ft/sec	Reynolds Number R	Particle Density s Slugs/cu.ft.	Computed Drag Coef. C_D	Boundary Correction m	Corrected Drag Coef. C_D
3. At 27.35°C, oil density 1.702 slugs per cu. ft., kinematic viscosity 0.2020 sq. ft. per sec., jar diameter 0.675 ft.							
C-1	0.01421	0.01284	0.000901	15.30	29,430	1.043	28,200
C-1	0.01196	0.00920	0.000545	15.18	47,850	1.033	46,250
P-4	0.01150	0.006595	0.000375	15.30	90,250	1.042	86,500
P-1	0.01445	0.01299	0.000927	15.30	29,400	1.040	28,250
P-1	0.01162	0.08360	0.000481	15.30	56,850	1.033	55,000
D-4	0.01593	0.01220	0.000965	15.30	36,200	1.070	32,600
D-1	0.01597	0.01579	0.001248	15.30	22,000	1.070	20,570
S-4	0.02027	0.02098	0.002105	15.30	15,780	1.099	14,390
4. At 28.05°C, oil density 1.701 slugs per cu. ft., kinematic viscosity 0.1900 sq. ft. per sec., jar diameter 0.469 ft.							
S-1/4	0.02119	0.02040	0.002275	15.30	17,500	1.195	14,650
The two following spheroids were dropped in a direction normal to the one stable in the surface drag zone. The dynamic properties and the jar diameter are the same as above.							
S-4-N	0.01242	0.01050	0.000686	15.30	38,600	1.065	36,200
S-1/4-N	0.02119	0.02890	0.003400	15.30	84,800	1.088	77,950
Summary of Results with Mixture of Oils No. 15967 and 15934, Standard Oil Company of Illinois							
1. At 26.40°C, oil density 1.671 slugs per cu. ft., kinematic viscosity 0.0412 sq. ft. per sec., jar diameter 0.675 ft.							
C-1/4	0.01182	0.0368	0.01057	15.18	3,025	1.051	2,880
C-1/4	0.00885	0.02042	0.00438	15.30	7,400	1.040	7,110

(Continued on next page)

Table 12
(Continued)

Particle	Nominal Diameter D ft	Velocity v ft/sec	Reynolds Number R	Particle Density s Slugs/cu.ft.	Computed Drag Coef. C'_D	Boundary Correction m	Corrected Drag Coef. C_D
C-1/4	0.00752	0.0149	0.00272	15.18	11,730	1.031	11,380
P-1/4	0.01131	0.0298	0.00819	15.30	4,450	1.051	4,225
D-4	0.01233	0.03945	0.01180	15.30	2,762	1.049	2,640
S-4	0.01242	0.0400	0.01207	15.30	2,720	1.048	2,595
S-4	0.00766	0.0154	0.00286	15.30	11,260	1.030	10,930
S-1/4	0.02119	0.1033	0.05300	15.30	692	1.130	612
2. At 29.80°C, oil density 1.667 slugs per cu. ft., kinematic viscosity 0.0317 sq. ft. per sec., jar diameter 0.675 ft.							
C-4	0.02264	0.1670	0.11950	15.30	285	1.107	258
C-4	0.01907	0.1210	0.07280	15.18	452.5	1.085	417
C-4	0.01183	0.04835	0.01807	15.18	1,760	1.050	1,677
C-1	0.01421	0.0876	0.03930	15.30	650	1.043	622
C-1	0.01196	0.0626	0.02360	15.18	1,062	1.033	1,027
3. At 30.00°C, oil density 1.667 slugs per cu. ft., kinematic viscosity 0.0312 sq. ft. per sec., jar diameter 0.675 ft.							
P-4	0.02295	0.1720	0.12650	15.30	271	1.098	247
P-4	0.01150	0.0458	0.01690	15.30	1,920	1.042	1,840
P-1	0.01445	0.0875	0.04050	15.30	662	1.040	637
P-1	0.01162	0.0576	0.02150	15.30	1,227	1.033	1,187
P-1/4	0.01551	0.0770	0.03828	15.30	921	1.080	852
D-4	0.01593	0.08375	0.04275	15.30	798	1.070	745
D-1	0.01597	0.1046	0.05350	15.30	512	1.070	478.5
D-1	0.01233	0.0641	0.02535	15.30	1,051	1.049	1,003
D-1/4	0.01713	0.0778	0.04265	15.30	996	1.133	880
D-1/4	0.01280	0.0491	0.02015	15.30	1,862	1.098	1,697
S-4	0.02027	0.1380	0.08970	15.30	374.2	1.099	341
S-1	0.01301	0.0758	0.03160	15.10	784	1.040	754

(Continued on next page)

Table 12
(Continued)

Summary of Results with Oil No. 15934, Standard Oil Company of Illinois

Particle	Nominal Diameter D ft	Velocity v ft/sec	Reynolds Number R	Particle Density ρ_s Slugs/cu.ft.	Computed Drag Coef. C'_D	Boundary Correction m	Corrected Drag Coef. C_D
1. At 26.90°C, oil density 1.643 slugs per cu. ft., kinematic viscosity 0.00525 sq. ft. per sec., jar diameter 0.675 ft.							
C-4	0.02264	0.731	3.158	15.30	15.12	1.040	14.55
C-4	0.01907	0.575	2.087	15.18	20.37	1.038	19.60
C-4	0.01183	0.268	0.604	15.18	58.27	1.036	56.30
C-1/4	0.01182	0.264	0.594	15.18	60.00	1.037	57.90
C-1/4	0.00885	0.164	0.276	15.30	117.2	1.033	113.4
C-1/4	0.00752	0.117	0.1672	15.18	193.9	1.031	188.0
P-1/4	0.01551	0.398	1.175	15.30	34.85	1.042	33.4
P-1/4	0.01131	0.236	0.5075	15.30	72.3	1.037	69.7
D-4	0.01233	0.289	0.677	15.30	52.6	1.036	50.8
S-4	0.00766	0.125	0.1887	15.30	174.6	1.030	169.6
S-1	0.01301	0.409	1.014	15.10	27.26	1.027	26.6
2. At 27.40°C, oil density 1.643 slugs per cu. ft., kinematic viscosity 0.00507 sq. ft. per sec., jar diameter 0.675 ft.							
C-1	0.01421	0.475	1.330	15.30	22.40	1.025	21.82
C-1	0.01196	0.354	0.834	15.18	33.62	1.023	32.82
P-4	0.02295	0.784	4.150	15.30	13.33	1.033	12.90
P-4	0.01150	0.260	0.5896	15.30	60.50	1.031	58.60
P-1	0.01445	0.477	1.592	15.30	22.64	1.019	22.25
P-1	0.01162	0.331	0.8885	15.30	37.70	1.021	36.88
D-4	0.01593	0.436	1.608	15.30	29.86	1.032	28.90
S-4	0.02027	0.668	2.672	15.30	16.17	1.041	15.51
S-4	0.01242	0.309	0.757	15.30	46.37	1.032	44.90

(Continued on next page)

Table 12
(Continued)

Particle	Nominal Diameter D ft	Velocity v ft/sec	Reynolds Number R	Particle Density ρ_s Slugs/cu.ft.	Computed Drag Coef. C'_D	Boundary Correction m	Corrected Drag Coef. C_D
3. At 25.30°C, oil density 1.645 slugs per cu. ft., kinematic viscosity 0.005915 sq. ft. per sec., jar diameter 0.675 ft.							
D-1	0.01597	0.471	1.272	15.30	25.58	1.038	24.63
D-1	0.01233	0.300	0.6252	15.30	48.80	1.037	47.10
D-1/4	0.01713	0.357	1.034	15.30	47.80	1.078	44.30
D-1/4	0.01280	0.226	0.489	15.30	89.10	1.072	83.00
4. At 32.80°C, oil density 1.638 slugs per cu. ft., kinematic viscosity 0.00345 sq. ft. per sec., jar diameter 0.469 ft.							
S-1/4	0.02119	0.825	5.060	15.30	11.11	1.066	10.41
Summary of Results with Oil No. 15933, Standard Oil Company of Illinois							
1. At 28.70°C, oil density 1.615 slugs per cu. ft., kinematic viscosity 0.000795 sq. ft. per sec., jar diameter 0.681 ft.							
C-4	0.02264	1.723	49.10	15.30	2.780	1.015	2.740
C-4	0.01907	1.440	34.55	15.18	3.315	1.013	3.268
C-4	0.01183	0.872	13.00	15.18	5.605	1.008	5.565
C-1	0.01421	1.430	25.60	15.30	2.530	1.007	2.510
C-1/4	0.01182	0.876	13.02	15.18	5.540	1.009	5.490
C-1/4	0.00885	0.602	6.695	15.30	8.840	1.008	8.770
C-1/4	0.00752	0.504	4.745	15.18	10.65	1.008	10.58
P-4	0.02295	1.770	51.00	15.30	2.650	1.016	2.610
P-4	0.01150	0.830	12.00	15.30	6.050	1.007	6.010
P-1	0.01445	1.400	25.41	15.30	2.675	1.008	2.655
P-1	0.01162	1.090	15.93	15.30	3.555	1.006	3.535
D-4	0.01593	1.140	22.80	15.30	4.448	1.012	4.390

(Continued on next page)

Table 12
(Continued)

Particle	Nominal Diameter D ft	Velocity v ft/sec	Reynolds Number R	Particle Density ρ_s Slugs/cu.ft.	Computed Drag Coef. C'_D	Boundary Correction m	Corrected Drag Coef. C_D
D-4	0.01233	0.914	14.17	15.30	5.370	1.009	5.330
S-4	0.02027	1.556	39.62	15.30	3.050	1.017	3.000
S-4	0.01242	0.952	14.88	15.30	4.965	1.009	4.925
S-4	0.00766	0.532	5.12	15.30	9.770	1.007	9.720
S-1	0.01301	1.370	22.41	15.10	2.480	1.007	2.463
2. At 27.20°C, oil density 1.616 slugs per cu. ft., kinematic viscosity 0.000864 sq. ft. per sec., jar diameter 0.681 ft.							
D-1	0.01597	1.360	25.15	15.30	3.130	1.012	3.090
D-1	0.01233	1.030	14.70	15.30	4.220	1.009	4.190
D-1/4	0.01713	0.900	17.87	15.30	7.680	1.025	7.490
D-1/4	0.01280	0.705	10.43	15.30	9.330	1.023	9.110
C-1	0.01196	1.096	15.00	15.18	3.582	1.005	3.561
3. At 28.60°C, oil density 1.615 slugs per cu. ft., kinematic viscosity 0.000800 sq. ft. per sec., jar diameter 0.681 ft.							
P-1/4	0.01551	1.088	23.01	15.30	4.765	1.014	4.700
P-1/4	0.01131	0.772	10.92	15.30	6.880	1.008	6.830
4. At 27.10°C, oil density 1.616 slugs per cu. ft., kinematic viscosity 0.000869 sq. ft. per sec., jar diameter 0.681 ft.							
S-1/4	0.02119	1.443	35.20	15.30	3.680	1.019	3.610

Summary of Results with Oil No. 5618, Standard Oil Company of California

1. At 28.40°C, oil density 1.674 slugs per cu. ft., kinematic viscosity 0.000245 sq. ft. per sec., jar diameter 0.681 ft.							
C-4	0.02264	2.260	209.0	15.30	1.551	1.011	1.533

(Continued on next page)

Table 12
(Continued)

Particle	Nominal Diameter D ft	Velocity v ft/sec	Reynolds Number R	Particle Density s Slugs/cu.ft.	Computed Drag Coef. C'_D	Boundary Correction m	Corrected Drag Coef. C_D
C-4	0.01907	1.980	154.1	15.18	1.681	1.010	1.664
C-4	0.01183	1.310	63.3	15.18	2.387	1.006	2.375
C-1	0.01421	2.130	123.7	15.30	1.093	1.003	1.090
C-1	0.01196	1.810	88.4	15.18	1.262	1.002	1.259
C-1/4	0.01182	1.260	60.75	15.18	2.580	1.006	2.561
C-1/4	0.00885	0.960	34.65	15.30	3.352	1.004	3.338
C-1/4	0.00752	0.818	25.10	15.18	3.888	1.005	3.870
P-1	0.01445	2.100	123.9	15.30	1.142	1.004	1.138
P-1	0.01162	1.700	80.7	15.30	1.404	1.003	1.399
P-1/4	0.01551	1.460	92.85	15.30	2.516	1.012	2.480
D-4	0.01592	1.630	106.10	15.30	2.090	1.009	2.074
D-4	0.01233	1.325	66.70	15.30	2.447	1.006	2.433
S-4	0.02027	2.090	173.1	15.30	1.620	1.012	1.600
S-4	0.01242	1.390	70.5	15.30	2.242	1.006	2.230
S-4	0.00766	0.880	27.5	15.30	3.460	1.003	3.450
S-1	0.01301	2.080	110.5	15.10	1.033	1.003	1.030
2. At 27.05°C, oil density 1.677 slugs per cu. ft., kinematic viscosity 0.0002585 sq. ft. per sec., jar diameter 0.681 ft.							
D-1	0.01597	1.835	113.2	15.30	1.650	1.009	1.638
D-1	0.01233	1.534	73.15	15.30	1.827	1.006	1.816
D-1/4	0.01280	0.950	47.12	15.30	4.940	1.015	4.860
3. At 32.20°C, oil density 1.670 slugs per cu. ft., kinematic viscosity 0.000209 sq. ft. per sec., jar diameter 0.681 ft.							
P-1/4	0.01131	1.176	63.51	15.30	2.870	1.006	2.855
P-4	0.02295	2.380	261.5	15.30	1.416	1.010	1.400
P-4	0.01150	1.381	76.0	15.30	2.102	1.005	2.092
S-1/4	0.02119	1.748	177.0	15.30	2.420	1.014	2.382

(Continued on next page)

Table 12
(Continued)

Summary of Results with Oil No. 5617, Standard Oil Company of California

Particle	Nominal Diameter D ft	Velocity v ft/sec	Reynolds Number R	Particle Density s Slugs/cu.ft.	Computed Drag Coef. C'_D	Boundary Correction m	Corrected Drag Coef. C_D
At 29.05°C, oil density 1.616 slugs per cu. ft., kinematic viscosity 0.0000425 sq. ft. per sec., jar diameter 0.675 ft.							
C-4	0.2264	2.590	1380	15.30	1.226	1.007	1.218
C-4	0.01907	2.360	1059	15.18	1.231	1.006	1.225
C-4	0.01183	1.845	513.5	15.18	1.252	1.003	1.248
C-1/4	0.00885	1.134	235.7	15.30	2.498	1.003	2.488
C-1/4	0.00752	1.073	189.6	15.18	2.345	1.003	2.338
D-4	0.01593	2.100	785	15.30	1.311	1.005	1.304
D-4	0.01233	1.850	536	15.30	1.310	1.003	1.304
D-1	0.01597	2.100	786	15.30	1.313	1.005	1.307
D-1	0.01233	1.830	529	15.30	1.337	1.003	1.332
S-4	0.02027	2.630	1252	15.30	1.064	1.006	1.059
S-4	0.01242	1.885	550	15.30	1.271	1.003	1.269
S-4	0.00766	1.383	248.7	15.30	1.451	1.001	1.450
S-1	0.01301	3.040	930	15.10	0.505	1.001	0.504

Table 13

Physical and Hydraulic Properties
of
Particles Studied by Wilde

-RANDOM SAMPLE.

No.	F	W	A	a	b	c	Vol.	s.g.	d_n	An	s.f. (A)	c/ab	a/b	ab	abc	ab/A	abc/Vol	DATA IN WATER: ν x 10³	V	C_d(A)	C_d(ab)	C_d(d_n)	R(ab) x10⁻³	R(d_n) x10⁻³	DATA IN OIL: ν	V	C_d(A)	C_d(ab)	C_d(d_n)	R(ab)	R(d_n)
1	18.82	30.44	800	3.48	2.91	1.95	11.62	2.62	2.81	620	0.78	0.62	1.20	1010	19.7	126	1.69	9.9	76.2	0.77	0.63	0.80	24.6	22.8	0.60	85.7	0.74	0.59	0.75	455	400
2	10.01	16.20	480	2.70	2.15	1.86	6.19	2.62	2.27	405	0.85	0.77	1.25	580	10.8	121	1.76	9.9	77.7	0.68	0.56	0.63	19.0	17.9	0.60	77	0.82	0.67	0.76	309	291
3	6.86	11.06	703	3.37	3.10	0.91	4.20	2.63	2.00	311	0.45	0.28	1.09	1040	9.5	148	2.26	9.6	37.2	1.46	1.03	2.65	12.6	7.8	0.60	43.1	1.21	0.82	2.14	232	144
4	7.75	12.44	557	3.17	2.30	1.29	4.69	2.65	2.05	330	0.61	0.48	1.38	730	9.4	131	2.00	10.0	49.1	1.14	0.87	1.50	13.2	10.1	0.60	56	1.03	0.78	1.36	252	191
5	8.97	14.42	726	3.19	3.00	1.46	5.45	2.65	2.18	373	0.52	0.47	1.06	960	13.9	132	2.55	10.0	48.8	1.04	0.80	1.56	14.9	10.5	0.60						
6	1.84	3.00	258	1.87	1.67	0.68	1.16	2.58	1.32	137	0.53	0.38	1.12	311	2.12	121	1.83	10.2	34.8	1.18	0.97	1.75	5.9	4.4	0.60	38.4	1.12	0.93	1.66	113	85
7	2.85	4.59	380	2.70	1.77	0.62	1.74	2.64	1.48	172	0.46	0.28	1.53	477	3.96	126	2.27	10.3	34.2	1.23	0.98	2.11	7.3	4.9	0.60	37.8	1.21	0.96	2.10	138	93
8	0.46	0.75	79	1.30	0.94	0.60	0.29	2.61	0.82	53	0.61	0.54	1.38	122	0.73	154	2.52	9.9	33.2	0.94	0.68	1.22	3.7	2.9	0.60	26.8	1.90	1.23	2.23	49	36.5
9	0.69	1.11	123	1.38	1.67	0.46	0.42	2.64	0.92	67	0.55	0.38	1.18	162	0.79	132	1.86	9.9	29.2	1.32	1.00	1.89	3.7	2.1	0.60	29	1.55	1.18	2.23	62	45
10	0.69	1.11	85	1.43	0.91	0.75	0.42	2.65	0.92	67	0.72	0.65	1.57	130	1.00	153	2.36	9.6	41.8	0.87	0.62	0.95	5.0	3.9	0.60	32.6	1.80	1.18	1.79	62	50
11	0.41	0.67	67	1.05	0.93	0.70	0.26	2.65	0.79	50	0.68	0.71	1.13	98	0.68	146	1.60	10.0	43.3	0.60	0.45	0.68	4.2	3.4	0.60	27.2	1.92	1.32	2.04	45	36
12	1.34	2.15	135	1.52	1.13	0.95	0.81	2.65	1.15	104	0.78	0.72	1.36	171	1.63	127	2.01	10.0	46.3	0.91	0.72	1.30	6.1	5.4	0.60	41.3	1.36	1.03	1.37	90	79
13	2.49	4.00	248	2.05	1.64	0.90	1.50	2.66	1.43	160	0.64	0.49	1.25	335	3.02	135	2.00	9.3	51.2	0.75	0.56	0.92	10.1	7.9	0.60	50.5	0.92	0.68	1.11	154	120
14	2.48	4.02	398	2.85	1.80	0.55	1.54	2.61	1.43	160	0.41	0.24	1.58	510	2.82	128	1.83	10.0	30.2	1.40	1.07	2.65	6.7	4.3	0.60	36	1.12	0.87	2.17	135	96
15	1.26	2.05	245	2.73	1.83	0.69	0.78	2.61	1.15	104	0.42	0.38	1.58	335	2.32	137	2.95	9.6	27.4	1.36	0.99	2.52	5.2	3.4	0.60	28.6	1.44	1.05	2.66	87	55
16	0.12	0.19	49	1.34	0.54	0.27	0.07	2.67	0.52	21	0.43	0.36	1.93	56	0.15	115	2.06								0.60	13.4	3.2	2.8	5.8	17	12
17	0.42	2.41	174	1.66	1.38	0.85	1.00	2.42	1.24	121	0.69	0.56	1.20	228	1.95	131	1.85	9.3	42.4	0.89	0.68	1.01	6.9	5.6	0.60-	38.8	1.25	0.96	1.42	98	80
18	0.95	1.61	135	1.70	1.01	0.80	0.61	2.63	1.05	87	0.64	0.61	1.68	172	1.37	127	2.23	9.8	39.6	0.92	0.73	1.13	5.3	4.3	0.60	33.9	1.50	1.17	1.83	74	59
19	1.42	2.29	132	1.46	1.26	1.05	0.88	2.61	1.29	111	0.81	0.78	1.16	184	1.93	139	2.20	9.8	47.2	0.95	0.69	0.90	6.3	5.9	0.60	45.7	1.19	0.85	1.11	103	91
20	4.58	6.93	287	2.51	1.49	1.22	2.35	2.95	1.64	211	0.74	0.64	1.70	378	4.62	132	1.31	9.9	51.8	1.12	0.85	1.19	10.3	8.2	0.60-						
21	3.95	6.34	287	2.07	1.91	1.55	2.39	2.65	1.55	214	0.75	0.76	1.08	395	6.13	138	1.57	9.9	52.7	1.07	0.78	1.13	11.3	9.4	0.60	58.9	0.93	0.67	0.98	195	161
22	0.44	0.71	55	0.95	0.77	0.75	0.27	2.65	0.80	50	0.92	0.88	1.23	73	0.55	133	2.03								0.60	33	1.70	1.28	1.46	47	44
23	4.63	6.90	278	2.37	1.87	1.23	2.26	3.05	1.63	208	0.75	0.64	1.51	345	4.57	124	1.71								0.60						
24	1.96	3.20	200	1.86	1.22	1.10	1.24	2.58	1.33	139	0.70	0.73	1.52	320	2.50	160	2.00	9.8	50.3	0.78	0.65	0.87	7.8	6.2	0.60	43.2	1.21	0.76	1.37	129	96
25	1.75	2.83	161	1.74	1.65	1.16	1.08	2.60	1.27	126	0.79	0.78	1.39	217	2.53	135	2.33	9.6	49.1	0.89	0.66	0.88	7.6	6.5	0.60	45.6	1.21	0.90	1.21	112	96
26	0.78	1.28	174	2.30	0.88	0.60	0.49	2.58	1.10	95	0.49	0.42	2.61	202	1.21	116	2.44	9.8	28.0	1.14	0.97	1.61	4.1	3.2	0.60	25.8	1.56	1.35	2.26	61	47
27	6.58	10.70	445	2.75	2.22	1.47	4.12	2.60	2.01	316	0.72	0.60	1.24	606	8.96	136	2.16	9.8	56.7						0.60	57.1	1.04	0.77	1.15	216	192
28	1.63	2.60	222	1.92	1.54	0.59	0.96	2.70	1.23	119	0.53	0.34	1.25	295	1.74	133	1.81	9.6	33.5	1.30	1.00	1.96	6.0	4.2	0.60	35.7	1.34	1.01	1.97	102	73
29	1.11	1.86	120	1.35	1.25	1.00	0.71	2.62	1.11	97	0.81	0.76	1.05	173	1.73	144	2.43	9.6	45.7	0.90	0.62	0.88	6.3	5.5	0.60	39.2	1.44	1.00	1.40	86	72
30	1.82	4.31	193	1.89	1.30	0.98	1.48	2.89	1.41	156	0.81	0.62	1.45	245	2.41	127	1.62	9.8	53.1	0.66	0.52	0.64	8.9	8.0	0.60						
31	2.16	3.50	168	1.57	1.51	1.20	1.34	2.60	1.36	145	0.88	0.81	1.11	221	2.66	132	1.97	9.3	63.7	0.63	0.47	0.58	10.2	5.9	0.60	50.9	1.19	0.90	1.08	126	115
32	1.55	2.49	197	1.75	1.51	0.76	0.94	2.65	1.21	115	0.59	0.48	1.24	246	1.88	125	2.00	9.8	40.3	0.96	0.76	1.27	6.5	5.0	0.60	39.9	1.44	0.92	1.54	104	80
33	2.46	3.96	284	2.64	1.42	0.91	1.49	2.65	1.42	158	0.56	0.47	1.86	374	3.41	132	2.28	9.8	41.8	0.97	0.74	1.38	8.3	6.1	0.60	41.8	1.32	0.87	1.42	135	199
34	2.27	3.66	232	2.05	1.50	0.91	1.38	2.65	1.38	149	0.64	0.52	1.37	306	2.80	132	2.02	9.5	43.6	1.02	0.77	1.24	7.9	6.3	0.60	45.5	1.10	0.83	1.34	133	105
35	3.75	6.14	452	3.55	1.82	0.76	2.38	2.57	1.65	214	0.47	0.30	1.95	645	4.91	143	2.06	9.8	39.0	1.16	0.78	1.85	10.0	6.5	0.60	41.9	1.10	0.77	1.02	177	115
36	3.17	5.09	264	2.06	1.53	1.10	1.92	2.64	1.54	186	0.71	0.62	1.36	318	3.73	120	1.94	9.6	50.3	0.94	0.77	1.04	9.4	8.1	0.60	55.5	0.90	0.75	1.00	165	142
37	1.06	1.74	197	2.01	1.16	0.56	0.67	2.58	1.12	99	0.50	0.37	1.74	233	1.31	118	1.94	9.8	39.0	1.04	0.86	1.58	6.2	4.5	0.60	29.1	1.48	1.25	2.33	74	54
38	2.38	3.54	246	2.21	1.40	0.68	1.16	3.05	1.30	132	0.54	0.39	1.58	309	2.10	125	1.81	9.8	38.7	1.36	1.10	2.00	7.0	5.1	0.60						
39	2.30	3.75	197	1.99	1.32	1.10	1.45	2.58	1.40	154	0.79	0.68	1.51	263	2.89	133	1.99	9.6	45.1	1.07	0.83	1.10	7.7	6.6	0.60	49.3	1.12	0.83	1.12	133	115
40	8.08	13.15	426	2.53	2.20	1.91	5.07	2.59	2.14	360	0.85	0.81	1.15	558	10.6	131	2.10	9.8	70.4	0.75	0.52	0.69	17.0	15.5	0.60	71	0.87	0.66	0.81	279	254
41	2.26	3.63	258	1.97	1.70	0.94	1.37	2.65	1.37	147	0.58	0.51	1.16	334	3.15	130	2.30	9.8	80.8	1.03	0.79	1.40	7.6	5.8	0.60	42.5	1.12	0.87	1.54	130	97
42	4.81	7.77	400	2.38	2.23	1.12	2.95	2.63	1.78	249	0.62	0.48	1.07	530	5.95	133	2.01	9.6	50.6	0.96	0.71	1.19	12.2	9.4	0.60	50.5	1.09	0.82	1.38	194	150
43	8.07	13.13	458	2.57	2.26	1.71	5.06	2.59	2.14	360	0.79	0.71	1.14	578	9.9	126	1.96								0.60	71.5	0.80	0.63	0.80	286	255
44	11.56	17.50	710	3.20	2.88	1.15	5.91	2.95	2.27	404	0.56	0.38	1.11	920	10.6	130	1.80	9.6	52.7	1.14	0.88	1.57	17.2	11.8	0.60	58.8	1.09	0.84	1.50	298	222
45	3.83	6.25	303	2.54	1.68	1.20	2.42	2.58	1.66	216	0.72	0.58	1.51	426	5.12	141	2.11	9.8	47.3	1.13	0.90	1.73	10.0	7.1	0.60	55	0.96	0.68	1.06	190	152
46	1.03	1.65	129	1.46	1.12	0.82	0.62	2.65	1.06	88	0.69	0.64	1.30	163	1.32	126	2.11	9.8	38.1	1.10	0.87	1..			0.60	35.6	1.47	1.16	1.68	76	63
47	0.68	1.08	145				0.40	2.68	0.71	66	0.45	---	---												0.60						
48	0.42	0.65	65	1.06	0.84	0.59	0.26	2.57	0.77	47	0.71	0.62	1.30	92	0.54	141	2.02	9.8	39.4	0.74	0.57	0.87	4.0	3.2	0.60	27.8	1.68	1.38	2.10	44.5	36
49	1.19	1.95	148	1.68	1.38	0.97	0.75	2.59	1.12	99	0.67	0.64	1.22	232	2.25	157	2.99	9.8	42.1	0.93	0.59	1.10	6.5	4.7	0.60	27.4	2.50	1.89	2.95	69.5	51
50	2.60	4.20	213	1.96	1.45	1.10	1.59	2.63	1.45	165	0.77	0.65	1.35	284	3.14	116	1.97	9.9	60.4	0.66	0.49	0.64	10.4	9.0	0.60	50.5	1.12	0.84	1.13	142	122
51	0.65	1.06	142				0.40	2.62	0.91	66	0.46	---	---											2.4	0.60					
52	1.21	1.94	144	1.70	1.20	0.84	0.73	2.64	1.12	99	0.68	0.59	1.42	195	1.72	134	2.33	9.3	44.2	0.85	0.63	0.98	7.0	5.6	0.60	38.3	1.34	0.99	1.53	89	71
53	1.00	1.63	116	1.59	1.06	0.73	0.63	2.67	1.06	88	0.77	0.58	1.41	159	1.18	137	1.86	9.6	42.1	1.19	0.87	1.22	5.0	4.2	0.60	38.2	1.38	1.00	1.42	80	67
54	2.93	4.71	248	2.05	1.46	1.12	1.78	2.65	1.50	176	0.73	0.65	1.40	299	3.37	124	1.89	9.8	55.5	0.77	0.63	0.83	9.8	8.5	0.60						
55	1.18	1.92	145	1.53	1.18	1.00	0.73	2.62	1.12	99	0.68	0.75	1.29	180	1.81	124	2.48	9.3	39.0	1.05	0.84	1.22	5.9	4.7	0.60	36.8	1.26	1.02	1.46	87	73
56	1.80	2.89	255	1.91	1.77	0.85	1.09	2.64	1.25	128	0.50	0.46	1.63	338	2.87	132	2.63	9.8	36.6	1.04	0.78	1.62	7.2	4.7	0.60	36.8	1.21	0.91	1.28	113	79
57	0.17	0.29	52				0.11	2.60	0.59	28	0.55	---	---											1.4	0.60					
58	0.27	0.25	56	1.13	0.80	0.34	0.11	2.60	0.59	28	0.49	0.36	1.41	90	0.31	160	2.82	9.8	23.2	1.20	0.75	1.91	2.3	1.4	0.60	16.7	2.62	1.63	4.18	26.4	16.5
59	0.30	0.48	52	0.95	0.74	0.55	0.18	2.63	0.70	38	0.75	0.66	1.26	71	0.39	137	2.11	9.8	36.0	0.89	0.65	0.93	3.1	2.6	0.60	25.2	2.13	1.56	2.25	35.4	29
60	1.92	3.07	184	1.63	1.39	1.08	1.15	2.63	1.32	136	0.72	0.72	1.17	226	2.45	123	2.13	9.6	55.1	0.67	0.55	0.71	8.7	7.7	0.60	43.9	1.26	1.02	1.33	110	97
61	1.48	2.39	168	1.84	1.36	0.97	0.90	2.63	1.20	113	0.68	0.61	1.35	250	2.42	149	2.67	9.8	44.8	0.87	0.68	1.00	7.3	5.5	0.60	39.7	1.30	0.87	1.51	104	79
62	0.82	1.33	96	1.29	0.98	0.76	0.51	2.60	0.99	77	0.50	0.66	1.32	126	0.96	131	1.86	9.8	42.7	0.91	0.70	0.99	4.9	4.4	0.60	37.1	1.45	1.11	1.40	69.5	61
63	2.31	3.84	152	1.40	1.40	1.40	1.53	2.51	1.42	152	1.00	1.00	1.00	196	2.75	129	1.80	9.8	75.5	0.50	0.41	0.41	11.1	11.1	0.60	57.8	1.06	0.82	0.80	135	137
64	2.83	4.71	181	1.51	1.51	1.51	1.88	2.50	1.53	181	1.00	1.00	1.00	228	3.45	127	1.83	9.6	76.5	0.51	0.41	0.41	11.7	11.7	0.60	62.5	0.93	0.74	0.72	158	159
65	3.46	5.77	206	1.61	1.61	1.61	2.31	2.49	1.64	206	1.00	1.00	1.00	256	4.20	127	1.82	9.8	80.5	0.48	0.40	0.40	14.3	14.3	0.60	66	0.90	0.72	0.69	177	180

Table 13 (continued)

Physical and Hydraulic Properties
of
Particles Studied by Wilde

-POUDRE RIVER SAMPLE.

No.	Seive Size	F	W	a	b	c	Vol	s.g.	d_n	An	c / $\sqrt{ab}$	a/b	WATER γ x10³	V	C_d	R(d_n) x10⁻⁴	OIL γ	V	C_d	R(d_n)
70	1 "	7.89	12.76	2.66	2.06	1.68	4.86	2.62	2.10	3h6	0.72	1.29	10.5	68.5	0.75	133	0.92	69	0.87	157
71	3/4"	9.25	14.97	2.74	2.37	1.82	5.72	2.61	2.22	387	0.71	1.16	"	70.0	0.82	1h3	"	6h.5	1.0h	155
72	"	9.36	15.21	2.95	2.20	1.69	5.85	2.60	2.23	392	0.66	1.3h	"	68.7	0.78	1h1	"			
73	"	11.1h	17.95	h.30	2.08	1.77	6.80	2.6h	2.35	h33	0.59	2.06	"	53.6	1.h3	115	"	58.1	1.38	1h9
7h	"	12.92	20.8h	3.25	2.62	1.79	7.92	2.61	2.h7	h79	0.61	1.2h	"	77.2	0.70	175	"	7h	0.89	199
75	"	7.26	11.87	2.80	2.06	1.h0	h.60	2.57	2.06	335	0.58	1.36	"	69.7	0.68	13h	"	62.5	1.00	1h0
76	"	1h.10	22.63	3.30	2.50	1.80	8.53	2.66	2.53	50h	0.63	1.32	"	6h.3	1.0h	1h9	"	7h	0.93	20h
77	"	9.19	1h.56	h.50	2.60	1.25	5.37	2.71	2.17	370	0.37	1.73	"	39.1	2.72	76	"	h9.7	1.83	90
78	"	1h.53	23.32	3.75	2.59	1.70	8.79	2.65	2.56	51h	0.55	1.h5	"	69.0	0.92	160	"	69.5	1.06	19h
79	"	6.90	11.16	2.78	2.h7	1.32	h.26	2.62	2.01	317	0.50	1.12	"	60.9	0.91	112	"	51.3	1.51	112
80	"	3.96	6.39	2.10	1.82	1.3h	2.h2	2.63	1.66	218	0.69	1.15	"	5h.8	0.9h	8h	"	h9.7	1.3h	90
81	"	5.76	9.2h	2.93	1.76	1.2h	3.h8	2.65	1.88	277	0.55	1.67	"	h8.8	1.36	8h	"	5h	1.29	110
82	1/2"	h.h5	7.17	2.55	1.76	1.1h	2.71	2.6h	1.73	235	0.5h	1.h5	"	h8.0	1.26	76	"	52.6	1.2h	99
83	"	6.27	10.21	2.86	1.98	1.h5	3.9h	2.59	1.96	301	0.61	1.hh	"	5h.h	1.08	98	"	52.6	1.36	112
8h	"	6.08	9.66	2.52	1.92	1.h5	3.58	2.70	1.90	283	0.66	1.21	"	6h.2	0.80	112	"	6h.5	0.9h	133
85	"	h.03	6.h7	1.77	1.80	1.32	2.hh	2.65	1.67	219	0.7h	1.02	"	70.5	0.57	109	"	57.1	1.02	10h
86	"	h.h2	7.1h	2.1h	1.97	1.1h	2.72	2.62	1.73	235	0.69	1.09	"	52.5	1.0h	8h	"	5h	1.17	101
87	"	h.35	7.08	2.01	1.95	1.5h	2.73	2.59	1.73	235	0.78	1.03	"	61.3	0.76	98	"	55.6	1.09	10h
88	"	h.88	7.93	2.13	1.82	1.h7	3.0h	2.60	1.80	255	0.75	1.17	"	63.5	0.73	105	"			
89	"	5.25	8.h0	2.71	1.95	1.15	3.1h	2.67	1.82	260	0.50	1.39	"	53.8	1.07	89	"	52.6	1.33	10h
90	"	1.99	3.21	2.27	1.26	0.97	1.21	2.6h	1.32	138	0.57	1.80	"	36.h	1.68	hh	"			
91	3/8"	1.56	2.53	1.h7	1.36	0.95	0.96	2.62	1.22	118	0.67	1.08	"	h7.1	0.92	53	"			
92	"	2.09	3.h3	1.78	1.hh	0.97	1.33	2.56	1.36	1h7	0.61	1.23	"	h5.3	1.06	58	"	hh.5	1.31	66
93	"	0.83	1.35	1.50	1.22	0.65	0.51	2.61	0.59	78	0.h8	1.23	"	3h.5	1.38	32	"	28.2	2.h5	31
9h	"	1.22	1.86	1.65	1.05	0.75	0.63	2.9h	1.06	89	0.57	1.57	"	h1.6	1.22	h1	"	37.7	1.77	hh
95	"	2.55	h.08	1.93	1.55	1.25	1.52	2.67	1.h3	161	0.72	1.25	"	50.h	0.96	66	"			
96	"	1.22	1.91	1.60	1.23	0.70	0.69	2.77	1.10	95	0.50	1.30	"	30.5	2.13	32	"	3h.5	1.95	h1
97	"	1.27	2.08	1.7h	1.17	0.83	0.80	2.59	1.15	10h	0.58	1.h9	"	---	--	--	"	36.6	1.67	h6
98	"	1.62	2.58	1.90	1.22	0.90	0.96	2.69	1.22	117	0.59	1.56	"	h6.2	0.99	52	"	38.6	1.70	51
99	"	1.08	1.70	1.90	1.35	0.53	0.62	2.7h	1.06	88	0.3h	1.35	"	30.0	2.09	29.2	"	27.6	2.92	32
100	"	0.20	0.32	1.09	0.96	0.22	0.12	2.56	0.62	306	0.21	1.13	"	18.8	2.81	11	"	1h.2	5.90	9.6
101	"	0.h8	0.76	1.65	1.21	0.29	0.28	2.67	0.81	52.5	0.20	1.36	"	--	--	--	"	18.9	h.7	16.8
102	No. h	0.1h	0.23	0.71	0.51	0.h5	0.09	2.59	0.56	2h.6	0.75	1.39	"	--	--	--	"	16.3	h.05	10
103	"	0.30	0.h8	0.78	0.70	0.57	0.18	2.67	0.70	38.5	0.77	1.11	"	--	--	--	"	23.7	2.52	18.0
10h	"	0.28	0.h6	0.90	0.82	0.50	0.17	2.58	0.69	38.3	0.58	1.10	"	32.5	1.07	21	"	20.9	3.06	15.8
105	"	0.26	0.60	0.95	0.90	0.56	0.23	2.58	0.76	h5.7	0.61	1.05	"	h1.8	0.71	29	"	23.5	2.66	19.2
106	"	0.h2	0.68	1.16	0.6h	0.50	0.26	2.58	0.79	h8.8	0.58	1.82	"	39.0	0.80	29	"	23.6	2.75	20.5
107	"	0.26	0.h2	0.90	0.70	0.55	0.15	2.70	0.66	35.1	0.69	1.28	"	32.5	1.05	20	"			
108	"	0.19	0.31	1.00	0.65	0.h5	0.12	2.60	0.61	29.5	0.56	1.5h	"	30.3	1.05	17	"	17.2	h.03	11.5
109	"	0.30	0.h8	1.1h	0.73	0.h6	0.18	2.63	0.70	39.0	0.50	1.56	"	30.3	1.29	20	"	19.8	3.60	15.2
110	"	0.09	0.16	0.71	0.hh	0.h1	0.06	2.62	0.h8	18.7	0.73	1.61	"	32.1	0.79	1h	"	1h.2	h.8	7.5
111	No. 6	0.05	0.09	0.50	0.39	0.35	0.03	2.63	0.h0	13.1	0.79	1.28	"	27.h	0.91	10	"	11.8	5.8	5.2
112	"	0.0h	0.07	0.61	0.h3	0.21	0.02	2.69	0.36	10.6	0.h1	1.h2	"	19.5	1.68	7	"			
113	"	0.10	0.18	0.85	0.h3	0.38	0.06	2.59	0.50	20.0	0.63	1.98	"	25.5	1.27	12	"	13.5	5.3	7.h
11h	"	0.06	0.11	0.61	0.h6	0.25	0.03	2.58	0.h1	13.6	0.h7	1.33	"	23.3	1.23	9	"	10.6	7.1	h.8
115	"	0.06	0.11	0.71	0.h2	0.31	0.0h	2.52	0.h3	1h.6	0.57	1.69	"	---	--	--	"	10.7	7.0	5.0
116	"	0.12	0.22	0.96	0.h8	0.33	0.07	2.60	0.52	21.5	0.h9	2.00	"	25.3	1.2h	12	"	13.7	5.h	7.8
117	"	0.06	0.11	0.53	0.5h	0.27	0.0h	2.5h	0.hh	15.3	0.h8	1.09	"	25.9	1.03	11	"	11.1	6.7	5.3
118	"	0.08	0.1h	0.61	0.60	0.29	0.05	2.60	0.h6	17.2	0.h8	1.02	"	--	--	--	"	11.5	6.9	5.9
119	"	0.03	0.0h	0.h6	0.38	0.29	0.02	2.5h	0.35	10.1	0.60	1.21	"	25.6	2.06	8	"	9.06	8.2	3.5

Table 13 (continued)

Physical and Hydraulic Properties
of
Particles Studied by Wilde

-CRUSHER PLANT SAMPLE.

No.	Seive Size	F	W	a	b	c	Vol	s.g.	d_n	An	$\sqrt{ab}$	$\frac{a}{b}$	WATER $\nu \times 10^5$	V	$C_{(d_n)}$	$R_{(d_n)} \times 10^5$	OIL ν	V	$C_{(d_n)}$	$R_{(d_n)}$
120	1 in	14.74	23.64	3.30	2.88	2.45	8.90	2.66	2.57	517	0.79	1.15	1.11	58.1	1.30	135	0.92	66.2	1.18	185
121	3/4"	10.24	16.52	3.27	2.44	2.36	6.27	2.63	2.29	411	0.84	1.34	"				"	60.6	1.23	151
122	"	5.72	9.14	3.18	2.47	1.18	3.42	2.67	1.87	274	0.42	1.29	"	36.1	2.45	61	"	42.2	2.13	90
123	"	7.50	12.14	3.21	2.35	1.58	4.64	2.62	2.07	336	0.58	1.37	"	52.7	1.23	99	"	55.6	1.31	125
124	"	3.75	6.05	3.59	2.40	1.13	2.30	2.63	1.64	211	0.39	1.50	"	62.5	0.70	94				
125	"	6.65	10.81	2.89	2.70	1.16	4.16	2.60	2.00	314	0.42	1.07	"	40.0	2.04	73	"	43.5	2.03	95
126	"	8.65	14.08	3.77	2.03	1.89	5.42	2.59	2.18	373	0.68	1.86	"	46.0	1.54	94	"	54.0	1.45	128
127	"	11.99	19.10	2.96	2.54	1.79	7.11	2.69	2.39	448	0.65	1.17	"	61.0	1.10	133	"	59.9	1.35	155
128	"	7.69	12.20	3.06	2.25	2.00	4.50	2.69	2.05	330	0.79	1.36	"	52.0	1.32	96	"	57.5	1.28	128
129	"	5.16	8.23	2.57	2.27	1.75	3.06	2.69	1.80	252	0.72	1.13	.62	53.5	1.09	86	"	50.5	1.44	99
130	"	4.23	6.81	2.49	2.26	1.24	2.57	2.65	1.70	227	0.52	1.10	"	45.5	1.38	70	"			
131	"	2.70	4.16	2.25	1.84	1.04	1.45	2.67	1.41	156	0.51	1.22	"	48.0	1.15	61	"	37.8	2.20	58
132	1/2"	4.20	6.72	3.66	1.71	0.90	2.52	2.66	1.69	224	0.36	2.14	"	47.0	1.30	72	"	37.0	2.50	68
133	"	2.88	4.68	2.45	1.70	1.33	1.80	2.60	1.51	179	0.65	1.84	"	40.9	1.48	56	"	40.4	1.80	66
134	"	5.77	9.35	3.02	2.06	1.85	3.57	2.62	1.90	284	0.74	1.46	"	50.3	1.23	87	"			
135	"	3.60	5.82	2.50	2.50	1.02	2.22	2.62	1.62	206	0.40	1.00	"	41.4	1.59	60	"	43.5	1.68	77
136	"	2.52	4.04	1.93	1.82	1.57	1.52	2.66	1.43	161	0.84	1.06	"				"			
137	"	3.91	6.27	3.12	2.00	1.10	2.35	2.66	1.65	214	0.44	1.56	"	36.0	2.18	54	"			
138	"	2.53	4.06	2.24	1.89	1.06	1.53	2.65	1.43	161	0.52	1.19	"	37.0	1.76	47	"	37.8	2.00	59
139	"	3.38	5.74	2.19	1.51	1.15	2.35	2.44	1.65	213	0.63	1.45	.56	49.0	1.01	73	"	46.3	0.63	83
140	"	1.71	2.74	2.02	1.45	0.80	1.03	2.66	1.25	123	0.47	1.39	"	39.0	1.41	44	"	32.2	2.45	44
141	"	0.56	0.91	1.47	1.30	0.47	0.34	2.64	0.87	59.3	0.36	1.13	"	29.7	1.60	24	"	20.6	4.08	19.8
142	3/8"																"	21.0	6.50	33
143	"	5.11	0.79	2.15	1.51	1.23	0.30	2.63	0.83	54.4	0.68	1.42	"	41.7	0.80	31	"			
144	"	1.02	1.64	1.59	1.49	0.80	0.62	2.65	1.06	88	0.52	1.07	"	36.9	1.30	36	"	27.4	2.80	32
145	"	1.27	2.05	3.08	1.74	0.36	0.78	2.64	1.14	102	0.16	1.77	"	30.7	2.04	32	"	19.6	5.90	24
146	"	0.57	0.92	1.61	1.61	0.40	0.34	2.67	0.87	59.3	0.40	1.00	"	21.7	3.18	17	"	20.4	4.23	19.6
147	"	0.85	1.38	1.32	1.01	0.99	0.52	2.64	1.00	78.6	0.86	1.31	"				"	32.6	1.87	35
148	"	0.96	1.52	1.91	1.51	0.67	0.56	2.70	1.02	82.5	0.39	1.27	"	26.5	2.54	25	"	24.0	3.70	27
149	"	0.67	1.08	1.73	1.19	0.61	0.41	2.62	0.92	67	0.43	1.45	.46	28.1	1.93	24	"	22.2	3.70	22
150	"	0.25	0.41	0.95	0.58	0.57	0.15	2.62	0.67	35.2	0.77	1.64	1.11	32.3	1.08	19	"	20.3	3.20	14.8
151	"	0.42	0.68	1.29	0.90	0.62	0.26	2.63	0.79	42.5	0.58	1.43	"	32.0	1.29	18	"	22.8	3.02	19.7
152	No. 4	0.55	0.86	2.03	0.65	0.45	0.21	2.75	0.84	56	0.39	3.13	"	37.0	1.12	28	"			
153	"	0.13	0.22	0.76	0.66	0.45	0.09				0.64	1.15	"	39.2			"	15.8		
154	"	0.28	0.44	1.30	0.73	0.51	0.16	2.67	0.68	36.7	0.51	1.78	"	27.6	1.55	17	"			14.3
155	"	0.39	0.63	1.17	0.99	0.45	0.24	2.65	0.77	86.6	0.42	1.18	"	29.6	1.49	20	"	20.8	3.59	17.5
156	"	0.33	0.54	1.06	0.73	0.72	0.20	2.63	0.73	42.2	0.82	1.45	"	37.3	0.88	25	"	22.0	3.01	17.5
157	"	0.22	0.36	1.41	0.96	0.28	0.13	2.66	0.64	32.2	0.24	1.47	"	18.9	3.03	11	"	14.0	6.6	9.7
158	"	0.15	.25	0.95	0.80	0.46	0.09	2.65	0.56	25.0	0.67	1.80	"	25.7	1.44	13	"	16.3	4.28	10
159	"	0.21	.34	0.77	0.61	0.60	0.12	2.67	0.62	30.9	0.87	1.26	.59	32.5	1.01	18	"	20.1	3.14	13.7

Table 13 (continued)

Physical and Hydraulic Properties
of
Particles Studied by Wilde

—GLACIAL MORRAINE SAMPLE

No.	Seive Size	F	W	a	b	c	Vol	s.g.	d_n	An	C $\sqrt{ab}$	a/b	WATER ν ×10³	WATER V	WATER C(d)/d_n	WATER R(d)/d_n ×10⁻³	OIL ν	OIL V	OIL C(d)/d_n	OIL R(d)/d_n
160	1 in	6.60	10.66	2.07	2.01	1.66	4.05	2.63	1.98	307	0.81	1.03	10.7				0.60	69.5	0.81	229
161	3/4"	10.92	17.11	3.15	2.56	1.67	6.19	2.77	2.27	450	0.59	1.23	"	61.5	1.09	132	"			
162	"	16.08	26.14	3.55	2.53	2.17	10.06	2.60	2.73	584	0.72	1.41	"	65.5	0.98	170	"	77.0	0.84	350
163	"	15.85	25.48	3.56	2.26	2.25	9.63	2.64	2.64	546	0.79	1.58	"	81.5	0.67	205	"	80.0	0.82	351
164	"	7.49	12.16	2.47	2.07	1.89	4.66	2.60	2.07	336	0.84	1.19	"	68.5	0.73	139	"	66.7	0.91	230
165	"	21.02	32.79	3.77	2.80	2.36	11.77	2.78	2.82	623	0.73	1.35	"	80.0	0.81	215	"	100	0.61	470
166	"	13.15	21.31	3.55	2.46	1.90	8.15	2.61	2.50	490	0.64	1.45	"	68.0	0.89	156	"	71.5	0.95	297
167	"	6.57	10.52	2.26	2.23	1.53	3.94	2.67	1.96	302	0.68	1.01	"	61.2	0.89	112	"			
168	"	14.52	23.17	3.56	2.72	1.85	8.64	2.68	2.54	507	0.60	1.31	"	74.3	0.80	173	"	64.5	1.26	273
169	"																			
170	3/4"	2.66	4.26	1.87	1.82	1.01	1.60	2.66	1.45	165	0.55	1.03	"	45.4	1.20	63				
171	1/2"	2.58	4.15	1.92	1.67	1.35	1.56	2.65	1.44	163	0.75	1.15	"	49.5	0.99	65	"	47.6	1.27	114
172	"	2.62	4.22	1.82	1.43	1.29	1.60	2.64	1.45	165	0.80	1.27	"	57.5	0.74	78	"	51.3	1.10	124
173	"	6.06	9.77	2.58	2.52	1.30	3.71	2.64	1.92	289	0.66	1.02	"	53.0	1.10	95	"			
174	"	5.01	8.09	2.70	1.80	1.29	3.08	2.62	1.80	255	0.59	1.50	"	54.0	1.04	93	"	55.9	1.14	168
175	"	2.88	4.63	2.64	1.40	1.12	1.74	2.65	1.49	176	0.58	1.88	"	42.6	1.38	59	"	47.0	1.36	116
176	"	5.81	9.31	2.74	1.62	1.60	3.50	2.66	1.88	277	0.76	1.69	"	53.2	1.14	93	"	62.0	0.99	194
177	"	3.09	4.94	2.07	1.61	1.04	1.84	2.68	1.52	181	0.57	1.28	"	54.5	0.89	77	"	55.2	1.02	140
178	"	5.26	8.45	2.53	2.09	1.25	3.18	2.65	1.82	260	0.54	1.21	"	59.0	0.89	97	"	58.9	1.06	178
179	"	3.60	5.87	2.04	1.80	1.18	2.27	2.58	1.63	208	0.62						"	55.6	1.01	151
180	"	1.00	1.61	1.40	1.07	1.03	0.61	2.65	1.05	86.5	0.84	1.31	"	45.0	0.88	43	"	40.0	1.33	70
181	"	1.88	3.04	2.62	1.25	0.75	1.16	2.62	1.30	134	0.41	2.10	"	42.8	1.18	52	"	39.4	1.65	86
182	3/4"	1.61	2.58	1.75	1.65	0.72	0.97	2.65	1.23	119	0.42	1.06	"	37.4	1.49	43	"	39.7	1.56	81
183	"	1.38	2.23	1.49	1.25	1.02	0.85	2.63	1.17	108	0.75	1.19	"	49.0	0.82	54	"	42.9	1.27	84
184	"	2.11	3.35	1.64	1.32	1.08	1.24	2.70	1.33	139	0.73	1.24	"	54.0	0.80	66	"	49.7	1.12	110
185	"	1.42	2.29	1.73	1.30	0.91	0.86	2.66	1.18	109	0.61	1.33	"	36.5	1.50	39.5	"	37.3	1.71	74
186	"	0.90	1.46	1.43	1.26	0.71	0.56	2.60	1.02	82.5	0.53	1.13	"	39.0	1.11	38	"	31.8	1.97	54
187	"	1.97	3.16	1.89	1.35	1.26	1.18	2.67	1.31	135	0.79	1.40	"	51.2	0.85	63	"	47.5	1.18	104
188	"	2.63	4.19	2.03	1.65	1.22	1.55	2.69	1.44	163	0.67	1.23	"	48.2	1.06	65	"	49.7	1.20	119
189	"	2.29	3.69	1.65	1.65	1.20	1.40	2.64	1.39	152	0.73	1.00	"	45.5	1.14	59	"	43.9	1.42	102
190	3/8"	0.57	0.76	1.57	0.70	0.54	0.24	3.08			0.52	2.24	"	35.2			"	27.3		
191	"	0.60	0.98	1.25	0.99	0.87	0.38	2.60	0.89	63.3	0.78	1.26	"	43.2	0.80	36	"	32.2	1.68	48
192	No. 4	0.23	0.38	0.81	0.69	0.59	0.14	2.65	0.65	33.2	0.79	1.37	"							
193	"	0.28	0.46	1.01	0.67	0.60	0.17	2.65	0.69	37.5	0.72	1.51	"	34.3	1.00	23				
194	"	0.23	0.37	0.92	0.73	0.57	0.14	2.66	0.64	32.9	0.70	1.26	"	30.7	1.17	21	"	21.0	2.91	23
195	"	0.33	0.53	1.09	0.82	0.59	0.20	2.66	0.72	41.5	0.62	1.33	"	35.1	1.02	24	"	22.7	2.85	27
196	"	0.34	0.54	1.11	0.78	0.57	0.20	2.69	0.73	41.8	0.62	1.42	"	33.2	1.15	22	"	24.8	2.44	30
197	"	0.17	0.28	0.78	0.76	0.39	0.11	2.55	0.59	28	0.51	1.03	"	29.0	1.14	16	"	19.3	3.03	18.2
198	"	0.60	.97	1.00	0.90	0.65	0.37	2.59	0.89	63	0.69	1.11	"	34.0	1.27	29	"	31.7	1.73	47
199	"	0.64	.03	1.40	0.94	0.77	0.38	2.62	0.90	64	0.67	1.49	"	35.6	1.22	31	"	31.1	1.90	47

Table 14

Physical and Hydraulic Properties
of
Particles Studied by Schulz

Particle Number	Mineral Type	Particle Dimensions a mm	b mm	c mm	Shape Factor	Volume cc	Nominal Diameter mm	S.G.	F gm	Kinematic Viscosity cm^2/sec	Fall Velocity cm/sec	Re (d_n)	$C_{D(d_n)}$
Sample of Rock Crusher Fragments Retained on No. 20 Tyler Standard Sieve													
B20.1	Q	1.12	1.04	.70	.694	.00038	.90	2.65	.00063	.0110	11.08	90.5	1.27
B20.2	Q	1.48	1.04	.91	.733	.00057	1.03	2.65	.00094	.0110	11.72	110	1.30
B20.3	M	2.80	1.93	.11	.038	.00018	.70	2.8	.000325	.0110	5.42	34.5	4.51
B20.4	F	1.52	1.34	1.005	.705	.00082	1.60	2.57	.00335	.0110	13.28	193	1.49
B20.5	Q	1.28	1.10	.78	.657	Lost							
B20.6	F	2.02	1.68	.71	.385	Lost							
B20.7	Q	1.56	1.04	.71	.557	Lost				.0110	11.71		
B20.8	Q	1.50	1.44	1.22	.833	Lost				.0109	13.02		
B20.9	Q	1.64	1.58	.60	.374	.00060	1.04	2.65	.00097	.0113	8.81	81	2.27
B20.10	F	1.16	1.15	.70	.608	.00037	.89	2.57	.00059	.0111	10.98	88	1.23
Retained on No. 24 Tyler Standard Sieve													
B24.1	Q	1.40	1.00	.43	.365	.00013	.63	2.65	.000217	.0113	7.00	39	2.24
B24.2	G	1.32	.94	.63	.566	.00028	.81	4.00	.0090	.0116	14.50	101	1.24
B24.3	F	2.16	1.00	.36	.246	.00031	.84	2.57	.000485	.0117	5.54	40	4.56
B24.4		1.04	.96	.58	.58	.00022	.74	2.65	.00032	.0118	8.57	54	1.74
B24.5	B	1.16	.90	.64	.625	.00035	.87	3.0	.00066	.0116	9.50	71	1.94
B24.6	B	1.56	1.00	.49	.393	.00039	.91	3.0	.00074	.0113	10.00	81	1.80
B24.7	X	1.48	1.12	.68	.528	.00050	.99	2.8	.00092	.0113	10.68	94	1.65
B24.8	F	1.90	1.10	.51	.353	.00054	1.01	2.57	.00084	.0113	8.25	74	2.44
B24.9	F	1.08	1.00	.66	.635	.00030	.83	2.57	.000465	.0113	8.84	65	1.74
B24.10	Q	1.30	1.12	.71	.695	.00045	.95	2.65	.00074	.0113	10.38	87	1.52

(Continued on next page)

Table 14
(Continued)

Particle Number	Mineral Type	Particle Dimensions a mm	b mm	c mm	Shape Factor	Volume cc	Nominal Diameter mm	S.G.	F gm	Kinematic Viscosity cm^2/sec	Fall Velocity cm/sec	Re (d_n)	$C_{D(d_n)}$
Retained on No. 28 Tyler Standard Sieve													
B28.1	M	1.46	1.00	.14	.116	.00009	.55	2.8	.000158	.0110	4.30	37	4.73
B28.2	F	1.32	1.06	.42	.355	.00025	.78	2.57	.00040	.0110	6.63	47.1	2.91
B28.3	F	1.28	.88	.45	.424	.00020	.72	2.57	.00030	.0110	7.14	47	2.34
B28.4	Q	.86	.80	.66	.797	.00019	.71	2.65	.00031	.0113	9.44	59	1.36
B28.5	F	1.36	.70	.67	.687	.00053	1.00	2.57	.00082	.0113	9.53	84	1.81
B28.6	Q	1.36	.96	.39	.341	.00025	.78	2.65	.000415	.0113	6.92	48	2.87
B28.7	Q	1.16	.70	.62	.688	.00024	.77	2.65	.00040	.0113	8.55	58	1.86
B28.8	Q	.94	.72	.49	.596	.00012	.61	2.65	.000195	.0113	5.58	30.2	3.46
B28.9	X	2.06	.76	.43	.343	.00030	.83	2.8	.00054	.0113	7.29	56	2.96
B28.10	F	1.08	.84	.60	.630	.00025	.78	2.57	.000395	.0109	7.96	57	2.01
Retained on No. 35 Tyler Standard Sieve													
B35.1	M	1.56	.78	.07	.064	.00003	.37	2.8	.000047	.0109	3.35	11.4	6.03
B35.2	X	.94	.76	.37	.437	.00012	.61	2.8	.000215	.0109	6.17	35	3.04
B35.3	Q	.88	.68	.30	.388	.00008	.53	2.65	.000130	.0110	5.83	28	2.71
B35.4	Q	.92	.70	.45	.562	.00015	.65	2.65	.000220	.0110	6.45	38	2.72
B35.5		.84	.80	.28	.342	.00009	.55	2.65	.000123	.0110	5.18	26	3.65
B35.6	Q	.78	.46	.45	.752	.00007	.51	2.65	.000108	.0113	6.23	28.2	2.26
B35.7	Q	.64	.62	.62	.985	.00013	.63	2.65	.00022	.0113	8.73	49	1.43
B35.8	Q	.88	.56	.40	.570	.00009	.55	2.65	.000148	.0113	5.98	29.2	2.65
B35.9	F	.92	.84	.24	.273	.00012	.61	2.57	.000186	.0116	4.93	26	4.20
B35.10	F	1.14	.61	.51	.612	.00026	.79	2.57	.00041	.0117	7.05	47.6	2.59

(Continued on next page)

Table 14
(Continued

Particle Number	Mineral Type	Particle Dimensions a mm	b mm	c mm	Shape Factor	Volume cc	Nominal Diameter mm	S.G.	F gm	Kinematic Viscosity cm²/sec	Fall Velocity cm/sec	Re (d_n)	$C_{D(d_n)}$
Retained on No. 48 Tyler Standard Sieve													
B48.1	B	.48	.42	.38	.849	Lost		3.0					
B48.2	Q	.76	.50	.23	.374	.00004	.42	2.65	.000576	.0101	3.85	16	4.96
B48.3	M	.64	.54	.09	.153	.00002	.33	2.8	.000033	.0101	2.79	9.1	8.20
B48.4	M	.44	.44	.14	.318	.00001	.26	2.8	.000018	.0100	3.01	7.8	5.50
B48.5	Q	.96	.40	.35	.567	.00006	.48	2.65	.000097	.0100	4.90	23.5	3.52
B48.6	Q	.74	.40	.16	.295	.00002	.33	2.65	.000031	.0100	3.32	10.9	5.17
B48.7	B	.88	.40	.26	.439	.00005	.45	3.0	.000090	.0101	4.07	18.1	5.45
B48.8	C	.92	.44	.22	.347	.00004	.42	2.72	.0000635	.0101	3.42	14.2	6.45
B48.9	Q	.62	.46	.26	.488	.00004	.42	2.65	.000057	.0102	4.14	17.1	4.31
B48.10	T	.56	.54	.30	.548	.00005	.45			.0102	5.47	24.2	
Retained on No. 60 Tyler Standard Sieve													
B60.1	Q	.40	.30	.26	.753	.000012	.27	2.65	.0000185	.0110	8.82	21.6	6.00
B60.2	Q	.68	.30	.25	.555	.000025	.35	2.65	.000037	.0110	4.12	13.1	3.58
B60.3	Ga	.48	.32	.18	.461	.000012	.27	7.50	.000039	.0114	3.63	8.6	7.28
B60.4	Q	.46	.32	.21	.549	.000013	.29	2.65	.000021	.0113	2.93	7.5	5.98
B60.5	Q	.40	.36	.18	.475	.000012	.27	2.65	.0000175	.0112	2.85	6.8	5.8
B60.6	Q	.48	.30	.26	.687	.000017	.31	2.65	.0000265	.0112	3.70	10.2	3.99
B60.7	Q	.50	.28	.20	.535	.000011	.25	2.65	.0000137	.0110	1.95	4.4	11.33
B60.8	B	.70	.36	.13	.260	Lost		3.0					
B60.9	M	.60	.42	.03	.060	.000005	.20	2.8	.0000074	.0102	0.96	1.9	12.80
B60.10	F	.50	.38	.03	.069	.000005	.20	2.57	.0000068	.0102	1.28	2.5	18.50

(Continued on next page)

Table 14
(Continued)

Particle Number	Mineral Type	Particle Dimensions a mm	b mm	c mm	Shape Factor	Volume cc	Nominal Diameter mm	S.G.	F gm	Kinematic Viscosity cm^2/sec	Fall Velocity cm/sec	Re (d_n)	$C_{D(d_n)}$
Retained on No. 65 Tyler Standard Sieve													
B65.1	Q	.28	.22	.20	.807	Lost		2.65					
B65.2	Q	.42	.28	.13	.381	Lost		2.65					
B65.3	Q	.48	.28	.23	.630	.000011	.25	2.65	.0000138	.0102	1.78	4.37	13.50
B65.4	Q	.30	.28	.21	.727	.000010	.24	2.65	.0000125	.0102	2.37	5.58	7.45
B65.5	M	.44	.36	.04	.101	Lost		2.8					
B65.6	Ga	.40	.30	.12	.347	.000008	.24	7.50	.0000235	.0102	1.23	2.9	4.40
B65.7	M	.40	.36	.04	.106	Lost		2.8					
B65.8	Q	.40	.28	.20	.60	Lost		2.65					
B65.9	F	.48	.24	.20	.592	.000011	.25	2.57	.0000134	.0102	2.03	4.97	9.82
B65.10	B	.68	.28	.12	.276	.000011	.25	3.00	.0000134	.0102	0.61	1.5	10.41

B - Biotite
C - Calcite
F - Feldspar
G - Garnet
Ga - Galena
M - Mica or Vermiculite
Q - Quartz or Chalcedony
X - Mixture

Table 14

Physical and Hydraulic Properties
of
Particles Studied by Schulz

Particle Number	Mineral Type	Particle Dimensions a mm	b mm	c mm	Shape Factor	Volume cc	Nominal Diameter mm	S.G.	F gm	Kinematic Viscosity cm^2/sec	Fall Velocity cm/sec	Re (d_n)	C_D (d_n)
Sample of sand from Wolf Creek below Ft. Supply Dam, Oklahoma													
Retained on No. 14 Tyler Standard Sieve													
L14.1	Q	1.94	1.78	1.00	.54	.00170	1.48	2.65	.00285	.0112	13.03	173	1.52
L14.2	Q	1.60	1.30	1.12	.78	.00108	1.27	2.65	.00175	.0112	15.62	177	0.90
L14.3	Q	1.56	1.44	1.34	.90	.00141	1.39	2.65	.00235	.0112	16.35	204	.83
L14.4	Q	1.64	1.52	1.17	.74	.00138	1.38	2.65	.00230	.0110	15.96	200	.95
L14.5	Q	1.80	1.62	1.19	.70	.00160	1.45	2.65	.00265	.0110	16.18	214	.96
L14.6	X	1.72	1.40	1.26	.81	.00141	1.39	2.65	.00235	.0110	16.04	203	.94
L14.7	X	1.92	1.60	.75	.43	.00108	1.27	2.65	.00175	.0108	10.36	122	2.04
L14.8	Q	1.68	1.56	1.14	.71	.00136	1.37	2.65	.00225	.0108	15.78	200	1.11
L14.9	Q	1.56	1.44	.95	.64	.00103	1.20	2.65	.00165	.0108	13.82	154	1.09
L14.10	Q	1.68	1.52	1.19	.76	.00158	1.48	2.65	.00285	.0108	16.20	222	.98
Retained on No. 16 Tyler Standard Sieve													
L16.1	Q	2.02	1.36	1.14	.69	.00150	1.42	2.65	.00251	.0106	15.95	214	1.05
L16.2	Q	1.56	1.38	.74	.51	.00080	1.15	2.65	.00132	.0106	12.26	133	1.33
L16.3	Q	1.72	1.42	.98	.63	.00118	1.31	2.65	.00193	.0106	13.58	168	1.26
L16.4	F	1.54	1.30	1.27	.90	.00112	1.28	2.57	.00171	.0106	15.05	182	.78
L16.5	Q	1.64	1.40	.51	.34	.00058	1.03	2.65	.00097	.0105	9.65	95	1.92
L16.6	Q	1.66	1.20	.82	.58	.00075	1.12	2.65	.00122	.0105	11.88	127	1.40
L16.7	F	1.70	1.40	1.02	.66	.00105	1.26	2.57	.00162	.0105	12.02	145	1.44
L16.8	Q	1.66	1.16	1.02	.74	.00095	1.22	2.65	.00156	.0100	13.95	170	1.10
L16.9	Q	1.44	1.26	.96	.71	.00084	1.17	2.65	.00140	.0100	14.65	172	.96
L16.10	X	1.38	1.26	1.03	.78	.00077	1.13	2.60	.00122	.0100	15.02	170	.83

(Continued on next page)

Table 14
(Continued)

Particle Number	Mineral Type	Particle Dimensions a mm	b mm	c mm	Shape Factor	Volume cc	Nominal Diameter mm	S.G.	F gm	Kinematic Viscosity cm²/sec	Fall Velocity cm/sec	Re (d_n)	C_D (d_n)
Retained on No. 20 Tyler Standard Sieve													
L20.1	Q	1.60	1.26	1.02	.72	.00092	1.20	2.65	.00150	.0100	13.98	168	1.075
L20.2		1.37	1.02	.78	.66	.00063	1.06	2.65	.00103	.0100	12.42	132	1.19
L20.3	X	1.44	1.16	.63	.49	.00036	0.88	2.65	.00059	.0100	8.89	78.3	1.94
L20.4	Q	1.20	1.00	.95	.87	.00051	0.99	2.65	.00084	.0100	14.06	139	0.87
L20.5	F	1.44	.88	.66	.59	.00037	0.89	2.57	.00058	.0110	9.38	76.0	1.71
L20.6	Q	1.40	1.16	.70	.55	.00048	0.97	2.65	.00087	.0110	9.48	83.7	1.87
L20.7	Q	1.40	1.04	.67	.56	.00043	0.93	2.65	.00070	.0110	9.57	81.2	1.75
L20.8	Q	1.34	1.28	.80	.61	.00061	1.05	2.65	.00099	.0110	12.23	117	1.21
L20.9	Q	1.30	1.26	.84	.66	.00063	1.06	2.65	.00103	.0110	12.06	116	1.26
L20.10	Q	1.34	1.04	1.05	.89	.00065	1.07	2.65	.00106	.0110	14.98	146	.83
Retained on No. 24 Tyler Standard Sieve													
L24.1	Q	1.22	1.00	.74	.67	.00040	0.91	2.65	.000655	.0112	10.17	82.8	1.54
L24.2	Q					Lost							
L24.3	Q	1.06	1.00	.81	.79	.00041	0.92	2.65	.00067	.0112	11.92	98.0	1.13
L24.4		1.26	1.12	.53	.45	.00035	0.87	2.65	.00057	.0110	9.10	72.1	1.82
L24.5	Q	0.88	0.80	.69	.82	.00023	0.76	2.65	.000385	.0110	10.56	73.0	1.18
L24.6	Q	0.94	0.86	.68	.74	.00023	0.76	2.65	.000385	.0110	8.65	59.8	1.66
L24.7	Q	1.40	0.96	.71	.61	.00044	0.74	2.65	.000345	.0108	7.65	52.5	2.19
L24.8	X	1.00	0.96	.65	.66	.00029	0.82	5.00	.002250	.0108	5.80	44.1	1.99
L24.9	F	1.06	0.80	.67	.73	.00024	0.77	2.57	.000375	.0106	9.87	71.8	1.31
L24.10		1.40	1.00	.77	.65	.00050	0.98	2.65	.000810	.0106	11.25	104	1.35

(Continued on next page)

Table 14
(Continued)

Particle Number	Mineral Type	Particle Dimensions a mm	b mm	c mm	Shape Factor	Volume cc	Nominal Diameter mm	S.G.	F gm	Kinematic Viscosity cm²/sec	Fall Velocity cm/sec	Re (d_n)	C_D (d_n)
Retained on No. 28 Tyler Standard Sieve													
L28.1	Q	.80	.72	.59	.77	.00015	0.66	2.65	.000250	.0110	9.00	54.0	1.42
L28.2	QQ	1.16	.80	.36	.37	.00013	0.62	2.65	.000210	.0110	6.25	35.3	2.75
L28.3	QQ	.94	.90	.53	.60	.00020	0.72	2.65	.000320	.0110	8.60	56.3	1.68
L28.4	QQ	1.00	.60	.56	.73	.00016	0.69	2.65	.000285	.0108	9.15	58.5	1.44
L28.5	QQ	.88	.74	.44	.55	.00013	0.62	2.65	.000210	.0108	7.28	41.8	2.02
L28.6	QQ	.88	.80	.54	.65	.00018	0.70	2.65	.000300	.0108	8.20	53.3	1.78
L28.7	QQ	1.28	.86	.64	.61	.00035	0.87	2.65	.000570	.0108	9.30	75.0	1.75
L28.8	QQ	1.00	.84	.52	.57	.00020	0.72	2.65	.000320	.0110	7.80	51.1	2.05
L28.9	Q	1.34	.94	.42	.38	.00025	0.78	2.65	.000415	.0110	6.69	47.4	3.02
L28.10	Q	1.04	.76	.53	.66	.00022	0.75	2.65	.000362	.0110	8.80	60.0	1.68
Retained on No. 32 Tyler Standard Sieve													
L32.1	Q	.90	.80	.36	.43	.00013	0.62	2.65	.000210	.0110	5.95	33.6	3.02
L32.2		.68	.60	.36	.56			Lost					
L32.3	QQ	.84	.74	.46	.79	.00013	0.62	2.65	.000210	.0110	8.93	51.3	1.35
L32.4	QQ	.86	.68	.60	.78	.00015	0.65	2.65	.000242	.0108	9.02	54.3	1.38
L32.5	F	1.06	.62	.48	.59	.00014	0.64	2.57	.000228	.0108	7.00	41.5	2.24
L32.6	QQ	.78	.76	.56	.73	.00014	0.64	2.65	.000228	.0108	8.52	50.5	1.53
L32.7	QQ	1.02	.84	.46	.49	.00018	0.70	2.65	.000300	.0108	7.15	46.4	2.35
L32.8	QQ	.70	.52	.47	.78	.00008	0.53	2.65	.000131	.0106	7.00	35.1	1.86
L32.9	QQ	.72	.64	.45	.67	.00009	0.55	2.65	.000145	.0106	6.05	31.4	2.61
L32.10	Q	.86	.58	.49	.69	.00010	0.57	2.65	.000162	.0106	6.39	34.4	2.45

(Continued on next page)

Table 14
(Continued)

Particle Number	Mineral Type	Particle Dimensions a mm	b mm	c mm	Shape Factor	Volume cc	Nominal Diameter mm	S.G.	F gm	Kinematic Viscosity cm^2/sec	Fall Velocity cm/sec	Re (d_n)	C_D (d_n)
Retained on No. 35 Tyler Standard Sieve													
L35.1	Q	.66	.50	.35	.61	.00005	0.45	2.65	.000080	.0103	5.08	22.20	3.05
L35.2	Q	.78	.52	.36	.55	.00006	0.48	2.65	.000096	.0103	5.01	23.35	3.37
L35.3	Q	.44	.40	.21	.49	.00002	0.32	2.65	.0000289	.0103	3.15	9.78	5.20
L35.4	Q	.60	.46	.33	.63	.00004	0.42	2.65	.000065	.0103	4.55	18.55	3.57
L35.5	Q	.52	.42	.23	.49	.00002	0.32	2.65	.0000289	.0101	3.34	10.57	4.72
L35.6	Q	.74	.44	.30	.52	.00005	0.45	2.65	.000080	.0101	4.45	19.80	4.05
L35.7	Q	.56	.50	.30	.56	.00004	0.42	2.65	.000065	.0101	4.30	17.88	3.98
L35.8	Q	.56	.40	.21	.45	.00002	0.32	2.65	.0000289	.0101	3.42	10.83	4.50
L35.9	Q	.68	.48	.47	.81	.00006	0.48	2.65	.000096	.0101	6.55	31.2	1.95
L35.10	Q	.62	.56	.43	.73	.00006	0.48	2.65	.000096	.0101	6.20	29.5	2.15
Retained on No. 42 Tyler Standard Sieve													
L42.1	Q	.46	.44	.23	.51	.00002	0.32	2.65	.0000289	.0100	3.40	10.89	4.60
L42.2	Q	.66	.52	.29	.49	.00005	0.45	2.65	.000080	.0100	3.70	16.62	5.03
L42.3	Q	.58	.38	.35	.75	.00004	0.42	2.65	.000065	.0100	6.05	26.45	2.03
L42.4	Q	.58	.44	.36	.70	.00005	0.45	2.65	.000080	.0100	6.10	27.40	2.10
L42.5	Q	.64	.46	.26	.48	.00003	0.38	2.65	.000049	.0100	3.38	12.83	5.80
L42.6	Q	.64	.38	.43	.88	.00005	0.45	2.65	.000080	.0100	6.30	28.3	1.95
L42.7	Q	.56	.36	.37	.82	.00003	0.38	2.65	.000049	.0101	4.25	15.98	2.92
L42.8	Q	.56	.40	.35	.75	.00003	0.38	2.65	.000049	.0101	4.25	15.98	3.68
L42.9	Q	.64	.40	.34	.67	.00004	0.42	2.65	.000065	.0101	4.45	18.48	3.73
L42.10	Q	.60	.48	.37	.68	.00005	0.45	2.65	.000080	.0101	5.20	23.15	2.90

(Continued on next page)

Table 14
(Continued)

Particle Number	Mineral Type	Particle Dimensions a mm	b mm	c mm	Shape Factor	Volume cc	Nominal Diameter mm	S.G.	F gm	Kinematic Viscosity cm^2/sec	Fall Velocity cm/sec	Re (d_n)	C_D (d_n)
Retained on No. 48 Tyler Standard Sieve													
L48.1	Q	.42	.40	.30	.75	.00002	0.32	2.65	.0000289	.0110	3.75	10.90	3.72
L48.2	Q	.38	.36	.24	.64	.00002	0.32	2.65	.0000289	.0110	3.10	9.00	5.36
L48.3	Q	.52	.46	.26	.53	.00003	0.38	2.65	.0000490	.0108	3.30	11.72	6.19
L48.4	Q	.54	.46	.20	.40	.00002	0.32	2.65	.0000289	.0108	2.91	8.70	6.21
L48.5	Q	.62	.38	.35	.71	.00003	0.38	2.65	.0000490	.0108	4.25	15.21	3.65
L48.6	Q	.42	.32	.27	.74	.00002	0.32	2.65	.0000289	.0106	4.07	12.30	3.20
L48.7	Q	.44	.40	.21	.51	.00002	0.32	2.65	.0000289	.0106	2.80	8.45	6.75
L48.8		.56	.38	.34	.75	.00003	0.38	2.65	.0000490	.0106	5.75	20.65	2.02
L48.9	Q	.54	.40	.31	.67	.00003	0.38	2.65	.0000490	.0106	3.65	13.08	4.97
L48.10	Q	.44	.36	.26	.64	.00002	0.32	2.65	.0000289	.0106	3.10	9.35	5.48
Retained on No. 60 Tyler Standard Sieve													
L60.1	Q	.44	.36	.04	.11			2.65			Lost		
L60.2	Q	.44	.34	.19	.50	.000012	0.28	2.65	.0000195	.0110	2.48	6.32	7.91
L60.3	Q	.44	.36	.20				2.65			Lost		
L60.4	Q	.42	.30					2.65			Lost		
L60.5	Q	.34	.30	.16	.48	.000007	0.24	2.65	.0000118	.0110	1.86	4.07	12.03
L60.6	Q	.42	.36	.18	.47	.000010	0.26	2.65	.0000255	.0108	2.20	5.30	9.40
L60.7	Q	.48	.26	.20	.58	.000009	0.25	2.65	.0000135	.0108	1.75	4.05	11.50
L60.8	Q	.42	.26	.12	.35			2.65			Lost		
L60.9	Q	.38	.34					2.65			Lost		
L60.10	Q	.60	.34					2.65			Lost		

(Continued on next page)

Table 14
(Continued)

Particle Number	Mineral Type	Particle Dimensions a mm	b mm	c mm	Shape Factor	Volume cc	Nominal Diameter mm	S.G.	F gm	Kinematic Viscosity cm^2/sec	Fall Velocity cm/sec	Re (d_n)	C_D (d_n)
Retained on No. 65 Tyler Standard Sieve													
L65.1	Q	.28	.28	.22	.78	.000007	0.23	2.65	.0000102	.0106	1.60	3.48	11.12
L65.2	Q	.40	.28	.19	.58	.000008	0.24	2.65	.0000118	.0106	1.12	2.54	14.00
L65.3	Q	.46	.26	.12	.34	.000005	0.21	2.65	.0000078	.0106	1.68	3.34	13.01
L65.4	Q	.30	.28	.23	.82	.000007	0.23	2.65	.0000102	.0110	2.27	4.75	7.95
L65.5	Q	.36	.20	.23	.87	.000006	0.22	2.65	.0000087	.0110	2.08	4.59	8.21
L65.6	Q	.32	.20	.17	.69	.000003	0.19	2.65	.0000071	.0100	1.92	3.65	9.43
L65.7	Q	.32	.30	.22	.68	.000009	0.25	2.65	.0000135	.0100	2.86	7.15	5.42
L65.8	Q	.36	.32					2.65		Lost			
L65.9	Q	.40	.30	.20	.58	.000011	0.27	2.65	.0000170	.0100	2.53	6.8	7.45
L65.10	Q	.40	.26	.19	.61	.000009	0.25	2.65	.0000135	.0100	1.72	4.3	9.79

F - Feldspar
Q - Quartz or Chalcedony
X - Mixture

Table 15

Drag Coefficient as a Function of Reynolds Number for Naturally Worn Sediments (Taken from Composite C_D:Re Graph, Fig. 14)

Re	C_D				
	sf = 0.3	0.5	0.7	0.9	1.0
1.5	25.0	21	19.4	--	19.0
2	20.2	16.8	15.4	--	14.9
3	14.9	12.4	11.2	--	10.8
4	12.0	9.9	8.9	--	8.6
5	10.3	8.5	7.5	--	7.2
6	9.1	7.45	6.5	--	6.3
7	8.1	6.7	5.85	--	5.6
8	7.5	6.1	5.3	--	5.05
9	6.9	5.65	4.9	--	4.65
10	6.5	5.25	4.55	--	4.3
15	5.05	4.1	3.45	--	3.23
20	4.3	3.4	2.88	2.75	2.68
30	3.5	2.72	2.28	2.14	2.08
40	3.1	2.35	1.94	1.81	1.75
50	2.85	2.11	1.74	1.59	1.56
60	2.70	1.95	1.60	1.45	1.40
70	2.60	1.83	1.49	1.33	1.29
80	2.52	1.75	1.41	1.25	1.21
90	2.47	1.67	1.35	1.18	1.14
100	2.45	1.61	1.30	1.12	1.08
150	2.36	1.45	1.14	.94	.895
200	2.34	1.38	1.07	.84	.79
300	2.37	1.30	1.02	.75	.67
400	2.40	1.30	1.00	.71	.60
500	2.45	1.31	1.00	.695	.555
600	2.50	1.33	1.02	.685	.528
700	2.55	1.37	1.03	.683	.502
800	2.59	1.40	1.04	.680	.488
1000	2.65	1.48	1.08	.675	.460
1500	2.70	1.61	1.14	.670	.428
2000	2.70	1.68	1.17	.670	.410
3000	2.63	1.70	1.20	.680	.400
4000	2.55	1.70	1.21	.682	.400
5000	2.46	1.67	1.20	.695	.401
6000	2.38	1.66	1.19	.700	.402
7000	2.31	1.63	1.18	.705	.404
8000	2.26	1.61	1.17	.705	.406
10000	2.17	1.57	1.14	.710	.410
15000	2.11	1.40	1.08	.711	.414

Table 16

Drag Coefficient as a Function of
Reynolds Number for Crusher Fragments
(Taken from Composite C_D:Re Graph, Fig. 15)

Re	C_D				
	sf = 0.3	0.5	0.7	0.9	1.0
1.5	24.5	21.3	19.5	--	19.0
2	19.9	16.9	15.5	--	14.9
3	14.6	12.3	11.3	--	10.8
4	11.8	9.9	8.9	--	8.5
5	10.2	8.55	7.5	--	7.15
6	8.95	7.5	6.6	--	6.25
7	8.05	6.7	5.9	--	5.55
8	7.33	6.15	5.35	--	5.1
9	6.80	5.7	4.95	--	4.65
10	6.40	5.3	4.60	--	4.3
15	5.02	4.13	3.55	--	3.26
20	4.28	3.52	3.00	2.75	2.7
30	3.5	2.85	2.38	2.18	2.10
40	3.15	2.5	2.06	1.86	1.76
50	2.92	2.28	1.86	1.66	1.56
60	2.8	2.14	1.72	1.52	1.41
70	2.70	2.05	1.63	1.41	1.30
80	2.66	1.98	1.54	1.34	1.21
90	2.62	1.94	1.47	1.27	1.15
100	2.60	1.88	1.43	1.22	1.09
150	2.67	1.78	1.30	1.06	.90
200	2.83	1.75	1.23	.98	.79
300	3.08	1.75	1.21	.89	.67
400	3.20	1.77	1.22	.865	.60
500	3.22	1.78	1.23	.858	.56
600	3.25	1.82	1.24	.855	.528
700	3.24	1.83	1.27	.855	.502
800	3.21	1.84	1.28	.855	.488
900	3.22	1.86	1.29	.857	.473
1000	3.18	1.88	1.29	.860	.460
1500	3.08	1.88	1.30	.863	.426
2000	2.99	1.90	1.32	.866	.410
3000	2.90	1.89	1.32	.869	.400
4000	2.79	1.86	1.31	.870	.400
5000	2.73	1.82	1.30	.868	.401
6000	2.68	1.80	1.29	.865	.402
7000	2.62	1.76	1.28	.855	.404
8000	2.57	1.72	1.27	.842	.406
9000	2.52	1.69	1.24	.825	.408
10000	2.48	1.67	1.22	.800	.410
15000	2.35	1.57	1.19	.750	.410

Table 17

Drag Coefficient as a Function of Size Coefficient for Natural Particles (Taken from Figs. 20 and 21)

C_s	C_D For naturally worn sediments					C_D For crusher fragments				
	sf = 0.3	0.5	0.7	0.9	1.0	0.3	0.5	0.7	0.9	1.0
20	28.0	21.1	18.2	--	16.3	28.0	21.2	18.2	--	16.3
100	10.3	7.73	6.45	--	5.95	10.3	7.90	6.65	--	5.95
400	5.35	3.96	3.20	--	2.85	5.39	4.11	3.32	--	2.85
1000	3.75	2.72	2.26	1.98	1.88	3.75	2.88	2.32	2.00	1.88
4,000	2.70	1.80	1.47	1.21	1.13	2.76	2.06	1.56	1.32	1.13
10,000	2.42	1.50	1.18	0.92	0.845	2.57	1.82	1.32	1.05	0.845
20,000	2.32	1.38	1.06	0.780	0.705	2.58	1.76	1.23	0.96	0.705
40,000	2.30	1.30	1.02	0.710	0.595	2.69	1.74	1.20	0.895	0.595
70,000	2.32	1.27	1.01	0.685	0.530	2.94	1.74	1.21	0.860	0.530
100,000	2.33	1.28	1.01	0.675	0.495	3.06	1.76	1.23	0.850	0.495
200,000	2.41	1.32	1.03	0.665	-.450	3.19	1.81	1.27	0.855	0.450
400,000	2.50	1.41	1.07	0.665	0.420	3.21	1.86	1.29	0.865	0.420
700,000	2.60	1.50	1.12	0.665	0.407	3.20	1.87	1.29	0.875	0.407
1,000,000	2.68	1.58	1.16	0.680	0.400	3.19	1.89	1.30	0.875	0.400
2,000,000	2.72	1.65	1.18	0.682	0.397	3.12	1.90	1.31	0.880	0.397
4,000,000	2.70	1.70	1.20	0.685	0.397	3.01	1.90	1.32	0.880	0.397
7,000,000	2.63	1.70	1.20	0.687	0.400	2.93	1.88	1.32	0.875	0.400
10,000,000	2.58	1.69	1.19	0.695	0.405	2.87	1.86	1.30	0.860	0.405
20,000,000	2.45	1.66	1.17	0.706	--	2.76	1.80	1.28	0.835	--
30,000,000	2.37	1.62	1.13	--	--	2.68	1.74	1.26	--	--
40,000,000	2.31	1.60	1.11	--	--	2.63	1.71	1.23	--	--
50,000,000	2.25	1.57	--	--	--	2.58	1.68	--	--	--

Table 18

Velocity Coefficient as a Function of Reynolds Number
(Taken from Figs. 22 and 23)

C_w	Re For naturally worn sediments					Re For crusher fragments				
sf =	0.3	0.5	0.7	0.9	1.0	0.3	0.5	0.7	0.9	1.0
.00000003	--	--	--	--	9800	--	--	--	--	9800
.00000007	--	--	--	6100	4000	--	--	--	8400	4000
.0000001	--	--	7700	4450	2800	--	--	8500	5950	2800
.0000002	7600	5600	4080	2290	1470	8600	6100	4450	3050	1470
.0000004	4250	2950	2030	1180	830	4670	3200	2260	1500	830
.0000007	2540	1620	1080	665	540	2800	1850	1280	850	540
.000001	1780	970	690	470	410	2000	1280	870	586	410
.000002	880	425	340	262	248	1070	625	408	302	248
.000004	416	225	186	158	153	540	294	210	173	153
.000007	226	142	117	107	103	280	165	128	112	103
.00001	151	106	90	84	80	180	119	96	85	81
.00002	82	64.5	55.6	52.5	50.5	86	66.5	58.	53.1	50.5
.00004	47.0	38.5	34.6	33.5	32.5	48	40.8	35.6	33.5	32.5
.0001	24.6	21.5	19.4	--	18.4	25.2	22.2	19.7	18.5	18.4
.0004	10.2	9.0	8.4	--	8.0	10.3	9.2	8.3	--	8.0
.001	5.8	5.2	4.85	--	4.70	5.9	5.2	4.85	--	4.70
.004	2.56	2.33	2.22	--	2.18	2.58	2.33	2.22	--	2.18
.008	1.72	1.58	1.50	--	1.48	1.72	1.58	1.51	--	1.48
.01	1.53	1.41	1.33	--	1.29	1.50	1.40	1.33	--	1.29